

**REGULATION AND SUBCELLULAR LOCALIZATION OF
AFLATOXIN BIOSYNTHESIS IN *ASPERGILLUS PARASITICUS***

By

Josephine Wee

A DISSERTATION

Submitted to
Michigan State University
in partial fulfillment of the requirements
for the degree of

Food Science--Environmental Toxicology--Doctor of Philosophy

2015

ABSTRACT

REGULATION AND SUBCELLULAR LOCALIZATION OF AFLATOXIN BIOSYNTHESIS IN *ASPERGILLUS PARASITICUS*

By

Josephine Wee

The filamentous fungus, *Aspergillus parasiticus* grows on a variety of susceptible food crops and produces aflatoxin, a carcinogenic secondary metabolite that is both a health and economic threat. Aflatoxin biosynthesis is one of the most well-characterized eukaryotic secondary metabolic pathways. Understanding **how** aflatoxin biosynthesis initiates and **where** aflatoxin is made are critical to control synthesis and export of fungal metabolites. A previous study conducted in the Linz laboratory using electrophoretic mobility shift analysis (EMSA) and chromatin immunoprecipitation (ChIP) found that the bZIP transcription factor AtfB binds to promoters of specific aflatoxin and stress response genes. Once aflatoxin gene expression initiates, our lab showed that *A. parasiticus* performs synthesis, compartmentalization, and export of aflatoxin in subcellular organelles called toxisomes. This dissertation is dedicated to further characterizing the role of transcriptional regulation and subcellular localization of aflatoxin biosynthesis specifically through two cellular targets, **AtfB** and **Vps34**. In order to study function of these two targets, we exploited a novel and endogenous CRISPR/*cas9*-like system in *A. parasiticus* to down-regulate function of AtfB and Vps34. This system is an easy, rapid, and highly efficient co-transformation method; 1 out of every 3 *niaD* + (the gene encoding nitrate reductase [*niaD*] is the selectable marker) transformants exhibited an atypical phenotype that we later showed was associated

with the presence and expression of the disruption construct. The disruption of AtfB resulted in a consistent phenotype of low aflatoxin production, lower conidiospore numbers, and lower levels of spore pigmentation. Down-regulation of AtfB targets involved in aflatoxin biosynthesis and stress response showed that the level of expression of target genes is consistent with the observed phenotype of the disruption strains. Of particular importance, global expression data and computer-based network analysis also suggested the AtfB network extends beyond mycotoxin biosynthesis and stress response. Interestingly, the disruption of Vps34 resulted in the opposite phenotype compared to disruption of AtfB. Vps34 transformants exhibited high aflatoxin production, high conidiospore numbers, and high levels of spore pigmentation. We conducted an independent experiment using 3-methyladenine, a biochemical inhibitor of Vps34. Treatment of *A. parasiticus* SU-1 with 3-methyladenine caused a 10-fold increase in aflatoxin levels detected in aflatoxin-inducing medium. This biochemical approach supports the phenotype of high aflatoxin levels observed in Vps34 disruption strains. We further propose that Vps34 negatively regulates the transport of toxisomes to the vacuoles. Vps34 also positively regulates the export pathway directing early endosomes carrying aflatoxin for export out of the cell. Fungal targets like AtfB and Vps34 that differentially regulate aflatoxin biosynthesis serve as useful tools to understand the molecular mechanisms that contribute to fungal virulence. From a public health perspective, our research goal is to use practical and sustainable natural inhibitors that target fungal specific cellular targets to block toxin production in the field and in storage.

**Copyright by
JOSEPHINE WEE
2015**

The mediocre teacher tells. The good teacher explains. The superior teacher demonstrates. The great teacher inspires. -- William Arthur Ward
To all my teachers and educators that have inspired me

ACKNOWLEDGEMENTS

I am grateful to the members of my guidance committee (my “scientific mentors”), Dr. Randy Beaudry, Dr. James Pestka, Dr. Gale Strasburg, and Dr. Frances Trail for their time, encouragement, and expertise during my PhD. Thank you for the inspiring conversations, challenging questions, and helpful suggestions throughout the course of this dissertation.

I would like to specifically thank Dr. Ludmila Roze, Dr. Sung-Yong Hong, and Dr. Anindya Chanda for their encouragement and support during my PhD journey. I am especially grateful to Devin Day for all her assistance during the final months of my PhD and for being a great friend. To the many friends that I have made during my time at MSU; you have impacted my life in various ways and you will be greatly missed.

There are people in my life that I share my success with. I thank my parents, who worked so hard to provide me with a good education. My sister, Jennifer and brothers, Justin and Jason for having faith in me and constantly breaking the “educational bar” I’ve set for them. Finally, I thank my husband, Shawn for his unconditional love as my equal half. I am excited to see what the future holds for us.

Without Dr. John Linz, pursuit of my advanced degree would never have started and completion of this work would be impossible. I’m forever indebted. I will really miss our thought-provoking conversations. His creative mind, optimistic support, and unflagging patience made this project both fun and rewarding. Dr. Linz is a brilliant scientist and a great mentor. I am truly blessed.

TABLE OF CONTENTS

| | |
|--|-----|
| LIST OF TABLES | x |
| LIST OF FIGURES | xi |
| KEY TO ABBREVIATIONS | xiv |
| CHAPTER 1: INTRODUCTION, CHAPTER SUMMARIES, LITERATURE REVIEW, AND SIGNIFICANCE | 1 |
| INTRODUCTION | 1 |
| CHAPTER SUMMARIES | 2 |
| LITERATURE REVIEW | 5 |
| Aflatoxins: background, toxicity, and global burden | 5 |
| Background | 5 |
| Toxicity and mechanism of carcinogenicity | 11 |
| Global health and economic burden associated with aflatoxin | 12 |
| Emerging risk of aflatoxin contamination due to global climate change | 17 |
| Proposed role of aflatoxin in fungal biology | 18 |
| Aflatoxin biosynthesis: Our previous work | 19 |
| Discovery of the key genes in the aflatoxin cluster | 22 |
| Regulatory elements in aflatoxin gene expression | 25 |
| Aflatoxin and oxidative stress | 26 |
| Studies on signal transduction pathways that mediate aflatoxin gene expression | 29 |
| Association between secondary metabolism and development | 33 |
| Studies on subcellular localization of aflatoxin enzymes and aflatoxin | 34 |
| Studies on compounds that potentiate/modulate aflatoxin synthesis | 41 |
| CHAPTER 2: THE FUNGAL TRANSCRIPTION FACTOR ATFB CONTROLS VIRULENCE-ASSOCIATED PROCESSES IN <i>ASPERGILLUS PARASITICUS</i> | 45 |
| ABSTRACT | 45 |
| INTRODUCTION | 46 |
| MATERIALS AND METHODS | 48 |
| Fungal strains and growth conditions | 48 |
| Disruption of <i>A. parasiticus</i> AtfB | 49 |
| DNA extraction and Southern blot analysis | 50 |
| Aflatoxin measurements in SU-1, JW-12 and JW-13 | 52 |
| RNA Isolation, transcript analysis, and <i>Hind</i> III cutting assay | 52 |
| Protein extraction and Western blot analysis | 53 |

| | |
|--|-----|
| RNA isolation and cDNA library preparation for RNA Seq analysis | 53 |
| RNA Seq analysis | 54 |
| RT-PCR analysis | 55 |
| Gene ontology (GO) pathway analysis and REViGO | 55 |
| RESULTS | 56 |
| Molecular analysis of JW-12 and JW-13 | 56 |
| AtfB disruption construct is directly linked to aflatoxin synthesis and fungal growth | 59 |
| Up-regulation of expression of <i>atfB</i> disruption transcript associates with a decrease of AtfB protein level in JW-12 and JW-13 | 61 |
| Accumulation of aflatoxin enzymes is decreased in JW-12 and JW-13 | 65 |
| AtfB protein levels impact expression of AtfB specific targets | 65 |
| Down regulation of “sentinel” gene expression in JW-12 and JW-13 | 71 |
| The fungal AtfB regulatory networks extends beyond secondary metabolism, stress response, and development | 74 |
| DISCUSSION | 76 |
| CHAPTER 3: UTILIZING A CRISPR/CAS9-LIKE MECHANISM TO ELUCIDATE THE ROLE OF VPS34 IN AFLATOXIN SYNTHESIS | 82 |
| ABSTRACT | |
| INTRODUCTION | 83 |
| MATERIALS AND METHODS | 86 |
| Fungal strains, media, and growth conditions | 86 |
| Identification, cloning, and disruption of <i>A. parasiticus</i> Vps34 | 87 |
| Molecular analysis of transformants | 88 |
| Aflatoxin measurements in strains SU-1, JW-17, and in 3-methyladenine experiments | 89 |
| RNA isolation and transcript analysis | 90 |
| RESULTS | 91 |
| Key domains in fungal Vps34 are highly conserved across different species | 91 |
| Vps34 mutant construct stability and potential loss of mutant phenotype | 95 |
| Multiple tandem integration of <i>vps34</i> knockout construct into an ectopic site in the <i>A. parasiticus</i> genome | 95 |
| Presence of the <i>vps34</i> disruption construct is directly linked to increased aflatoxin synthesis and conidiospore development | 100 |
| <i>Vps34</i> mutant transcript expression levels increase over time | 104 |
| 3-methyladenine increases aflatoxin synthesis in wild-type strain SU-1 | 106 |
| DISCUSSION | 108 |

| | |
|---|-----|
| CHAPTER 4: <i>A. PARASITICUS</i> GENOME SEQUENCE, PREDICTED CHROMOSOME STRUCTURE, AND DIFFERENTIAL GENE EXPRESSION | 112 |
| ABSTRACT | 112 |
| INTRODUCTION | 113 |
| MATERIALS AND METHODS | 115 |
| Microorganisms and culture conditions | 115 |
| DNA preparation and Illumina next generation sequence (NGS) analysis | 115 |
| Comparison of chromosome structure and gene distribution in <i>A. parasiticus</i> SU-1 and <i>A. flavus</i> 3357 | 116 |
| RNA preparation and RNA sequence (RNA Seq) analysis | 117 |
| Identification and function of “uniquely expressed loci” in <i>A. parasiticus</i> | 119 |
| RESULTS | 120 |
| <i>A. parasiticus</i> SU-1 genome sequence and predicted chromosome structure | 120 |
| Comparison of <i>A. parasiticus</i> SU-1 and <i>A. flavus</i> 3357 gene expression under aflatoxin inducing conditions | 133 |
| Identification of “uniquely expressed genes” in <i>A. parasiticus</i> | 141 |
| DISCUSSION | 145 |
| CHAPTER 5: PROPOSED FUTURE STUDIES | 149 |
| APPENDICES | 151 |
| APPENDIX A: COMPUTER-AIDED ALGORITHMS REVEAL NOVEL CIS-REGULATORY ELEMENTS IN AFLATOXIN BIOSYNTHESIS | 152 |
| APPENDIX B: BIOCHEMICAL COMPOUNDS THAT TARGET AFLATOXIN BIOSYNTHESIS | 162 |
| APPENDIX C: HETEROLOGOUS EXPRESSION AND PURIFICATION OF THE <i>ASPERGILLUS PARASITICUS</i> ATFB DNA BINDING DOMAIN | 170 |
| BIBLIOGRAPHY | 182 |

LIST OF TABLES

| | | |
|---------|--|-----|
| Table 1 | Summary of the major aflatoxins produced by various <i>Aspergillus</i> spp. | 10 |
| Table 2 | Top 31 <i>A. parasiticus</i> SU-1 scaffolds by length | 122 |
| Table 3 | Secondary metabolism gene clusters in the <i>A. parasiticus</i> SU-1 genome screened by BLAST analysis | 127 |
| Table 4 | Expression of selected genes involved in secondary metabolism, stress response, and development | 135 |
| Table 5 | Predicted function of selected proteins by functional category | 144 |
| Table 6 | Potential compounds to control toxic secondary metabolite synthesis by <i>A. parasiticus</i> | 164 |

LIST OF FIGURES

| | | |
|-----------|--|----|
| Figure 1 | Molecular structures of fungal secondary metabolites | 6 |
| Figure 2 | Chemical structures of the four major types of aflatoxins | 8 |
| Figure 3 | Fungal secondary metabolic gene clusters for polyketides, non-ribosomal peptides, and terpenes | 21 |
| Figure 4 | The aflatoxin gene cluster in <i>A. parasiticus</i> | 24 |
| Figure 5 | Proposed model (2007) for aflatoxin biosynthesis in <i>A. parasiticus</i> during the transition from exponential growth to the stationary phase | 32 |
| Figure 6 | Two major categories of fungal secondary metabolites grouped by their chemical backbone and starter units | 36 |
| Figure 7 | Effective ways to block aflatoxin biosynthesis at the cellular level | 42 |
| Figure 8 | Disruption of <i>A. parasiticus attB</i> | 51 |
| Figure 9 | Southern hybridization analysis of <i>A. parasiticus</i> strains NR-1, JW-12, and JW-13 using an <i>attB</i> probe | 58 |
| Figure 10 | Characterization of fungal growth, conidiospore number/pigment, and aflatoxin production (phenotype) in strains SU-1, JW-12, and JW-13 | 60 |
| Figure 11 | Analysis of <i>attB</i> transcript levels in strains SU-1, JW-12, and JW-13 using semi-quantitative real time PCR and a novel <i>HindIII</i> cutting assay | 63 |
| Figure 12 | AttB protein levels analyzed by Western blot analysis | 66 |
| Figure 13 | Aflatoxin enzyme accumulation shows similar pattern of expression to AttB protein | 67 |
| Figure 14 | Comparison of the transcriptome in strains SU-1, JW-12 and JW-13 by RNA Seq analysis | 69 |
| Figure 15 | AttB regulates expression of selected sentinel virulence-associated genes | 72 |

| | | |
|-----------|---|-----|
| Figure 16 | Gene ontology (GO) analysis of candidate genes in the AtfB regulatory network in JW-12 and JW-13 | 75 |
| Figure 17 | Alignment of Vps34 amino acid sequences from aspergilli, yeast, mouse and human | 94 |
| Figure 18 | Molecular characterization of Vps34 transformants | 97 |
| Figure 19 | Disruption of Vps34 and Southern hybridization (blot) analysis | 99 |
| Figure 20 | Characterization of fungal growth, conidiospore number/pigment, and aflatoxin production (phenotype) in strains SU-1 and JW-17 | 101 |
| Figure 21 | Aflatoxin levels and growth measurements of SU-1 and JW-17 | 102 |
| Figure 22 | Mutant <i>vps34</i> transcript levels are up-regulated in Vps34 strain JW-17 | 105 |
| Figure 23 | 3-methyladenine increases aflatoxin levels in wild-type SU-1 under aflatoxin inducing GMS liquid medium | 107 |
| Figure 24 | Predicted chromosome structure of <i>A. parasiticus</i> SU-1 and <i>A. flavus</i> 3357 | 123 |
| Figure 25 | Analysis of genome identity between <i>A. parasiticus</i> SU-1 and <i>A. flavus</i> 3357 | 125 |
| Figure 26 | RNA SEQ analysis of gene expression in secondary metabolite Clusters 54 and 55 in <i>A. parasticus</i> SU-1 and <i>A. flavus</i> 3357 | 138 |
| Figure 27 | Aflatoxin accumulation in <i>A. parasiticus</i> SU-1 and <i>A. flavus</i> 3357 grown in culture | 140 |
| Figure 28 | KOBAS GO pathway analysis of uniquely expressed genes in <i>A. parasiticus</i> SU-1 | 143 |
| Figure 29 | Sequence analysis of aflatoxin gene promoters using MEME | 155 |
| Figure 30 | Example image of input .txt. format of promoter regions | 157 |
| Figure 31 | Screenshot view of MEME job submission | 158 |
| Figure 32 | Six highest reoccurring motifs based on preliminary analysis | 159 |
| Figure 33 | Location and distribution of 30 motifs | 160 |

| | | |
|-----------|--|-----|
| Figure 34 | TPEN decreases aflatoxin biosynthesis on PDA solid media | 166 |
| Figure 35 | TPEN decreases aflatoxin biosynthesis in GMS solid media | 167 |
| Figure 36 | Wortmannin differentially affects aflatoxin synthesis on solid media | 168 |
| Figure 37 | Secondary structure prediction of ApAtfB | 172 |
| Figure 38 | Physicochemical properties of ApAtfB | 173 |
| Figure 39 | Sequence comparison of Atf2, CREB, and ApAtfB | 174 |
| Figure 40 | Plasmid map of synthetic gene construct ApAtfB159-242_C2S | 175 |
| Figure 41 | Purification of recombinant 6xHis-ApAtfB (column fractionation) | 178 |
| Figure 42 | Purification of the recombinant 6xHis-ApAtfB (SDS-Page) | 179 |
| Figure 43 | Purification of ApAtfB | 180 |

KEY TO ABBREVIATIONS

| | |
|------------------|---|
| 3-MA | 3-methyladenine |
| A. | <i>Aspergillus</i> |
| AFB ₁ | Aflatoxin B ₁ |
| AtfB | Activating transcription factor B |
| CD | Conidiospore development |
| ChIP | Chromatin immunoprecipitation |
| CVT | Cytoplasm-to-vacuole targeting |
| EGFP | Enhanced green fluorescent protein |
| ELISA | Enzyme-linked immunosorbent assay |
| EMSA | Electrophoretic mobility shift assay |
| GMS | Glucose Minimal Salts |
| HBV | Hepatitis B virus |
| HCC | Hepatocellular carcinoma |
| IARC | International Agency for Research on Cancer |
| NA | Norsolorinic acid |
| NRP | Non-ribosomal peptide |
| PCR | Polymerase chain reaction |
| PI3K | Phosphatidylinositol-3 kinase |
| PKS | Polyketide synthase |
| RT-PCR | Reverse transcriptase polymerase chain reaction |
| SM | Secondary metabolism |

| | |
|-------|----------------------------|
| SMS | Sucrose Minimal Salts |
| SR | Stress response |
| ST | Sterigmatocystin |
| TLC | Thin-layer chromatography |
| VA | Versicolorin A |
| Vps34 | Vacuole sorting protein 34 |
| WHO | World Health Organization |
| YEG | Yeast Extract Glucose |
| YEP | Yeast Extract Peptone |
| YES | Yeast Extract Sucrose |

CHAPTER 1: INTRODUCTION, CHAPTER SUMMARIES, LITERATURE REVIEW, AND SIGNIFICANCE

INTRODUCTION

Filamentous fungi in the genus *Aspergillus* synthesize a variety of mycotoxins with important human health consequences including aflatoxin, sterigmatocystin, patulin, cyclopiazonic acid, gliotoxin, and aspergillilic acid. *Aspergillus parasiticus*, *A. flavus*, and *A. fumigatus* are important fungal pathogens of plants, animals, and humans. Aflatoxin has received the most public health attention compared to other foodborne mycotoxins because it is a potent carcinogen in animals and epidemiological evidence provides a strong link to incidences of liver and lung cancer in humans. *A. parasiticus* produces aflatoxin on a variety of economically important crops in the field (such as corn, peanuts, tree nuts) and in storage. Current methods to prevent or treat crop infection by aspergilli have limited efficacy and aflatoxin contamination remains a significant and longstanding problem. Our long-term goal is to utilize fungal-specific genetic and biochemical approaches to prevent aflatoxin (mycotoxin) contamination of crops in field and in storage to reduce human and animal exposure to foodborne mycotoxins.

The research in this dissertation expands on the work of others by identification of fungal-specific genetic and biochemical approaches to dissect the molecular and cellular mechanisms that drive aflatoxin biosynthesis. Early work in our laboratory demonstrated that the bZIP transcription factor AtfB is unique to aspergilli and regulates several genes involved in aflatoxin biosynthesis and oxidative stress response. We also

demonstrated that aflatoxin synthesis and export are mediated by endosomes (aflatoxisomes) in *A. parasiticus* that carry proteins involved in development, stress response, and secondary metabolism. The work conducted in this dissertation will enable us to understand in greater detail the specific mechanisms by which functional networks are controlled during aflatoxin biosynthesis and to test fungal-specific strategies to control synthesis in culture, in the soil environment, and on host plants.

CHAPTER SUMMARIES

Chapter 1 presents a concise review of the literature beginning with the discovery of aflatoxins (mycotoxins) and their initial characterization in the 1960s. This chapter is comprised of two major sections: 1) aflatoxins (what they are, where they come from, associated toxicities, and global burden of health and the economy related to mycotoxins); and 2) aflatoxin biosynthesis, which focuses on the work conducted in the Linz laboratory on the molecular and cellular mechanisms that trigger aflatoxin synthesis in the model organism, *Aspergillus parasiticus*. Contributions from the Linz laboratory from the discovery of the aflatoxin gene cluster (early 2000s) up to the complete sequence of the *A. parasiticus* genome (2014) have been significant and instrumental in directing previous and current work in the area of mycotoxin research. Chapter 1 is also aimed at providing background information for the motivation guiding my research in the Linz laboratory since January 2009.

Together, Chapter 2 and 3 represent first authored manuscripts prepared for publication in scientific journals. The focus of **Chapter 2** is to demonstrate that the bZIP transcription factor AtfB regulates several genes involved in secondary metabolism

(SM), stress response (SR), and conidiospore development (CD). SM, SR, and CD contribute to fungal virulence and are important virulence-associated cellular processes in *A. parasiticus*. We present evidence that the disruption of AtfB down-regulates AtfB regulatory networks involved in expression of virulence-associated cellular processes at the molecular and cellular level. These data serve to confirm that AtfB represents an important fungal-specific target to control *Aspergillus* virulence in culture, on plants, and in humans.

Chapter 3 further explores the idea of subcellular localization of aflatoxins in aflatoxisomes. I propose that a Class III lipid kinase, Vps34 plays a role in maturation of early endosomes and the export of aflatoxin in *A. parasiticus*. I present evidence that the down-regulation of *vps34* by a novel and endogenous CRISPR/*cas9*-like system down-regulates Vps34 function, down-regulates the cytoplasm-to-vacuole (CVT) pathway, and increases synthesis and export of aflatoxins. We propose that the cellular process of compartmentalization and export of secondary metabolites can be considered a virulence-associated process in *A. parasiticus*. These data serve to confirm that Vps34 represents a critical target (in addition to AtfB) to control *Aspergillus* virulence in culture, on plants, and in humans.

Chapter 4 will shift the focus to Illumina next generation sequence and bioinformatics analyses based on the recently published genome sequence of *A. parasiticus* wild type strain SU-1. We present the SU-1 genome sequence, its predicted chromosome structure, and comparative gene expression (RNA Seq analysis) under aflatoxin inducing and non-inducing conditions. We compared these observations to the previously published *A. flavus* genome to understand the genetic basis for differences in

biochemistry and morphology between *A. parasiticus* and *A. flavus*. These data help explain species-specific differences in the type and quantity of mycotoxins synthesized, as well as in morphology of mycelia and conidiospores. We concluded our discussion by suggesting that fungal specific C6-transcription factors and unique genes involved in secondary metabolism and stress response/cellular defense in *A. parasiticus* SU-1 could determine distinct species characteristics. This chapter has been published in Eukaryotic Cell and can be found at <http://www.ncbi.nlm.nih.gov/pubmed/24951444>.

In **Chapter 5**, I briefly propose future research directions based on the findings of Chapters 2-4. These future directions will enable us to better understand the cellular processes and regulatory networks controlled by two *A. parasiticus* regulators, AtfB and Vps34. Lastly, the research implications are related back to the control of toxic metabolite synthesis by filamentous fungus like *A. parasiticus* and how this information can help us to control production and export of secondary metabolites.

Building upon the findings of Chapter 2 on the role of AtfB in controlling fungal virulence-associated processes, **Appendices A and C** highlight my contributions to our understanding of the *cis*-regulatory elements in promoters of genes in the aflatoxin gene cluster as well as to express and purify the DNA binding domain of AtfB to characterize its affinity and binding to sequence-specific DNA regions. The data presented in **Appendix B** on biochemical compounds that target aflatoxin synthesis was included to enable researchers to use the preliminary data to guide future studies on identifying potential compounds to modulate secondary metabolism.

LITERATURE REVIEW

Aflatoxins: background, toxicity, and global burden

Background

Fungi have the ability to produce structurally diverse and highly specialized low molecular weight compounds called secondary metabolites. **Figure 1** highlights examples of secondary metabolites produced by fungi¹ and illustrates the chemical diversity of these metabolites. Generally, the production of secondary metabolites is not essential for growth (primary metabolism)^{2,3}. This means that secondary metabolism is not a requirement for growth. The ecological niches in which these fungi grow and thrive influence their capabilities to produce such metabolites. Many of these compounds are found to be bioactive and possess pharmaceutical or toxigenic properties. Although not essential for growth, from an evolutionary perspective, it is thought that fungi use secondary metabolites as molecules of communication for defense and protection^{1,4}.

Conservative estimates propose that there are at least 1.5 million fungal species in our ecosystem⁵. Assuming that each fungus has the ability to produce an array of secondary metabolites, the wealth of chemical compounds with potential bioactivity and pharmaceutical properties is largely unexplored. For example, the filamentous fungi *A. parasiticus* and *A. flavus* carry the genetic capacity to produce up to 90 secondary metabolites⁶, however a relatively small number of such metabolites are actually detected under standard laboratory conditions. Fungal secondary metabolites have beneficial properties such as pharmaceuticals and medical drugs (penicillin, cyclosporin, statins) as well as potent toxins like aflatoxins, gliotoxins, and sterigmatocystin². Among the mold toxins (mycotoxins), aflatoxin is the most well-known and best characterized.

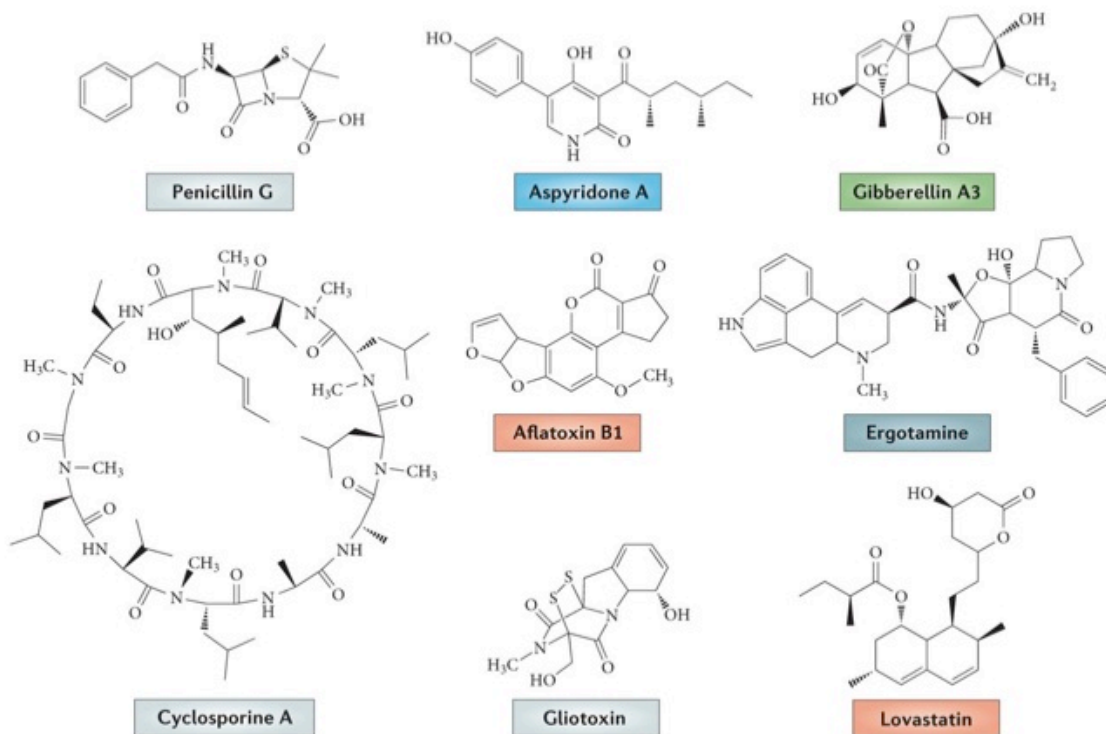


Figure 1 Molecular structures of fungal secondary metabolites

Secondary metabolites are low molecular weight compounds that are not essential for primary metabolism and growth. These natural products have positive and/or negative impacts on human health. Penicillin G (produced by *Penicillium chrysogenum*) is used as a β -lactam antibiotic, cyclosporine A (produced by *Tolypocladium inflatum*) is used as an immunosuppressant whereas lovastatin (produced by *Aspergillus terreus*) is used as a cholesterol-lowering drug. Many secondary metabolites have toxic properties such as aflatoxin produced by *A. flavus* and *A. parasiticus* as well as gliotoxin produced by *A. fumigatus*. Moderate cytotoxic activity has been associated with aspyridones (produced by *A. nidulans*). *Fusarium fujikuroi* produces the plant hormones gibberellins and ergot alkaloids (ergotamines) are predominantly produced by *Claviceps purpurea*. Figure reprinted from Brakhage (2014) with permission from the publisher, the Nature Publishing Group¹.

In the early 1960s, there was a mysterious death of thousands of turkeys in England that was later traced back to the same Brazilian peanut meal^{7,8}. The feed was later found to be contaminated by a mold toxin that was later characterized as “aflatoxins” by thin layer chromatography (TLC) on the contaminated peanut meal⁹. Aflatoxins derived their name from *A. flavus* from which they were originally isolated¹⁰.

Aflatoxins are predominantly produced by *Aspergillus flavus* and *A. parasiticus* when they colonize agricultural crops such as corn, barley, wheat, rye, tree nuts, and cottonseed¹¹. Aflatoxins are polyketide-derived furanocoumarins and consist of four major chemical groups (**Figure 2**); AFB₁, AFB₂, AFG₁, and AFG₂ named after their blue (B) and green (G) fluorescence under ultraviolet light¹². The number 1 and 2 indicate major and minor compounds based on their relative separation by TLC. Aflatoxin B₁ is the most toxic form of aflatoxin and is the most potent naturally occurring carcinogen known¹³. It is also the major aflatoxin derivative produced by toxigenic strains². Hence, WHO classifies AFB₁ as a Class I carcinogen¹⁴.

Although *A. flavus* and *A. parasiticus* are predominant producers of aflatoxin in agricultural crops, other *Aspergillus* spp. are also known to produce aflatoxin¹⁴. These aflatoxin-producing species are encountered less frequently: *Aspergillus bombycis*, *Aspergillus ochraceoroseus*, *Aspergillus nomius*, and *Aspergillus pseudotamari*². Aflatoxigenic strains differ in the amount and type of aflatoxin they produce. These qualitative and quantitative differences are important from a mycological standpoint. For example not all strains of *A. flavus* and *A. parasiticus* produce aflatoxin. *A. flavus* strains synthesize predominantly B aflatoxins while *A. parasiticus* strains produce both B and G type aflatoxins^{6,15}. *A. parasiticus* strains generally synthesize greater quantities of

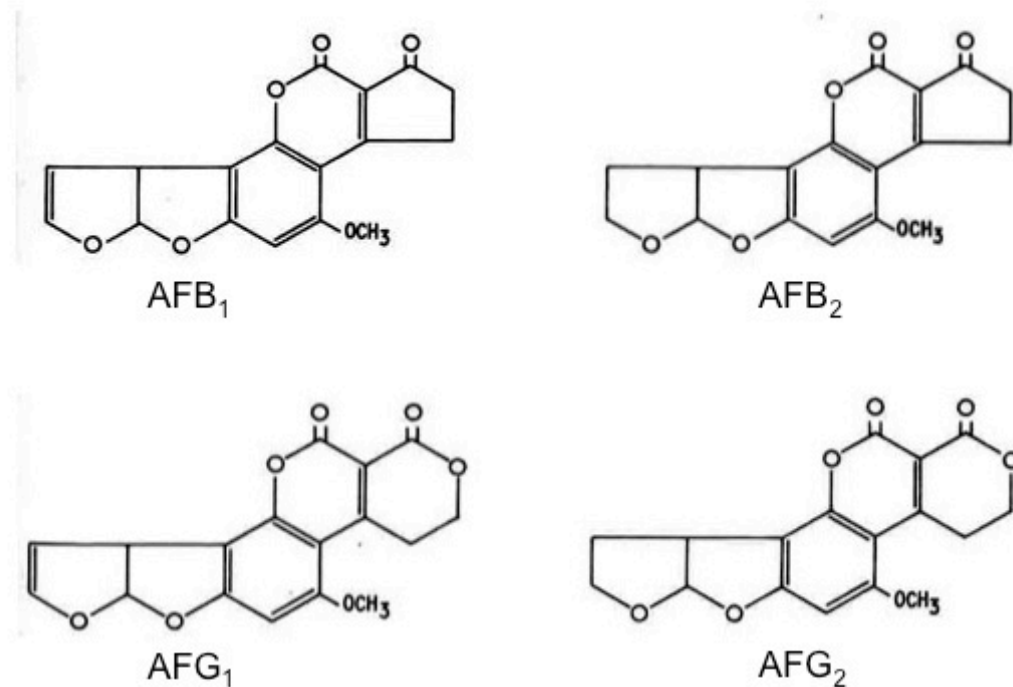


Figure 2 Chemical structures of the four major types of aflatoxins

Aflatoxins are polyketide-derived furanocoumarins and consist of four major chemical groups, AFB₁, AFB₂, AFG₁, and AFG₂. The number 1 and 2 indicate major and minor compounds based on their relative separation by TLC. Aflatoxin B₁ is the most toxic form of aflatoxin and is the most potent naturally occurring carcinogen known¹³.

aflatoxin than *A. flavus*. Other derivatives of the aflatoxin family are aflatoxin M₁ and M₂, which are oxidized forms of aflatoxin B₁. Aflatoxin M₁ and M₂ were first isolated from the milk of lactating animals fed with contaminated feed. In addition, aflatoxin can go through bio-transformation in the gastrointestinal (GI) tract of some animals and can be isolated from urine and feces^{2,16}. **Table 1** summarizes toxins produced from many other aflatoxin-producing species that have been identified and characterized¹⁴.

Table 1 Summary of the major aflatoxins produced by various *Aspergillus* spp.
Aflatoxins are produced predominantly by *A. flavus* and *A. parasiticus*¹⁴.

| Difuranocoumarins | Type of aflatoxin | <i>Aspergillus</i> specie(s) |
|--|--|--|
| Difurocoumaro-cyclopentenone series | Aflatoxin B ₁ (AFB ₁) | <i>A. flavus</i> , <i>A. arachidicola</i> , <i>A. bombycis</i> , <i>A. minisclerotigenes</i> , <i>A. nomius</i> , <i>A. ochraceoroseus</i> , <i>A. parasiticus</i> , <i>A. pseudotamarii</i> , <i>A. rambellii</i> , <i>Emericella venezuelensis</i> |
| | Aflatoxin B ₂ (AFB ₂) | <i>A. arachidicola</i> , <i>A. flavus</i> , <i>A. minisclerotigenes</i> , <i>A. nomius</i> , <i>A. parasiticus</i> |
| | Aflatoxin B _{2a} (AFB _{2a}) | <i>A. flavus</i> |
| | Aflatoxin M ₁ (AFM ₁) | <i>A. flavus</i> , <i>A. parasiticus</i> ; metabolite of aflatoxin B ₁ in humans and animals and comes from a mother's milk |
| | Aflatoxin M ₂ (AFM ₂) | Species not defined; metabolite of aflatoxin B ₂ in milk of cattle fed on contaminated foods |
| | Aflatoxin M _{2A} (AFM _{2A}) | Species not defined; metabolite of AFM ₂ |
| | Aflatoxicol (AFL) | <i>A. flavus</i> , metabolite of AFB ₁ |
| | Aflatoxicol M ₁ | Metabolite of AFM ₁ |
| Difurocoumaro-lactone series | Aflatoxin G ₁ (AFG ₁) | <i>A. arachidicola</i> , <i>A. flavus</i> , <i>A. minisclerotigenes</i> , <i>A. nomius</i> , <i>A. parasiticus</i> |
| | Aflatoxin G ₂ (AFG ₂) | <i>A. arachidicola</i> , <i>A. flavus</i> , <i>A. minisclerotigenes</i> , <i>A. nomius</i> , <i>A. parasiticus</i> |
| | Aflatoxin G _{2A} (AFG _{2A}) | Species not defined; metabolite of AFG ₂ |
| | Aflatoxin GM ₁ (AFG ₁) | <i>A. flavus</i> |
| | Aflatoxin GM ₂ (AFGM ₂) | Metabolite of AFG ₂ |
| | AFGM _{2A} | Metabolite of AFGM ₂ |
| | Aflatoxin B ₃ (AFB ₃) | Species not defined |
| | Parasiticol (P) | <i>A. flavus</i> |
| | Aflatrem | <i>A. flavus</i> , <i>A. minisclerotigenes</i> |
| | Aspertoxin | <i>A. flavus</i> |
| | Aflatoxin Q ₁ (AFQ ₁) | Major metabolite of AFB ₁ in in-vitro liver preparations of other higher vertebrates |

Table adapted from Bbosa et al. (2013) obtained from open access publisher, InTech.

Toxicity and mechanism of carcinogenicity

Fungi are important pathogens of plants, animals, and humans. There are relatively few pathogenic fungi associated with severe medical diseases as compared to pathogenic bacteria². The term 'mycotoxicoses' refers to a toxic response caused by dietary, respiratory, dermal, and other exposures to toxic fungal metabolites produced by filamentous fungi, including *Aspergillus*, *Penicillium*, and *Fusarium*^{17,18}. In contrast, mycoses refers to a response to the growth of the fungus itself². The degree of mycoses ranges from localized skin infections (such as athlete's foot) to more systemic infections of the pulmonary tract (such as invasive aspergillosis). Most mycoses are caused by opportunistic fungal pathogens that colonize an immune-compromised host.

Aflatoxins are immunosuppressive, mutagenic, teratogenic, and hepatocarcinogenic in experimental and domestic animals¹⁶. The disease symptoms caused by aflatoxin consumption are collectively known as 'aflatoxicoses' and the major site for aflatoxin toxicity is in the liver, hence the term 'hepatocarcinogen'. Similar to characteristics of other toxicological outcomes, factors that affect the magnitude of toxicity are related to dose, time of exposure, and nutritional status of patients¹¹. Acute toxicity is associated with a rapid onset and/or obvious toxic response which is characterized as the lack of appetite, loss of body weight, GI tract infections, necrosis of the liver, bile duct proliferation, acute hepatitis, and even death^{2,11}. Chronic, low dose exposure to aflatoxin has been associated with liver and lung cancer, and immune suppression^{2,11}.

What puts the 'toxin' in aflatoxin? Aflatoxin is metabolized in the liver by a group of cytochrome P450 enzymes. Liver cytochrome P450 enzymes convert aflatoxin into

an unstable reactive intermediate, aflatoxin-8,9-epoxide. The oxidation of double-bonds present in the chemical structure of the epoxide is thought to be responsible for the ability of aflatoxin to interact with cellular proteins and DNA. This short lived epoxide may act at the level of protein and/or DNA: binding of aflatoxin-8,9-epoxide to proteins in the liver causes aflatoxicosis (acute toxicity) whereas binding to DNA induces hepatocellular carcinoma (chronic toxicity). Aflatoxin B₁ may be the most toxic among the aflatoxins due to its flat conformation that allows close interaction with ring 7 nitrogen in guanine residues present in the DNA double helix. This enables the formation of aflatoxin-8,9-epoxide DNA adduct.

Global health and economic burden associated with aflatoxin

It is estimated that up to 4.5 billion people worldwide may be exposed to aflatoxin in their food or as part of the air they breathe¹⁹. This is because aflatoxin is a naturally occurring contaminant of food and its formation is unavoidable². Dietary exposure to aflatoxin is the primary route of exposure. Environmental exposure to aflatoxin has been strongly correlated to incidences of liver and lung cancer¹¹. For populations that have been predisposed to the hepatitis B virus, aflatoxin synergistically increases the risk of hepatocellular carcinoma (HCC) or liver cancer compared to either exposure alone²⁰.

According to the World Health Organization (WHO), HCC is the third leading cause of cancer deaths worldwide and its prevalence is 32 times higher in developing nations. Based on animal toxicological data, the International Agency for Research in Cancer (IARC) classifies mixtures of aflatoxin in foods as a Group 1 human carcinogen. This classification means that aflatoxin is a known human carcinogen characterized by

sufficient evidence of toxicity in experimental animals and strong epidemiological link between human aflatoxin exposure and HCC. Of the 600,000 new HCC cases worldwide each year, approximately 4-28% (up to 155,000) may be attributable to aflatoxin exposure²¹.

Dietary exposure to aflatoxin and hepatitis B virus (HBV) infection are the main risk factors of HCC. The risk of liver cancer in individuals exposed to chronic HBV infection and aflatoxin is up to 30 times greater than the risk in individuals exposed to one risk factor alone²¹. The synergistic effect of aflatoxin and HBV is particularly important in areas of increased HCC prevalence in Southeast Asia and sub-Saharan Africa²¹. Although much is known about the association of HBV and HCC, the underlying mechanisms contributing to the increased risk of HCC by the combination of HBV and foodborne aflatoxin are still unknown.

In developing countries in Asia and Africa, dietary exposure to aflatoxin has also been shown to be immunosuppressive and strongly associated with HIV/AIDS and malaria²². Immunotoxicity caused by aflatoxin could be one explanation of childhood malnutrition that leads to growth stunting in children of Asia and Africa. This is largely due to aflatoxin contamination of staple crops such as corn (maize) and peanuts (groundnuts) as well as food scarcity in the region. In addition, corn and peanuts are incorporated as a basic weaning food for children, thus placing children in these countries at a higher risk to aflatoxin exposure and its adverse effects.

Due to the health impacts of aflatoxin in humans and animals, the United States Food and Drug Administration (FDA) places action levels on the amount of aflatoxin allowed in human food and animal feed. The human food action level is set at 20 ppb

(0.5 ppb for milk) which is a level considered to be an acceptable risk of liver cancer. The action levels range in animal feed between 100-300 ppb for poultry, swine, and beef cattle and 20 ppb in dairy cattle. In the EU countries, action levels are more stringent and as low as 2 ppb is deemed unacceptable in human food¹¹.

The result of aflatoxin regulations (despite their focus on health) imposes significant barriers to trade. Using the trade of corn and groundnuts as example, these agricultural crops are highly susceptible to aflatoxin contamination with higher prevalence in Asia and Africa due to climate conditions and drought stress²³. Yet, these countries depend on the export of such crops to developed countries. The failure to comply to higher standards imposed by developed countries (example, the 20 ppb action level set by the FDA) causes significant difficulty in meeting requirements for food imports. On one hand, developed countries are protected from the adverse risk of aflatoxin but on the other hand 'contaminated crops' may be returned or redistributed to countries with lower or no aflatoxin safety standards.

In the United States and developed countries, chronic exposure to aflatoxin is less frequent as compared to developing nations^{19,21}. However, major losses in the USA attributed to aflatoxin contamination are estimated at about \$ 500 million on an annual basis largely due to screening, decontamination, and/or destruction of contaminated crops¹¹. Farmers bear a large proportion of this burden.

Khlangwiset and Wu described current strategies to control human exposure to aflatoxin as primary and secondary interventions²⁴. The aim of primary intervention is to decrease or eliminate aflatoxin levels in susceptible crops. These include agricultural interventions in the field (preharvest), during transportation, and in storage (post-

harvest). Drought stress and insect damage are factors contributing to the aflatoxin problem in the field. Insects serve as reservoirs and vehicles for fungal spores and insect damage predisposes corn to fungal infection. Genetically modified corn (BT corn) is less susceptible to insect damage thereby indirectly decreasing the ability of the fungus to infect corn kernels. Lower levels of aflatoxin have been reported in BT corn²⁵. Hence, strategies like genetically modified crops that are more drought tolerant and resistant to insect damage provide a promising approach for preharvest reduction of aflatoxin contamination.

Biocontrol methods have been employed in attempts to reduce aflatoxin levels in maize, groundnuts, and cottonseed. Biocontrol strategies involve competitive exclusion of toxigenic aflatoxin-producing strains using atoxigenic (non-aflatoxin producers) strains. More importantly, naturally occurring atoxigenic *A. flavus* strains have been found in regions of sub-Saharan Africa and may be effective in controlling aflatoxin in maize cultivars in the region^{26–28}. Such strategies appear to be economically feasible and sustainable.

Postharvest aflatoxin contamination is less common in developed countries but remains a threat in developing countries located in tropical regions. Effective prevention strategies dealing with proper drying, sanitation, storage, and pest management can be successful depending on efforts to educate farmers and crop growers through community education^{22,29}. Hand sorting aflatoxin-contaminated grain (physical separation) is still a common practice in less developed countries and has been shown to significantly decrease aflatoxin levels in postharvest maize³⁰. Although proven effective in reducing aflatoxin levels, such methods of sorting grains increases the risk

of environmental exposure (through air) to aflatoxin predominantly in women who usually are responsible to prepare grains to be sold.

Secondary interventions do not reduce human exposure to aflatoxin but they aim at decreasing the bioavailability and toxicity of aflatoxin through dietary and clinical interventions. High prevalence of dietary exposure to aflatoxin in Asia and Africa is due to food scarcity as well as dependence on dietary staples like maize and peanuts. Bandyopadhyay proposed a simple dietary intervention to shift from crops heavily contaminated with aflatoxin (maize, peanuts) to crops with lower aflatoxin levels (sorghum, beans)³¹. Since usage of these staples is intrinsically tied to traditions and crop feasibility is dependent on availability, community education could focus on helping farmers to diversify their crops.

Absorption of aflatoxin by incorporation of dietary absorbents such as clay (NovaSil®)²⁹, green tea polyphenols³², and chlorophyllin^{33,34} has been used as a successful intervention in Africa and China. NovaSil® (calcium montmorillonite) acts by binding aflatoxin with high affinity in the GI tract subsequently decreasing the bioavailability and downstream toxicity of aflatoxin. NovaSil® has also been used to prevent aflatoxicosis in animal studies. Clinical studies have shown that incorporation of green tea polyphenols and chlorophyllin in the human diet is anticarcinogenic; green tea was shown to affect aflatoxin metabolism where as chlorophyllin was shown to impede aflatoxin adsorption and aid with detoxification³²⁻³⁴.

The risk of liver cancer in individuals exposed to chronic HBV infection and aflatoxin is up to 30 times greater than the risk in individuals exposed to one risk factor alone. Thus, HBV vaccination prevents the synergistic impact of HBV and aflatoxin-

induced HCC by lowering HBV risk. Vaccinating children against HBV in populations where 65 million out of 350 million people are chronically infected by HBV could decrease aflatoxin-induced HCC.

Overall, there still exists a gap between scientific knowledge and economic feasibility. Khlangwiset and Wu performed a cost benefit analysis of agricultural interventions against dietary interventions to control aflatoxin exposure and found that efficacy tends to be higher for the former than the latter to reduce aflatoxin-related health risks²². In the end, the impact of such strategies should be targeted at the lifestyle and culture of the community; strategies should influence the daily life of a mother sorting through moldy grain deciding on whether to go hungry without food or to feed her children aflatoxin-contaminated grain.

Emerging risk of aflatoxin contamination due to global climate change

Aflatoxin production is exacerbated by environmental changes such as fluctuations in temperature and water activity in warm and humid climates. Plant stress and climate change are also contributing factors for aflatoxin contamination in tropical regions like Asia and Africa. Changes in the environment may increase aflatoxin contamination at both the pre- and post-harvest levels. Climate changes (such as global warming) alter the complex ecosystems that house aflatoxin-producing fungi. These changes affect the quantity of aflatoxin produced and perturb the fungal community structure. A study (both *in vitro* and in maize grain) conducted to assess the effect of temperature and water activity combinations showed that changing the temperature from 25°C to 30°C and water activity from 0.90 to 0.99 increased the amount of AFB₁

from 3 ng/g to approximately 3000 ng/g (a 1000-fold increase)³⁵. Fungal community structure is characterized by fungal-fungal interactions, fungal-plant interactions, and plant-insect interaction. Production of aflatoxin in the field is divided into two phases: (1) infection and toxin contamination of the developing crop and (2) infection of the crop after maturation followed by toxin contamination²³. Dry and hot climates favor the first phase whereas warm and wet climates favor the second phase.

Aflatoxin contamination is a major threat to human health and to the world's food supply. As global climate change continues to impact regions of Europe and North America, the potential impact of aflatoxin contamination may extend beyond regions with tropical climate currently affected by the aflatoxin problem. The ability to evaluate climate changes and correlate this factor to fungal infection and subsequent aflatoxin contamination will help in identifying, predicting, and dealing with this emerging risk. In support of this idea, aflatoxin was reported in Michigan field corn in the summer of 2012 during a period of record high temperatures and record low rainfall (Michigan Farm Bureau). Aflatoxin is not normally an issue in this northern tier state.

Proposed role of aflatoxin in fungal biology

In laboratory culture, fungal secondary metabolites are produced during a transition from active growth to stationary phase and their production does not affect growth. Hence, their function is not essential for growth (primary metabolism). Why are aflatoxins produced? There are two primary roles of aflatoxin in fungal biology: Secondary metabolites play different roles in (1) fungal fitness and development and (2) fungal defense and resistance (the 'chemical-shield' hypothesis).

To date, the role of aflatoxin (secondary metabolites) in fungal biology is based on correlative experiments from fungus-grazer interactions. The first genetic support for the shield hypothesis was conducted in the fungivorous springtail *Folsomia candida* (a soil arthropod that feeds on fungi)^{36,37}. *Folsomia candida* (springtail) exhibited a feeding preference on an *Aspergillus nidulans* strain that was lacking secondary metabolite production (this strain was a deletion mutant of an important secondary metabolite regulator, *laeA*) compared to the wild-type *A. nidulans* strain. The deletion of the *laeA* gene in *A. nidulans* reduced or eliminated a variety of secondary metabolites including sterigmatocystin (ST), a toxic intermediate of the aflatoxin biosynthetic pathway. These data strongly suggest that filamentous fungi in the soil environment have evolved secondary metabolism capabilities to defend their habitat and to inhibit growth of competitors such as springtails.

Aflatoxin biosynthesis: Our previous work

A hallmark of fungal secondary metabolism is the clustering of biosynthetic pathway genes. Examples of well-characterized secondary metabolite gene clusters include those involved in the biosynthesis of the β -lactam antibiotic penicillin and cephalosporin and pharmaceutical drugs such as compactin and lovastatin^{38,39}. Gene clusters for other secondary metabolites include mycotoxins like the trichothecenes and the polyketides aflatoxin and sterigmatocystin^{38,39}. These clusters can span more than 70,000 bases (aflatoxin biosynthesis) and comprise large portions of the chromosome. Most secondary metabolite gene clusters contain one or more key pathway genes encoding extremely large multidomain, multimodular enzymes that catalyze synthesis of

various intermediates in the pathway leading to the final product¹. The most common clusters in filamentous fungi are those dedicated to the synthesis of polyketides (PKSs) and non-ribosomal peptides (NRPs)⁴⁰. Many of these secondary metabolite clusters are physically located within sub-telomeric regions of the chromosome suggesting that secondary metabolism has evolved as a 'playground' for adaptive evolution. What is surprising, however, is that these clusters are highly conserved among members of the same species and remain relatively intact throughout evolution, which also suggests an adaptive advantage of maintaining such large gene clusters.

Bioinformatic analysis coupled with manual and experimental methods suggest that filamentous fungi in the genus *Aspergillus* have the genetic capacity to produce anywhere from 39 to 90 metabolites catalyzed by up to 250 enzymes encoded by their biosynthetic genes (**Figure 3**)⁶. The phenomenon of gene clustering in eukaryotes is thought to provide selective advantage in regards to regulation of gene expression. The close proximity of biosynthetic genes encoding intermediates in a pathway may enable fine-tuning of control by one or more regulatory elements.

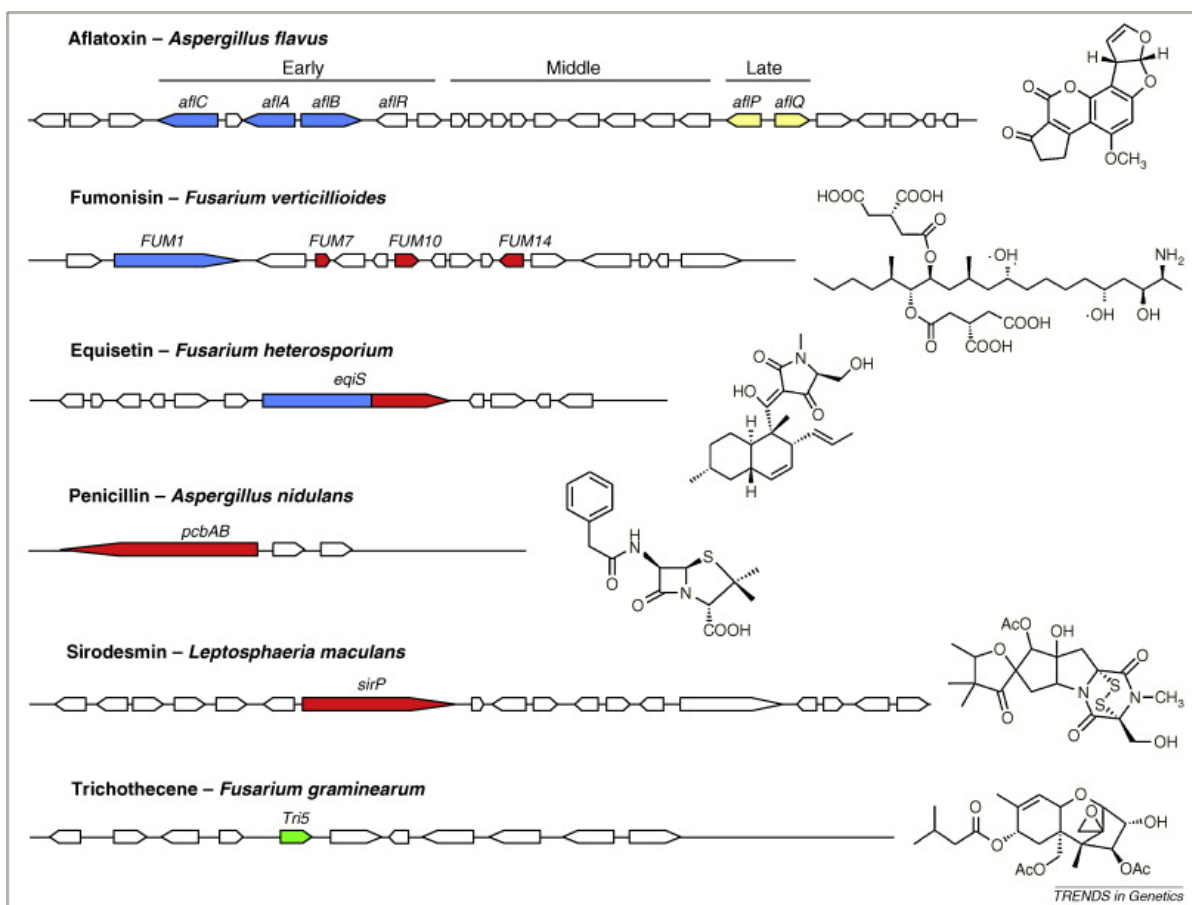


Figure 3 Fungal secondary metabolic gene clusters for polyketides, non-ribosomal peptides, and terpenes

Key enzymes present in specific pathways are designated as follows: PKS (aflatoxin cluster: *afiC*, *afiA*, *afiB* and fumonisin cluster: *FUM1*), NRPS (penicillin cluster: *pcbAB* and sirodesmin cluster: *sirP*), NRPS-PKS hybrid (equisetin cluster, *equS*), and terpene synthase (trichothecene cluster: *Tri5*). The three red genes in the fumonisin cluster (*FUM7*, *10* and *14*) encode separate domains of an NRPS-like multimodular enzyme. The two genes in the aflatoxin cluster that enable conversion of sterigmatocystin into aflatoxins (*afiP* and *afiQ*) are in yellow. Figure reprinted from Osbourn (2010) with permission from the publisher, Elsevier⁴¹.

Discovery of the key genes in the aflatoxin cluster

The aflatoxin and sterigmatocystin gene clusters (mycotoxin biosynthesis) are the most extensively studied fungal secondary metabolite gene clusters in *Aspergillus* spp. due to the detrimental health effects associated with these mycotoxins. Peng-Kuang Chang and Chris Skory from the Linz laboratory first cloned the *nor-1* (B-62 strain)⁴² and *ver-1* (CS-10 strain)⁴³ aflatoxin pathway genes in 1992. Subsequently, Chris Skory and Frances Trail characterized the genetic linkage and molecular functionality of Ver-1 and Nor-1 in aflatoxin biosynthesis^{44,45}. By 1995, a physical and transcript map of the aflatoxin genes cluster was generated and the gene cluster was characterized^{39,46}. By the early 2000s, the complete nucleotide sequence of the aflatoxin biosynthetic pathway including functions of structural genes was outlined^{17,47} in *A. flavus* (NCBI Accession # AY371490.1).

Aflatoxins are polyketide-derived furanocoumarins produced through a series of conversion steps that include acetate → polyketide → anthraquinones → anthones → aflatoxin. The initial building block of aflatoxin is acetate. In the early stages of aflatoxin synthesis, a specialized two-subunit fatty acid synthetase (hexanoate synthetase, comprised of Fas-1 and Fas-2) catalyzes condensation of one molecule of acetyl CoA and two molecules of malonyl CoA to form hexanoyl-CoA¹⁸. A polyketide synthase (PksA) extends this 6-carbon molecule to form the 20-carbon decaaketide, norsolorinic acid (NA), the first stable polyketide pathway intermediate. NA is converted via a series of enzymes to versicolorin A (VA), the first toxic pathway intermediate. VA is the first pathway intermediate to contain a bisfuran ring structure with a double bond.

A. parasiticus is known to produce four kinds of aflatoxins (AFB₁, AFB₂, AFG₁, AFG₂) whereas *A. flavus* produces predominantly AFB₁ and AFB₂^{6,18}. *A. nidulans* another closely related species, contains a similar gene cluster to both *A. parasiticus* and *A. flavus*. One notable difference in *A. nidulans* is its ability to synthesize sterigmatocystin, the next to last aflatoxin pathway intermediate. A comprehensive understanding of the *A. nidulans* sexual cycle makes *A. nidulans* a useful genetic tool to study the biosynthesis of aflatoxin. Aflatoxin biosynthesis is catalyzed by 25 or more enzymes encoded by up to 30 genes clustered at the sub-telomeric region of chromosome 3 in *A. flavus* and *A. parasiticus*^{48,49}. The genes for this biosynthetic pathway are well conserved between aspergilli and are located within a large 75 kb region in the genome (**Figure 4**). Adjacent to the aflatoxin cluster is a four-gene sugar utilization cluster (*nadA*, *hxtA*, *glcA*, and *sugR*), which may function to regulate nutrient signals that play a critical role in aflatoxin biosynthesis (see Section 4 on page **29**).

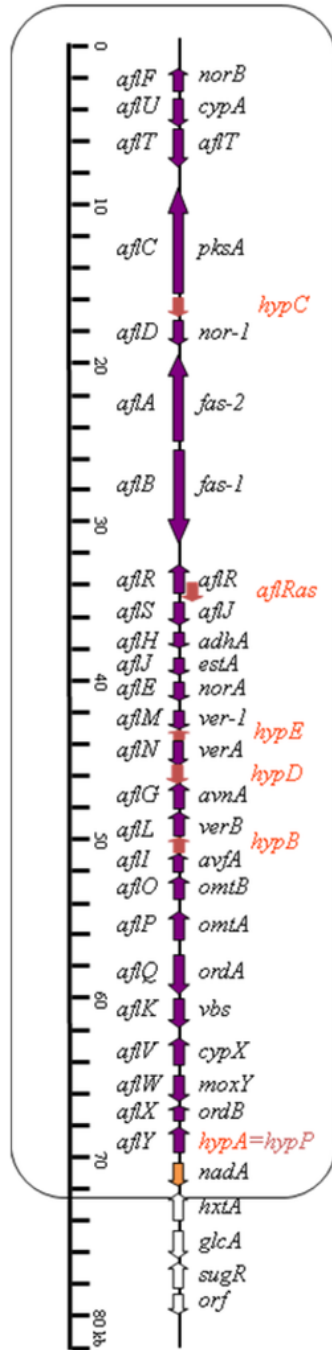


Figure 4 The aflatoxin gene cluster in *A. parasiticus*

The old gene names are labeled to the left of the vertical line and the new gene names are labeled to the right¹⁷. Arrowheads along the vertical line represent direction of transcription. The ruler at the far left indicates the relative sizes of these genes in kilobases. Reproduced with permission from MDPI open access publisher⁵⁰.

Regulatory elements in aflatoxin gene expression

As mentioned earlier, one of the functional advantages of gene clustering in secondary metabolism is the close proximity for regulation by one or more cluster-specific transcription factors. Correct positioning of regulatory transcription factors within the gene cluster enables fine-tuning of the transcriptional regulation of secondary metabolite genes. One such transcription factor is a Gal4-type zinc binuclear cluster protein called AflR. AflR is required for expression of most genes involved in aflatoxin/sterigmatocystin biosynthesis⁵¹. AflR was identified as a key positive regulator in 1993⁵². Gene knockout of AflR completely down-regulated expression of most genes in the biosynthetic pathway and subsequently eliminated aflatoxin or sterigmatocystin production under the conditions studied. It is also important to note that within promoter regions of aflatoxin pathway genes there is a conserved 11 bp palindromic sequence 5'-TCG(N5)CGA-3' present that is critical for gene activation by AflR.

Protein coding regions of closely related species like *Aspergillus flavus* and *A. parasiticus* exhibit >90% sequence similarity as compared to approximately 46% similarity in their intergenic regions, suggesting species-specific differences in regulation at the level of the promoter region by the transcriptional machinery⁵³. Our studies focused on identifying cis-regulatory signatures within aflatoxin promoter regions as well as novel binding proteins important for regulation and functionality of such promoter domains. Early work in the Linz laboratory focused on the *nor-1* promoter region; *nor-1* encodes an early aflatoxin pathway enzyme. Miller showed that AflR, novel DNA binding proteins (NorLbp and CRE1bp), a TATA binding protein, and specific *cis*-acting binding sites are required for maximal *nor-1* transcriptional activation⁵⁴.

Roze et al. 2004 showed that a 32-kDa protein co-immunoprecipitates with AtfB (using anti-AflR antibodies) and specifically binds to norR⁵⁵. The authors hypothesized that p32 (protein with molecular mass size of 32-kDa) assists AflR in binding to the *nor-1* promoter. p32 was later identified as AtfB (based on 96% identity to *A. oryzae* AtfB protein) a member of the bZIP/CREB family and a stress-related transcription factor⁵³. Chromatin immunoprecipitation (ChIP) studies using antibodies specific to AtfB demonstrated that AtfB (p32) binds to seven promoters in the aflatoxin cluster that contain CRE sites and does not bind to promoters lacking CRE sites. Interestingly, composite and bioinformatics analysis supported the presence of a novel motif (which includes the CRE motif) present 11 times in promoters of aflatoxin genes. For the first time, our studies provided a functional role for the stress-related transcription factor, AtfB in aflatoxin biosynthesis. The data prompted us to propose that AtfB integrates secondary metabolism and the cellular response to oxidative stress.

Aflatoxin and oxidative stress

Several lines of research evidence suggest that aflatoxin is produced by the fungus as a mechanism to cope with stress. In other words, aflatoxin synthesis allows the fungus to tolerate stress. In support of the genetic, molecular, and biochemical observations that demonstrate an association between oxidative stress and aflatoxin synthesis, factors that impact redox balance also modulate aflatoxin levels. Antioxidants can be used to block aflatoxin synthesis; and pro-oxidants increase aflatoxin synthesis. Compounds that stimulate or inhibit aflatoxin biosynthesis will be covered in more detail in Section 7 (page 41). Although the association has been long

established, the functional and molecular significance of this association remains unclear.

In support of the ChIP studies conducted using anti-AtfB⁵³ (mentioned at the end of the previous section), Hong et al. 2014 expanded the analysis to show AtfB binding to promoters of antioxidant and stress response genes using EMSA⁵⁶. In addition to *nor-1*, Hong showed that AtfB is a master co-regulator that binds to early (*fas-1*), middle (*ver-1*), and late (*omtA*) pathway genes as well as stress response genes (mycelial-specific catalase, *cat1* and mitochondrial-enzyme *Mn sod*). Binding of AtfB to these promoters was dependent on the presence of a cAMP response element motif (CRE). This work suggests that AtfB together with other canonical oxidative stress transcription factors (SrrA, MsnA, and AP-1) induce aflatoxin biosynthesis as part of the cellular response to oxidative stress.

These studies were motivated by the initial work conducted by Subramanyam and co-workers^{57,58}, Sakamoto^{59,60}, and Reverberi⁶¹ between 2000 to 2009. Briefly, Jayashree and Subramanyam showed that toxigenic strains of *A. parasiticus* accumulate far greater amounts of metabolites and significantly higher activities of enzymes that are indicative of enhanced oxidative stress in comparison to the non-toxigenic strains⁵⁷. They were the first to provide a biochemical link between oxidative stress and aflatoxin biosynthesis. Using well-thought out studies with genetic mutants in the aflatoxin biosynthetic pathway that accumulated different intermediates in the pathway, Narasaiah and Subramanyam showed that these mutants accumulate different levels of reactive oxygen species (ROS) under aflatoxin inducing conditions⁵⁸. Highest ROS levels were observed in the toxigenic strain and lowest ROS levels were

observed in the non-toxigenic strains. ROS levels correlated with metabolites and enzymes indicative of oxidative stress.

Sakamoto and his group compared two related transcription factors, AtfA and AtfB in a food safe and industrially important fungus, *Aspergillus oryzae*. Using genetic knockouts of *atfA* and *atfB*, Sakamoto showed that $\Delta atfA$ and $\Delta atfB$ conidia exhibited increased sensitivity to heat shock and oxidative stress treatment^{59,60}. Expression analysis on mutant strains showed down-regulation of candidate genes in stress response pathways such as catalase and trehalose-6-phosphate synthase.

Reverberi and co-workers studied the role of a stress-related transcription factor, AP-1 and showed that *A. parasiticus* Apyap1 is important for the timing of ROS accumulation, the timing of conidiospore development, and the level of stress tolerance in conidiospores⁶¹. Apyap1 did not stimulate aflatoxin biosynthesis but aflatoxin production was detected at an earlier time point under standard conditions. Putative AP-1 binding sites were identified in promoter regions of aflatoxin genes suggesting a direct functional role for AP-1 in regulation of aflatoxin biosynthesis.

In a previous study, we concluded our discussion by proposing that AtfB is a major node in the regulatory circuit that integrates secondary metabolism and the cellular response to oxidative stress⁵³. As mentioned briefly in the chapter summaries (page Error! Bookmark not defined.), **my research** was aimed at investigating the direct role of AtfB in aflatoxin biosynthesis. The hypothesis tested in this study is that the **loss of AtfB function in *A. parasiticus* would impact aflatoxin gene regulatory networks and down-regulate aflatoxin biosynthesis**. Beyond this direct role, I also hypothesized that AtfB plays a **central regulatory role** to modulate gene targets

beyond the aflatoxin gene cluster. Finally, I propose a new perspective to rethink the potential role of secondary metabolism in fungal survival. I collectively define secondary metabolism (SM), stress response (SR), and conidiospore development (CD) as **virulence-associated cellular processes** in *A. parasiticus*. Subsequently, specific gene targets within this network are termed **sentinel genes that mediate virulence**; tracking their expression enables one to monitor function of the AtfB regulatory network. This work is presented in Chapter 2 (page **45**) where I describe in greater detail how “The fungal transcription factor AtfB controls virulence-associated processes in *Aspergillus parasiticus*”.

Studies on signal transduction pathways that mediate aflatoxin gene expression

An inherent ability of cells is the capacity to sense and respond to changes in environmental signals, such as light, nutrients, hormones, pH, and stress signals. Carbon, nitrogen, trace elements, pH, and temperature are shown to impact aflatoxin gene expression (Miller 2006, dissertation). These studies provided the rationale for our research on upstream signaling mechanisms in *A. parasiticus*. G protein-mediated signaling has been intensively studied in various filamentous fungal species. Signaling pathways provide important clues to dissect secondary metabolite biosynthesis, whose regulation is closely associated with fungal development (see page **33**).

A. parasiticus produces aflatoxin in the presence of sucrose (yeast extract sucrose, YES medium) but not in the presence of peptone (yeast extract peptone, YEP medium)^{55,62}. *A. parasiticus* begins aflatoxin production at approximately 24 h under standard aflatoxin inducing conditions (100 mL YES liquid medium, shake culture, 30°C,

in the dark) and production increases exponentially until 48 h. Aflatoxin synthesis begins to slow down after 48 h⁶³. Aflatoxin transcripts and proteins are detected between 24 h and 40 h in support of aflatoxin production in the medium⁶⁴. Our lab seeks to understand and characterize the molecular switch that triggers production of aflatoxin. Part of this molecular switch is the transition from high to low sucrose/glucose levels (transition from primary to secondary metabolism), which the cell senses and responds by activating a signal transduction cascade.

The first link between a signaling cascade and secondary metabolite production was proposed in *A. nidulans* where it was shown that FadA, an α -subunit of a heterotrimeric G protein, binds GTP which results in inhibition of sterigmatocystin production⁶⁵. Further expansion of this pathway to include cAMP levels and PKA was elucidated in *A. nidulans* and *A. parasiticus* and this signaling pathway was shown to regulate aflatoxin biosynthesis and conidiation^{66,67}. The Linz laboratory demonstrated that a FadA-mediated mechanism similar to the one in *A. nidulans* controls cAMP levels in a PKA-dependent regulatory network that affects conidiation and aflatoxin biosynthesis in *A. parasiticus*⁶⁶.

The Linz laboratory also discovered an association between the initiation and spread of histone H4 acetylation in aflatoxin promoters that correlated with the onset of accumulation of aflatoxin proteins and aflatoxin in the growth medium⁶⁴. We proposed that a specific stress signal (such as decrease in sucrose/glucose levels) is sensed by a G-protein coupled receptor (like FadA) and this triggers the activity of a cAMP/PKA signaling cascade⁶⁶, down regulation of PKA activity, and activation of transcription factors such as AtfB (CRE1bp) binding to the *pkxA/nor-1* promoter. AtfB binding to

promoters recruits histone acetyltransferase (HAT) to initiate a wave of histone H4 acetylation and unwinding of the chromatin (conversion of heterochromatin to euchromatin). The bidirectional wave of histone unwinding exposes promoters for binding of pathway specific regulators like AfIR. This entire process is reinforced by the presence of additional CRE sites and by further recruitment of AtfB/AfIR/HAT complexes to these sites⁶⁴ (see proposed model in **Figure 5**).

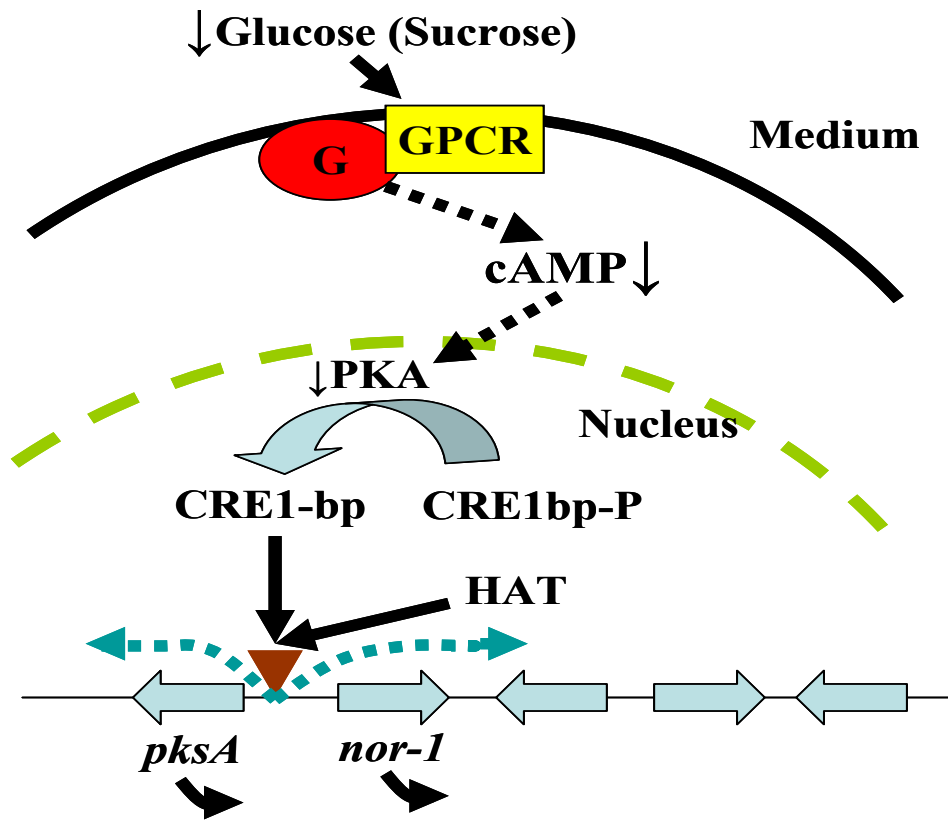


Figure 5 Proposed model (2007) for aflatoxin biosynthesis in *A. parasiticus* during the transition from exponential growth to the stationary phase

This model shows how a decrease in glucose/sucrose triggers the G-protein-coupled receptor (GPCR) to decrease levels of cAMP and dephosphorylate CRE1-bp (now known as AtfB). Dephosphorylation of CRE1-bp/AtfB then binds to the nor-1/pksA region and activates transcription by recruiting histone acetyltransferase (HAT)⁶⁴.

Association between secondary metabolism and development

Secondary metabolism is closely linked to fungal development (reviewed by Calvo and others^{68,69}). Our lab found that mutants which accumulate intermediates between norsolorinic acid and versicolorin A have reduced sclerotial (asexual survival structure) development^{39,43}. On the other hand, when the early pathway genes *fas1A* (encodes a fatty acid synthase) or *pksA* (encodes a polyketide synthase) were disrupted, mutants showed increased production of sclerotia⁷⁰. Our lab also studied another gene encoding a polyketide synthase (*fluP*) and found that disruption mutants of *fluP* exhibited reduced sclerotial development⁷¹.

Joan Bennett conducted the earliest study demonstrating a close relationship between aflatoxin production and fungal development in 1978. She observed “fan” and “fluff” phenotypes that correlated with a decrease in aflatoxin production⁷². Various conidiation mutants showed a reduction in aflatoxin production in a later study⁷³. Hicks et al. identified a genetic mechanism that involved a G-protein/cAMP/PKA-dependent pathway that linked sterigmatocystin and aflatoxin production to fungal development. When the G-protein/cAMP/PKA pathway is upregulated, the alpha subunit FadA is activated and bound to GTP, conidiation and sporulation is repressed and ST/AF production is down-regulated⁶⁵.

VeA, a global regulator of secondary metabolism that participates in a multiprotein complex mediates light-dependent developmental regulation in *A. nidulans*⁷⁴. VeA gene disruption in *A. parasiticus* resulted in elimination of sclerotial formation and blockage of the production of aflatoxin intermediates⁷⁵. Taken together, these data strongly support a close regulatory link between fungal development and

secondary metabolism in *Aspergillus* spp. However, the functional significance of this link remains to be understood.

Studies on subcellular localization of aflatoxin enzymes and aflatoxin

Now that we have some understanding of the molecular mechanisms (genes and enzymes involved, regulatory elements, signal transduction pathways) that mediate aflatoxin biosynthesis, it is necessary to understand other steps that are required complete aflatoxin biosynthesis: these steps include aflatoxin enzyme compartmentalization, localization within the cell, and export. From an application standpoint, a holistic approach to understanding aflatoxin biosynthesis at the molecular and cellular level is critical to design effective strategies to block aflatoxin production (our long term goal). This section will include a summary of our previous subcellular localization studies of aflatoxin proteins in *A. parasiticus*, a parallel study conducted by the Kistler laboratory on *Fusarium graminearum*⁷⁶, and how my research was aimed at contributing to the expansion of this idea.

There are two major categories of fungal secondary metabolites occurring in nature grouped by their chemical backbone⁴⁰ and starter units⁷⁷ (examples of secondary metabolites derived from each category are highlighted in **Figure 6**); (1) polyketides (fatty acid derivatives from acyl-CoA) and (2) non-ribosomal peptides (amino acid-derived compounds). The first group includes aflatoxin/sterigmatocystin, trichothecene, gibberellin A3, paxilline, aromatic polyketides, lovastatin/compactin and related compounds such as oxylipins and spore/ hyphal pigments. The second group includes penicillin, fumiquinazoline, siderophores, AK-toxins, ergot alkaloids,

cephalosporin, cyclosporine, and catorenoids. Examples of other fungal metabolite categories are the terpenes, siderophores, and cyclic peptides. Unlike plants, little is known about sub-cellular organization of fungal secondary metabolites.

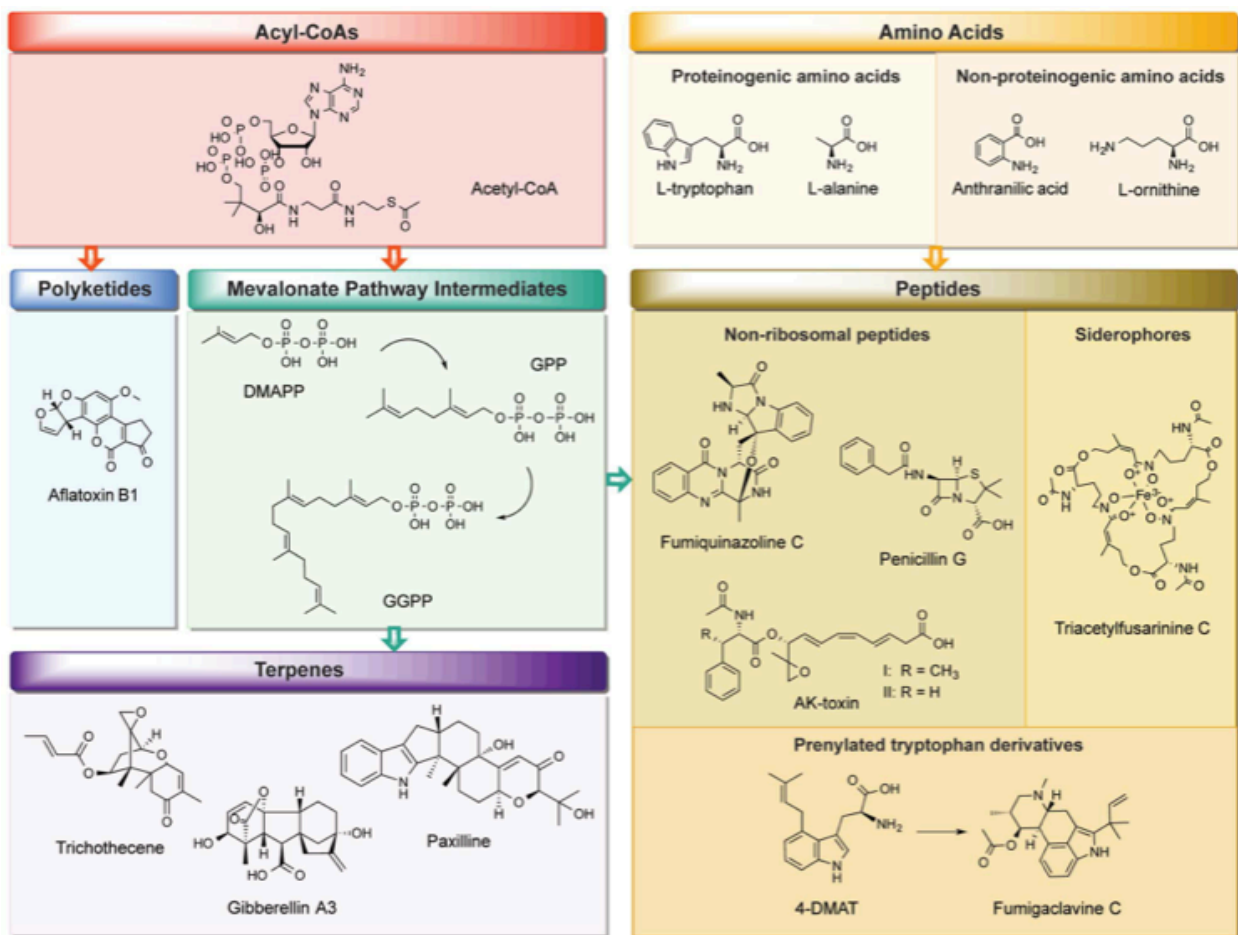


Figure 6 Two major categories of fungal secondary metabolites grouped by their chemical backbone and starter units

Examples of secondary metabolites derived from polyketides and peptides demonstrate structures of increasing complexity. Abbreviations: DMAPP (dimethylallyl diphosphate); GPP (geranyl diphosphate); GGPP (geranylgeranyl diphosphate); DMAT (dimethylallyl tryptophan). Figure reprinted from Lim and Keller (2014) with permission from the publisher, the Royal Society of Chemistry⁷⁷.

As early as 1977, Lawellin et al. used antibodies against aflatoxin as part of an immunohistochemical approach to visualize aflatoxin granules deposited within 72 h old mycelia; these granules were described as dark brown 'spots' around the hyphae⁷⁸. Subcellular localization of enzymes involved in aflatoxin biosynthesis has been studied extensively in our laboratory. Early work utilized a novel "concentric circle colony fractionation" procedure developed to determine the sub-cellular location of four aflatoxin enzymes in specific fractions of *A. parasiticus* grown on solid aflatoxin inducing media⁷⁹. Specific fractions corresponded roughly to 24 h periods of growth on solid media. Immunofluorescence microscopy using specific rabbit polyclonal antibodies developed in our laboratory against an early pathway enzyme Nor-1 (Zhou 1997, dissertation), the middle pathway enzymes Ver-1⁶³ and Vbs (Chiou 2003, dissertation), and a late pathway enzyme OmtA (Lee 2003, dissertation) suggested that these enzymes accumulated in different subcellular compartments in a time dependent manner. Between 24 h to 36 h of growth, Nor-1, Ver-1, Vbs, and OmtA localize in the cytoplasm. Later in growth (48 h to 72 h), these enzymes were found in vesicles and vacuoles^{79,80}. These studies provided the first evidence that early, middle, and late aflatoxin enzymes Nor-1, Ver-1, and OmtA are synthesized on free ribosomes in the cytoplasm but then these enzymes are transported to subcellular organelles.

In 2008, Sung-Yong Hong from the Linz laboratory developed an enhanced green fluorescence protein (EGFP) reporter system in which expression of Nor-1 and Ver-1 can be monitored in real time^{81,82}. Nor-1 and Ver-1 was fused to an EGFP reporter and expression of these fusion proteins was under the control of their respective wild-type promoters. Confocal laser scanning microscopy (CLSM)

demonstrated that both Nor-1 and Ver-1 were synthesized in the cytoplasm between 24 h to 48 h, and then localized in vesicles and vacuoles by 48 h to 72 h.

Based on the data obtained, two pathways were proposed for the fate of aflatoxin enzymes. Once the aflatoxin genes are activated and aflatoxin proteins are made, they are transported to the vacuole for protein turnover/degradation (via CVT pathway) or they fuse to the cytoplasmic membrane for export (secretory pathway). In 2009, Chanda et al. 2007 developed a novel technique unique to our laboratory, to isolate and purify a vesicle/vacuole fraction from *A. parasiticus* liquid cultures⁸³. Using genetic and biochemical studies, Chanda showed that aflatoxin enzymes are housed in subcellular compartments called aflatoxisomes⁶². These toxosomes complete the aflatoxin biosynthetic pathway. He targeted a small GTPase protein, AvaA (previously identified in *A. nidulans*⁸⁴) that functions in the fusion of late endosomes to the vacuole in yeast. Genetic knockout of *avaA* caused disruption strains to accumulate increased levels of aflatoxin proteins as detected by Western blot analysis and increased production of aflatoxin. This observation was proposed to be associated with the down-regulation of the endosome-to-vacuole pathway and activation of the secretory pathway, thus increasing export of aflatoxin. To further strengthen this model, Chanda et al. 2009 used Sortin3 (a biochemical inhibitor known to block a class C tethering complex protein, Vps16). Chanda observed a similar phenotype of Sortin3-treated cells to *avaA* mutants. The genetic knockout of AvaA and Sortin 3 treatment supports our hypothesis that the down-regulation of the vacuole targeting pathway and subsequent activation of the export pathway increases aflatoxin export.

Chanda et al. 2009 demonstrated a role for late endosomes in the compartmentalization and export of aflatoxin by blocking the function of AvaA (GTPase associated with late endosome) and use of Sortin 3 (inhibitor of Vps16 protein which is part of the early and late endosome tethering complex, CORVET and HOPS respectively). **My research** was aimed at investigating the role of early endosomes (particularly a class III PI3K Vps34 associated with early endosomes) in aflatoxin export. We hypothesize that **disruption of Vps34 function will increase aflatoxin export** by activation of the export pathway and down-regulation of the cytoplasm-to-vacuole (CVT) targeting pathway. This observation will strengthen the previous model proposed by Chanda⁶². Second, we hypothesize that a **co-transformation system** (similar to that used to down-regulate AtfB function) **will block Vps34 function** in Vps34 knockdown mutants. Finally, I propose that the cellular process of compartmentalization and export of secondary metabolites contributes to **fungal virulence and can be considered as a part of a virulence-associated process** in *A. parasiticus*. This work is presented in Chapter 3 (see page **82**) where I describe in greater detail “Utilizing a CRISPR/cas9-like system to elucidate the role of Vps34 in aflatoxin synthesis”. To our knowledge, we are the first to demonstrate and describe hallmarks of an endogenous CRISPR/cas9-like system in filamentous fungi. Also novel to the Linz laboratory is the role of an early endosome-associated lipid kinase, Vps34 in synthesis, storage, and export of aflatoxin, a polyketide secondary metabolite.

Collectively, studies conducted in the Linz laboratory on the sequential compartmentalization of aflatoxin in *A. parasiticus* were the first studies to link synthesis of aflatoxin to endosome biogenesis. Recently, Menke et al. (2013) observed a similar

phenomenon of subcellular localization and export of trichothecene (DON) biosynthesis⁸⁵. The Kistler laboratory found that two cytochrome P-450 oxygenases involved in early and late steps of trichothecene synthesis co-localize to vesicles called “toxisomes”. Tri4p and Tri1p were fluorescence-tagged and shown to display dynamic “shuttling” with motile vesicles containing a major transporter Tri12p involved in DON export and tolerance in *Fusarium graminearum*. Parallel to the synthesis and export of aflatoxin in *A. parasiticus*, Menke and co-workers suggested that toxin synthesis occurs within subcellular compartments called toxisomes within *F. graminearum*. Findings from the Kistler lab and others provide a very important feature of this cellular process; both *A. parasiticus* and *F. graminearum* have evolved similar mechanisms for toxin synthesis and export that appear to be uniquely adapted to suit their lifestyle and environment.

Manual and bioinformatics analyses of PKS and NRP secondary metabolite gene clusters estimate that 60% of secondary metabolite gene clusters in *A. parasiticus* are dedicated to the synthesis of PKSs and NRPs. What this could imply is that evolutionary forces have shaped the timing and level of fungal metabolite output by directing subcellular localization of secondary metabolite enzymes. It is also reasonable to postulate that virulence-associated processes described above (SR, SM, CD) co-evolved with the ability to compartmentalize and export secondary metabolites possibly as a defense mechanism (intracellular) and/or as a means to establish infection of hosts and plants (extracellular).

Studies on compounds that potentiate/modulate aflatoxin synthesis

Our laboratory has focused extensive research effort on identifying and characterizing compounds (natural products from plants, lichens, and fungi) that inhibit aflatoxin biosynthesis. As mentioned earlier, aflatoxins have gained much attention due to their toxicity and global burden. The long-term goal of elucidating the specific cellular mechanism of aflatoxin biosynthesis is crucial to carefully select practical and effective ways to block/eliminate aflatoxin contamination in food and animal feed. Research efforts in the Linz laboratory have targeted different cellular levels (**Figure 7**).

The exposome is comprised of specific stress signals such as light, oxidative stress, pH levels, water activity, and nutrient limitation. The exposome of the filamentous fungus, *A. parasiticus* can be defined as an aggregate measure of all the exposures from the environment. Cross talk between the exposome and signal transduction pathways activates specific components in the signalosome such as the FadA/cAMP/PKA signaling cascade. Signal transduction pathways activate transcription factors in the nucleus like AflR and AtfB. Recruitment of AflR and AtfB to promoters within the aflatoxin gene cluster triggers expression of aflatoxin structural genes. Once aflatoxin proteins are made, they are housed in subcellular compartments called toxisomes. These endosomes complete aflatoxin biosynthesis, and they can either fuse to the vacuole for protein turnover/degradation or they can fuse to the cytoplasmic membrane for export. Ultimately, these concurrent, sequential, and partially overlapping cellular processes are what determine the timing and level of aflatoxin production and export out of the cell. The ability to effectively and persistently target one or more of

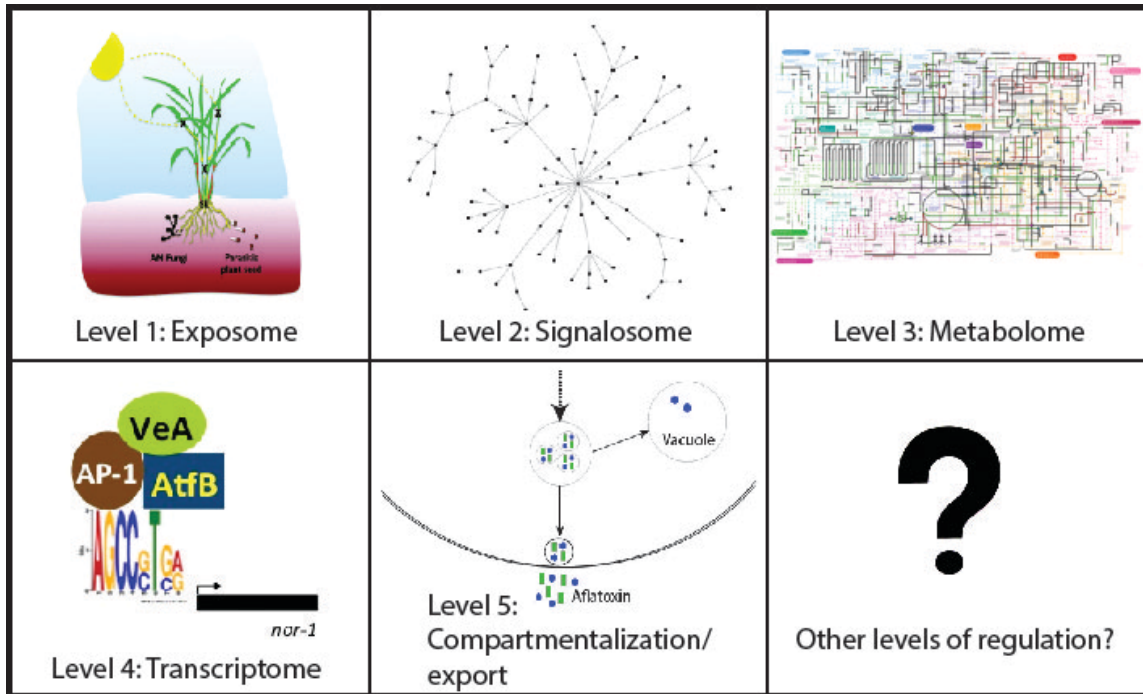


Figure 7 Effective ways to block aflatoxin biosynthesis at the cellular level

these levels will successfully block toxin production in *A. parasiticus*. The ability to block regulation at some of these levels is more practical to achieve in the field and in storage. I will highlight some previous work conducted in the Linz laboratory, provide some supporting evidence from others, and suggest that studying biochemical compounds that stimulate toxin synthesis is equally valuable to studying inhibitors of toxin synthesis. My contribution to the lab's long-term goal of studying inhibitors to block toxin synthesis is highlighted in Appendix II (see page **162**). For the purpose of this dissertation, we will define an inhibitor as a compound that inhibits aflatoxin biosynthesis under aflatoxin inducing conditions and focus on compounds that are specific inhibitors of aflatoxin biosynthesis and not compounds that alter fungal growth (anti-fungal properties).

Initial work in our laboratory was focused on identification of compounds that inhibit aflatoxin synthesis as illustrated by the inhibitory effects of food safe gases including ethylene and carbon dioxide^{86,87}. Biochemicals like crotyl alcohol and wortmannin⁸⁸ serve as useful tools to understand the molecular mechanisms by which aflatoxin biosynthesis is affected and aid in selection of specific cellular targets that block its synthesis. Extensive work has been done to further understand the mechanism and effect of natural plant volatiles and their activity on aflatoxin biosynthesis. Our laboratory's contribution in this area includes analysis of the inhibitory effects of ethylene and carbon dioxide (as mentioned above) as well as willow bark volatiles⁸⁹, black walnut tree volatiles, and lichen volatiles (Roze, unpublished). A concise review on various inhibitors of aflatoxin biosynthesis was published⁹⁰ in 2008.

It is important to note that one main challenge in identifying and utilizing effective inhibitors of aflatoxin production in field and in storage is strongly associated with the fact that humans and the host plants that support mycotoxin synthesis are eukaryotic organisms. Any inhibitor that non-specifically targets fungal growth (fungi are also eukaryotes) likely will have significant side effects in humans. Thus, development of unique fungal-specific strategies (like targeting AtfB) could potentially provide an effective treatment option. Current methods using inhibitors that lack specificity, have limited efficacy, and are not practical in developing countries in Asia and Africa where the mycotoxin problem remains significant and longstanding. So, the use of volatiles derived from locally grown plants may provide a lucrative and sustainable avenue for local farmers to control mycotoxin contamination in food and feed crops.

CHAPTER 2: THE FUNGAL TRANSCRIPTION FACTOR ATFB CONTROLS VIRULENCE-ASSOCIATED PROCESSES IN *ASPERGILLUS PARASITICUS*

This chapter is under review: **Wee J**, Hong SY, Roze LV, Day DM, Chanda A, Linz JE; submitted to Molecular Microbiology.

ABSTRACT

The bZIP transcription factor AtfB is unique to aspergilli and regulates several genes involved in conidiospore development, stress response, and secondary metabolism in *Aspergillus parasiticus*. These three functional networks represent important virulence-associated cellular processes in aspergilli. Here we conducted a gene disruption of *atfB* in *A. parasiticus*, a well-characterized fungal pathogen of plants, animals, and humans that produces the secondary metabolite and carcinogen aflatoxin to determine the mechanisms by which AtfB contributes to virulence. We exploited a novel co-transformation system to down-regulate the AtfB regulatory network and the 3 virulence-associated processes. We show that up-regulation of expression of the *atfB* disruption transcript associates with a decrease in AtfB protein levels, a decrease in three aflatoxin enzymes and aflatoxin accumulation, and a decrease in conidiospore development. Finally, we show that the fungal AtfB regulatory network extends beyond the 3 virulence-associated processes to novel targets in cellular defense as well as to actin and cytoskeleton arrangement/transport. These data suggest that exploiting the fungal-specific target AtfB will enable us to successfully control synthesis of fungal secondary metabolites with positive (pharmaceutical drugs) or negative (mycotoxins) impacts on human health. Future work will focus on using this novel endogenous system to further

study the function of newly identified AtfB targets and how they impact virulence of *A. parasiticus*.

INTRODUCTION

Activation of transcription factors plays a critical role in regulating expression of gene clusters involved in secondary metabolism in filamentous fungi^{37,91–94}. Fungal genomes can carry up to 250 secondary metabolite genes and 70 or more secondary metabolite gene clusters. To control this complex genetic organization, filamentous fungi including *Aspergillus* spp. have developed complex and hardwired cluster-specific transcriptional machinery^{1,95–97}. Protein coding regions of closely related species like *Aspergillus flavus* and *A. parasiticus* exhibit >90% sequence similarity as compared to approximately 46% similarity in their intergenic regions, suggesting species-specific differences in regulation at the level of the promoter region by the transcriptional machinery⁵³.

One group of cluster-specific transcription factors is collectively known as the basic leucine zipper (bZIP) transcription factor family. bZIPs in aspergilla including AP-1, AtfA, AtfB, and RsmA coordinate and integrate multiple functional networks including secondary metabolism, oxidative stress response, fungal development and cellular defense mechanisms^{37,53,56,59–61}. For example, the oxidative stress-related transcription factor, AP-1 was demonstrated to regulate the timing and level of conidiospore formation and aflatoxin biosynthesis as well as susceptibility to oxidative stress in *A. parasiticus*⁶¹. Fungal specific bZIPs belonging to the ATF/CREB family such as AtfA and AtfB were first characterized relative to their roles in stress tolerance of *Aspergillus oryzae* conidiospores^{59,60}. An *A. nidulans* putative YAP-like bZIP protein, RsmA was

demonstrated to be involved in fungal defense against fungivorous insects^{37,98}. Although numerous studies established the association between fungal bZIPs and secondary metabolism (SM), stress response (SR), and conidiospore development (CD), details of this association at the molecular level were largely unknown. Collectively, we refer to SM, SR, and CD as important fungal virulence-associated cellular processes.

At the molecular level, fungal-specific bZIPs like AtfB regulate a specific subset of promoters that are co-regulated as part of SM. In *A. parasiticus*, AtfB physically interacts with a positive pathway regulator, AflR, which likely up-regulates *nor-1* (an early pathway gene)^{54,55}. Under aflatoxin inducing conditions, AtfB binds to promoters of seven aflatoxin genes (including *nor-1*) harboring cyclic-AMP response elements (CRE) and does not bind to promoters that do not contain CRE sites. Under aflatoxin non-inducing conditions, this binding effect is almost abolished⁵³. Although evidence supports AtfB binding to promoters in the aflatoxin gene cluster, details of how AtfB regulates gene expression remained unclear. The goal of the current study was to characterize the role of AtfB in regulation of virulence-associated genes at the level of transcriptional activation. We collectively define genes associated with SM, SR, and CD as “sentinel” genes because we can use their expression to monitor AtfB function.

In previous work, we proposed that AtfB is a major node in the regulatory circuit that integrates secondary metabolism and cellular response to oxidative stress⁵³. Although it was clear that this association exists, it was not known if AtfB directly impacts aflatoxin synthesis. In the current study, we hypothesized that the loss of AtfB function in *A. parasiticus* would impact aflatoxin gene regulatory networks and down-

regulate aflatoxin biosynthesis. Thus, we disrupted the function of native AtfB in *A. parasiticus* through a novel co-transformation method (see **Methods**, page 48). Our data suggest that a reduction in AtfB production at the protein level down-regulates aflatoxin synthesis and impairs fungal development. RNA Seq and RT-PCR data analyses demonstrate an overall down-regulation of target sentinel genes in the disruption strains (JW-12 and JW-13) compared to the wild-type strain, SU-1. Gene ontology (GO) analysis conducted on JW-12 and JW-13 demonstrate that AtfB is associated with regulation of virulence-associated processes as well as gene targets of other cellular defense pathways and actin cytoskeleton arrangement and transport. These observations confirm that AtfB directly regulates at least three functional gene networks and integrates SM, SR, and CD in *A. parasiticus*.

MATERIALS AND METHODS

Fungal strains and growth conditions

A. parasiticus strain SU-1 (ATTC 56775) was the wild-type aflatoxin-producing strain used in this study. *A. parasiticus* NR-1 which harbors a non-functional gene encoding nitrate reductase (*niaD*) was derived from SU-1 and used as a recipient and control strain for co-transformation⁹⁹.

YES liquid medium (2% yeast extract and 6% sucrose, pH 5.8) was used as an aflatoxin-inducing growth medium. Conidiospores from frozen mycelia stock solutions were inoculated into 100 mL liquid medium at a final concentration of 10^4 spores per mL; each flask contained five 6-mm glass beads (Sigma)⁴⁴. Cultures were incubated at 30°C with shaking at 150 rpm in the dark for designated time periods (standard

conditions). Potato dextrose agar (PDA; Becton Dickinson, Franklin Lakes, New Jersey) was used as an aflatoxin-inducing solid growth medium. 10^4 spores (10 μ l) were center-inoculated onto the solid medium surface which was then incubated for 24 h to 120 h at 30°C in the dark.

For RNA Seq analysis, duplicate samples of SU-1, JW-12, and JW-13 were grown in YES liquid medium for 40 h and 60 h under standard growth conditions (30°C with shaking at 150 rpm in the dark).

Disruption of *A. parasiticus* AtfB

AtfB was previously identified and designated AFLA_094010 (92.m03394) using a published *A. flavus* genome database (<http://www.aspergillusflavus.org/>) by strong sequence identity (96%) to the transcription factor AtfB in *A. oryzae*⁵³. The *A. parasiticus* AtfB sequence identity was confirmed by cloning, nucleotide sequence analysis, and comparison against the recently published *A. parasiticus* genome sequence, which was determined by Illumina sequence analysis^{6,53}. The nucleotide sequence accession number for *atfB* is ADZ06147.1 and the *A. parasiticus* SU-1 genome sequence is available through the NCBI database (Accession: JMUG00000000) (<http://www.ncbi.nlm.nih.gov/>).

We amplified two fragments (Fragment 1, 5'-ATGTCGGTGGACCAAACCCT-3', forward primer, Fragment 2, 5'-GGCGAAGAAGCTTAGAACAGTTGCTCACTCTGGTCGACG-3', reverse primer; Fragment 2, 5'-TGTTCTAAGCTTCTTCGCCGAAAAATTCCTAGAACGGAA-3', forward primer, 5'-CTAAACATTAATCAGCTCTT-3', reverse primer) from an intronless *atfB*

ORF of 957 bp by PCR. Overlap extension PCR of Fragment 1 and 2 resulted in a 20 bp deletion and insertion of a *HindIII*- site in the disruption construct (see schematic map of the *atfB* disruption construct in **Figure 8**). A circular and uncut plasmid pSL82 containing a 6.3-kb *HindIII* fragment with the selectable marker *niaD* was used together with the disruption construct for co-transformation of strain NR-1⁹⁹. Protoplasts were obtained as previously described^{99,100} from strain NR-1 (*niaD*⁻, aflatoxin⁺). PCR and Southern blot analyses of *niaD*⁺ transformants identified several in which multiple tandem copies of the disruption construct integrated into the *A. parasiticus* genome at ectopic sites.

DNA extraction and Southern blot analysis

Genomic DNA from *A. parasiticus* NR-1, JW-12, and JW-13 was isolated from frozen fungal mycelium using the phenol-chloroform method previously described¹⁰⁰. Southern hybridization analysis was performed as previously described⁸² with minor modifications. Briefly, 2.5 µg genomic DNA was digested with 20 U of *Bam*HI-HF, *Eco*RI-HF or *Hind*III at 37°C for 16 hours (NEB, Ipswich, MA). Digested DNA was separated on a 0.8% agarose gel and transferred onto a Nytran® SuPerCharge membrane (Schleicher and Schell, Inc., Keene, NH) by capillary transfer. Membranes were UV cross-linked (120,000 µJ/cm²) in a UV Stratalinker® 2400 (Stratagene, Inc., La Jolla, CA). A 600 bp *atfB* probe was generated by PCR (5'-ATGTCGGTGGACCAAACCCT-3', forward primer; 5'-TCGCCTTTCTTGCTGGATAC-3', reverse primer). PCR products were purified with a Qiagen Gel Purification kit (Qiagen, Valencia, CA). Probe labeling, hybridization, and detection were performed using an

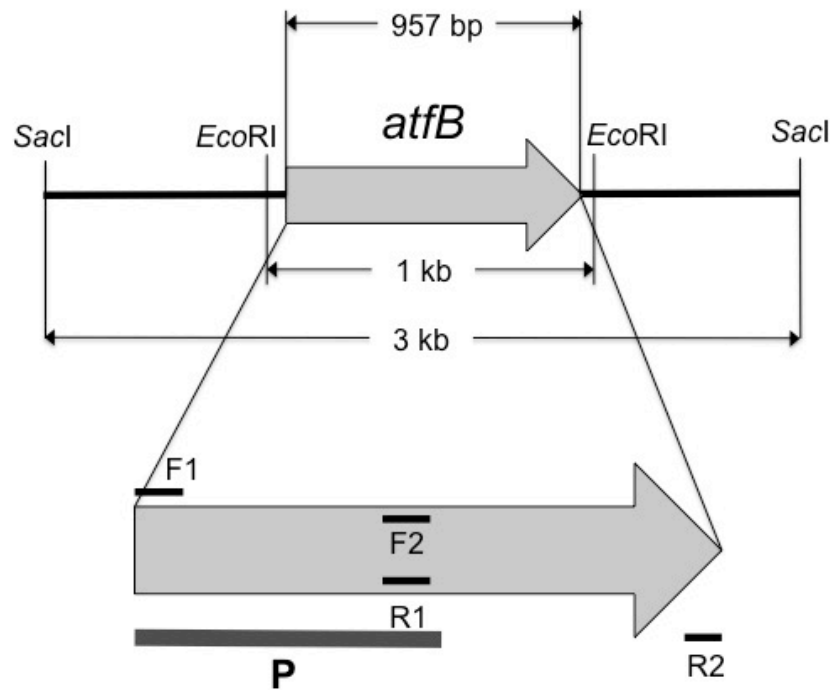


Figure 8 Disruption of *A. parasiticus atfB*

Schematic diagram depicting integration of the *SacI* linear fragment (3kb) or the *EcoRI* linear fragment (1kb) carrying the 957 bp *atfB* disruption construct co-transformed together with the circularized psL82 plasmid carrying the selectable marker, *niaD* (see **Methods**). Primers used to amplify the construct for overlap PCR and Southern probe (designated P) are as follow. F1: Fragment 1, 5'-ATGTCGGTGGACCAAACCCT-3', forward primer; R1: Fragment 1, 5'-GGCGAAGAAGCTTAGAACAGTTGCTCACTCTGGTCGACG-3', reverse primer; F2: Fragment 2, 5'- TGTTCTAAGCTTCTTCGCCGAAAATTCTAGAACGGAA-3', forward primer; R2: Fragment 2, 5'- CTAAACATTAATCAGCTCTT-3', reverse primer. A 600 bp southern probe (designated P) was generated by PCR using forward primer 5'-ATGTCGGTGGACCAAACCCT-3' and reverse primer 5'-TCGCCTTTCTTGCTGGATAC-3'.

Amersham Gene Images AlkPhos Direct Labeling and Detection System (GE Healthcare, Pittsburg, PA) according to manufacturer's instructions.

Aflatoxin measurements in SU-1, JW-12 and JW-13

Triplicate cultures of SU-1, JW-12, and JW-13 were grown in YES liquid medium under standard conditions (30°C with shaking at 150 rpm in the dark) and harvested at designated time points. Aflatoxin B₁ concentration (µg) in the medium was quantified by ELISA using anti-aflatoxin B₁ polyclonal antibodies (Sigma-Aldrich, St. Louis, MO) and normalized to mycelial dry weight (g) as previously described^{66,82}.

RNA Isolation, transcript analysis, and *HindIII* cutting assay

Triplicate cultures of SU-1, JW-12, and JW-13 were grown in YES liquid medium under standard conditions, harvested at 24 h, 40 h, and 60 h and fungal cells disrupted using a mortar and pestle in the presence of liquid nitrogen. TRIzol® reagent (Invitrogen, Grand Island, NY) was used to extract total RNA from ground mycelium⁵³. An Agilent 2100 Bioanalyzer (Agilent Technologies, Santa Clara, CA) was used to assess RNA quality. Total RNA (1 µg) was reverse-transcribed into cDNA with the QuantiTect reverse transcription kit (Qiagen).

Full length *atfB* transcript was amplified with *atfB* specific primers (5'-ATGTCGGTGGACCAAACCCT-3', forward primer; 5'-CTAAACATTAATCAGCTCTT-3', reverse primer) by semi-quantitative PCR of cDNA prepared from cultures after 24 h, 40 h, and 60 h of growth. A 1 kb *atfB* fragment was purified using a Qiagen Gel Purification System. An equal volume of purified 1 kb *atfB* fragment was digested with 20 U of

*Hind*III for 1 h or left undigested to serve as a control. Band intensities and the ratio of wild-type (WT) to disruptant (MT) transcripts were quantified using ImageJ¹⁰¹.

Protein extraction and Western blot analysis

Triplicate cultures of SU-1, JW-12, and JW-13 were grown in YES liquid medium for 40 h under standard conditions, harvested and disrupted with a mortar and pestle under liquid nitrogen, and a protein extract was prepared as previously described⁵³. Total protein concentrations were measured using the Pierce® BCA Protein Assay Reagent (Thermo Scientific, Waltham, MA). 100 µg of total proteins per lane was separated by SDS-PAGE using a 4–20% gradient Tris-HCl Ready Gel® (Bio-Rad, Hercules, CA) and transferred to PVDF membranes (PerkinElmer Life Sciences, Waltham, MA). Membranes were exposed to polyclonal anti-AtfB antibodies (YSR, 5 µg/ml) and incubated with goat anti-rabbit secondary antibodies conjugated to the fluorescent tag IRDye 800CW (Li-Cor Biosciences, Lincoln, NE) as previously described⁵³. For aflatoxin enzymes, highly specific antibodies against Nor-1, OmtA, and Ver-1 were used as previously described^{79–82}. Visualization of proteins was performed using an Odyssey infrared imaging system (Li-Cor Biosciences) at 795 nm as previously described⁵³.

RNA isolation and cDNA library preparation for RNA Seq analysis

Duplicate cultures of SU-1, JW-12, and JW-13 were grown in YES liquid medium under standard conditions, harvested after 40 h, ground in a mortar and pestle under liquid nitrogen and RNA was extracted as described above. Library construction and

RNA quality analysis for all six isolates were conducted by Orogenetics (Norcross, GA) and Functional Biosciences (Madison, WI). Integrity and purity of the RNA samples were assessed using an Agilent 2200 TapeStation Bioanalyzer System (Agilent, Santa Clara, CA). All samples had an RNA Integrity Number (RIN) of 9.0 or higher with an OD260/280 between 1.78 – 1.80.

cDNA library construction was conducted as follows: Fragment AnalyzerTM (AATI, Ames, IA) and Qubit[®] were used to assess cDNA quality. 100 ng of total RNA was reverse transcribed into cDNA using a Clontech SmartPCR cDNA kit (Clontech, Mountain View, CA). Restriction enzyme digestion end repair was conducted by removing adaptor sequences and fragmentation of the resulting cDNA was conducted using a Covaris M220 focused-ultrasonicator (Woburn, MA). Fragmented cDNA was subjected to Illumina library preparation with NEBNext-based reagents (NEB, Ipswich, MA). The quality, quantity, and size distribution of Illumina libraries were determined using an Agilent Bioanalyzer 2100. cDNA clusters were generated on a cBot automated station and the Illumina libraries were submitted for Illumina HiSeq2000 2x100 bp Paired-End sequencing (Illumina, San Diego, CA).

RNA Seq analysis

RNA Seq data analysis was performed by ContigExpress, LLC (New York, NY). Six *A. parasiticus* samples (duplicates of SU-1, JW-12, and JW-13) prepared as described above were used in this analysis. Detailed methods for QC of Illumina sequence reads, mapping, annotation, and differential expression analysis were recently published⁶.

RT-PCR analysis

Semi-quantitative PCR analyses was used to validate differential gene expression analysis obtained from RNA Seq. Total RNA (1 µg) was reverse-transcribed into cDNA with the QuantiTect reverse transcription kit (Qiagen) according to the manufacturer's instructions. 1 µl (50 ng) of cDNA was used as a template in the subsequent PCR using a Robocycler Gradient 96 (Stratagene, La Jolla, CA) under the following conditions: initial denaturation at 94 °C for 4 min; followed by 30 cycles of 94 °C for 1 min, 60 °C for 2 min, and 72 °C for 1 min, with a final extension at 72 °C for 9 min. The PCR products were separated by electrophoresis on a 0.8% agarose gel.

Gene ontology (GO) pathway analysis and REViGO

GO and pathway analysis was conducted by ContigExpress, LLC (New York, NY). The entire transcriptome of JW-12 and JW-13 was annotated against the *A. fumigatus* database using KOBAS 2.0¹⁰². About eighty percent of genes were annotated in at least one GO term or pathway. Differentially expressed genes in JW-12 vs. SU-1 and JW-13 vs. SU-1 were subject to GO and pathway enrichment analysis using KOBAS 2.0. Enriched GO terms with p-values <0.05 were used as an input list for REViGO analysis (free software available at <http://revigo.irb.hr/>)¹⁰³.

RESULTS

Molecular analysis of JW-12 and JW-13

93 *niaD* + transformants were obtained from transformation of the *atfB* construct into the control strain, NR-1. 61 *niaD* + transformants were observed having wild type (WT) phenotype by initial visual screening (conidiospore levels similar to control strain, aflatoxin + on a coconut agar screening medium) while 32 transformants were observed with atypical phenotype (either low sporulation or aflatoxin – on screening medium). Among the 61 *niaD* + WT transformants, 9 out of 9 transformants analyzed were negative in screening for the disruption construct. Out of 32 atypical transformants, PCR analysis was conducted on 5 and all 5 transformants screened positive for the disruption construct. Two of these 5 isolates designated JW-12 and JW-13 were analyzed further. PCR + transformants JW-12 and JW-13 carried multiple copies of the *atfB* gene disruption construct that integrated at a single, but unique ectopic site. These transformants were subjected to 2 rounds of single spore isolation and analyzed in greater detail. We determined that even though the gene disruption construct in JW-12 and JW-13 integrated at different ectopic locations, the phenotype of these transformants was nearly identical (marked decrease in levels of aflatoxin and decrease in conidiospore number and pigment). There was a 100% correlation between phenotype and the presence of the gene disruption construct. Of critical importance, we analyzed 4 representative transformants out of 9 transformants that initially screened as *niaD* + and these did not carry the gene disruption construct; we observed the wild type phenotype (normal levels of conidiospores and aflatoxin) in all 4.

NR-1 (recipient and control strain), JW-12, and JW-13 were grown in YES medium and the extracted genomic DNA was analyzed by Southern blot analysis under high stringency conditions. Genomic DNA isolated from NR-1 was digested with *Bam*HI, *Eco*RI, or *Hind*III and the resulting pattern of fragments suggested the presence of two or more copies of *atfB* (**Figure 9A**). A more intense band at 7.0 kb in the *Bam*HI digest suggested higher identity or more than one identical copy of *atfB* whereas a less intense 5.0 kb band suggested an additional copy of *atfB* of lower sequence identity. The 5.0 kb and 7.0 kb bands observed in the recipient and control strain NR-1 appeared intact at the same location in JW-12 and JW-13 (**Figure 9B**) indicating that the wild-type *atfB* gene copies were not replaced by the *atfB* disruption construct by co-transformation. However, we did observe ectopic integration (non-native recombination) of the *atfB* construct at different locations in JW-12 and JW-13 (**Figure 9B**). This is supported by a 12.0 kb *Bam*HI band in JW-12, which is absent in JW-13 and NR-1, but a smaller 4.0 kb *Bam*HI band in JW-13 that is absent in JW-12 and NR-1. Different locations of ectopic integration of the *atfB* mutant construct in JW-12 and JW-13 is further supported by the *Eco*RI-digest. Band intensity of the ectopically integrated construct is approximately 2-3 times higher than that of the native locus (**Figure 9B**) suggesting multiple tandem integration of the *atfB* mutant construct at the non-native locus. The presence of a *Hind*III-site created within the *atfB* construct supports restriction patterns observed in *Hind*III-digested genomic DNA. Two additional bands at different locations were detected in JW-12 and JW-13 strongly supporting the integration of the disruption construct into the NR-1 genome. So, multiple tandem integration of the disruption construct at different ectopic sites in JW-12 and JW-13

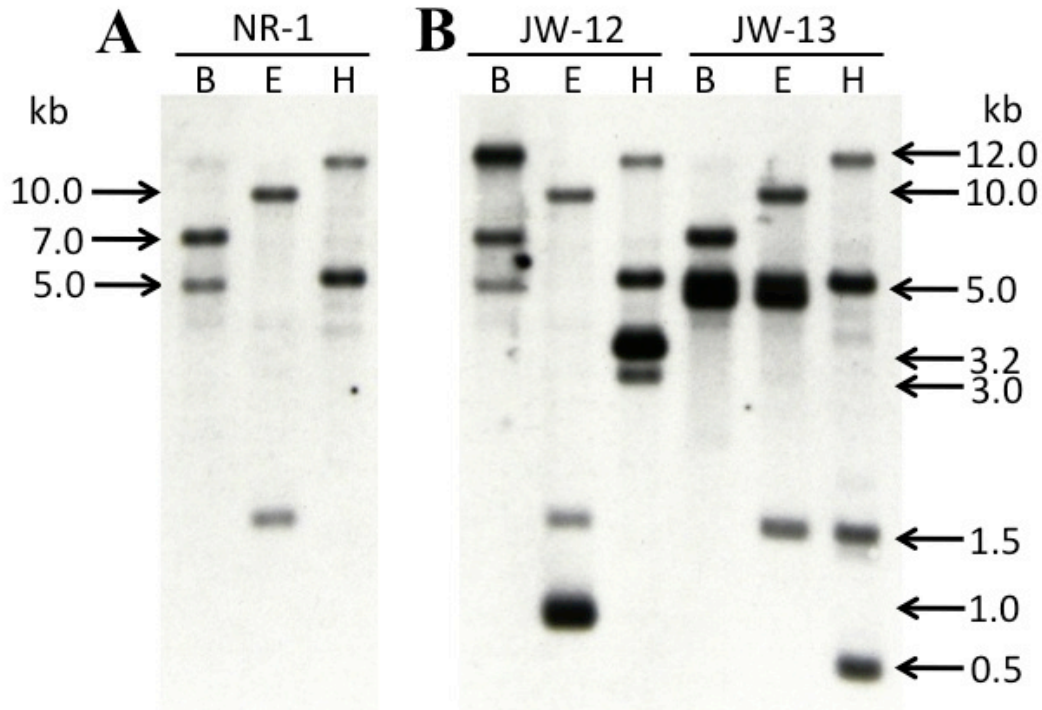


Figure 9 Southern hybridization analysis of *A. parasiticus* strains NR-1, JW-12, and JW-13 using an *attB* probe

Strains NR-1, JW-12, and JW-13 were grown in YES liquid medium for 40 h and genomic DNA was extracted for Southern hybridization analysis with an *attB* probe (see **Methods**). DNA was digested with *Bam*HI (B), *Eco*RI (E), or *Hind*III (H) and analyzed using standard methods (see **Methods**). **Panel A.** Southern analysis of NR-1 (recipient and control strain) derived from wild-type SU-1 depicts the number of copies of *attB* present in the *A. parasiticus* genome. **Panel B.** Southern analysis of *attB* disruption strains, JW-12 and JW-13 shows the location and extent of integration of the disruption construct into the genome by co-transformation. Additional bands in the *Hind*III digest are due to a *Hind*III site created in the *attB* disruption construct.

generated highly similar phenotypes (**Figure 10A**). Therefore, we hypothesized that disruption of *atfB* in JW-12 and JW-13 was caused by a transcriptional or posttranscriptional effect on *atfB* expression and not on removal of the wild type gene.

AtfB disruption construct is directly linked to aflatoxin synthesis and fungal growth

On an aflatoxin-inducing solid growth medium (PDA), growth of strains JW-12, JW-13, and SU-1 was observed for 24 h to 120 h. Although the ectopic integration of the *atfB* construct did not alter fungal growth rate significantly, conidiospore formation and spore pigmentation were significantly affected in JW-12 and JW-13 (**Figure 10A**). JW-12 and JW-13 showed marked decreases in conidiospore formation from 48 h to 120 h (**Figure 10A**) by visual inspection. This observation is supported by evidence in *Aspergillus oryzae*, where *atfB* deletion reduced conidiospore number and generated a 'white fluffy' mycelium phenotype⁵⁹.

Under standard aflatoxin inducing conditions, *A. parasiticus* initiates aflatoxin synthesis between 24 and 30 h, and maximum levels of synthesis occurs by 40 h^{62,64}. Comparing aflatoxin levels produced by SU-1, JW-12, and JW-13 in YES medium, JW-12 produced 200-fold less aflatoxin at 40 h and 40-fold less at 60 h when compared to SU-1 (**Figure 10B**). JW-13 produced 20-fold less aflatoxin at 40 h and 10-fold less at 60 h when compared to SU-1.

Taken together, these data support a strong direct association between the presence of the *atfB* disruption construct in the *A. parasiticus* genome (genetic

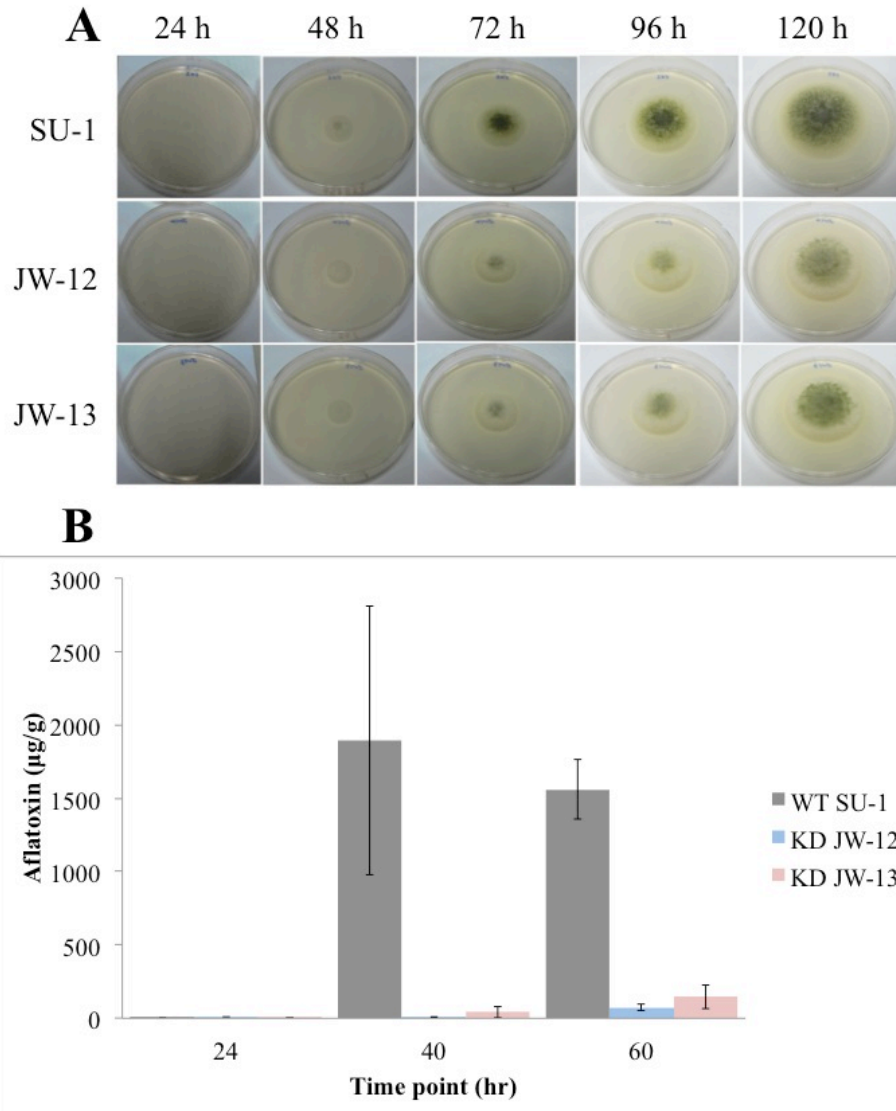


Figure 10 Characterization of fungal growth, conidiospore number/pigment, and aflatoxin production (phenotype) in strains SU-1, JW-12, and JW-13

A. parasiticus strains were grown for 24, 48, 72, 96, and 120 h on aflatoxin inducing PDA agar (**Panel A**) or for 24, 40, and 60 h (**Panel B**) on aflatoxin-inducing YES liquid medium and analyzed for growth and conidiospore number/pigment (**Panel A**) as well as for aflatoxin production (ELISA, **Panel B**). Aflatoxin levels are the means \pm SEMs of triplicates from two independent biological replicates (total of 6 samples per time point) of the experiment.

alteration) with the occurrence of a 'white fluffy' mycelia morphology, low conidiospore formation, and low aflatoxin production in JW-12 and JW-13.

Up-regulation of expression of *atfB* disruption transcript associates with a decrease of AtfB protein level in JW-12 and JW-13

We amplified full length *atfB* transcript by semi-quantitative PCR to make cDNA from SU-1, JW-12 and JW-13 at 24 h, 40 h, and 60 h. Densitometric analysis of agarose gels on which we resolved the full length *atfB* transcript showed a significant increase in transcript levels in JW-12 and JW-13 when compared to SU-1 at 24 h (**Figure 11A**) strongly suggesting that the disruption construct in both strains was expressed at the transcript level. At 24 h, both JW-12 and JW-13 produced a 3-fold increase of full-length transcripts when compared to SU-1. Full-length transcripts appear relatively unchanged at 40 h. At 60 h, total transcripts of JW-13 remained higher than SU-1, whereas JW-12 remain unchanged (**Figure 11B**). This observation is reasonable considering that the net amount of transcript produced in the disruption strains represents the sum of the transcripts expressed at the native locus and those expressed at the ectopic site. Differences in the level of full-length *atfB* transcript in JW-12 and JW-13 could suggest differential regulation of *atfB* transcripts at the time points analyzed prompting us to hypothesize that different promoters drive expression of the *atfB* disruption construct in JW-12 and JW-13.

To assess the ratio of wild-type (WT) to disruption (MT) transcript produced at 24, 40, and 60 h, we conducted a *HindIII*-cutting assay (see **Methods**). We amplified a 957 bp cDNA fragment in SU-1, JW-12, and JW-13 at three time points. This fragment

was excised from the agarose gel and digested with *HindIII*. The presence of a *HindIII*-site inserted in the disruption construct enabled us to subsequently analyze the level of WT and MT transcript as detected by digestion with *HindIII*. The data demonstrated that the MT transcript is not produced in SU-1 but is produced in JW-12 and JW-13 (**Figure 11C**). In JW-12 and JW-13, different levels of MT transcript were detected at 24, 40, and 60 h of growth supporting the hypothesis that different promoters drive transcription of these constructs. These data are in agreement with the unique location of ectopic integration of the disruption construct in each strain. We then calculated a WT to MT transcript ratio to depict differences in transcript levels produced by WT *atfB* compared to transcripts being produced by the *atfB* disruption construct (MT). The MT transcript was produced at highest amounts at 24 h in JW-12 (**Figure 11D**) and transcript levels decreased markedly at 40 and 60 h. In contrast, in JW-13, high levels of MT transcript were produced at 24 h and the level continued to increase with the highest levels of MT transcript detected at 60 h (**Figure 11E**). Of particular significance, there was an inverse relationship observed between the quantity of MT transcript and WT transcript in JW-12 and JW-13. We also observed a large decrease in WT transcript in JW-13 that in general, expresses higher levels of MT transcript than JW-12.

We analyzed expression of AtfB protein in SU-1, JW-12, and JW-13 using *atfB*-specific anti-peptide polyclonal antibodies generated previously⁵³. Anti-AtfB detected a 34-kDa protein in cell extracts of SU-1, JW-12, and JW-13 at 40 h consistent with the previously reported mass for the AtfB protein⁵³ and supported by an AtfB immunoprecipitation (data not shown) and peptide competition analysis (data not shown). The 34 kDa protein was clearly detectable in SU-1 but was observed at

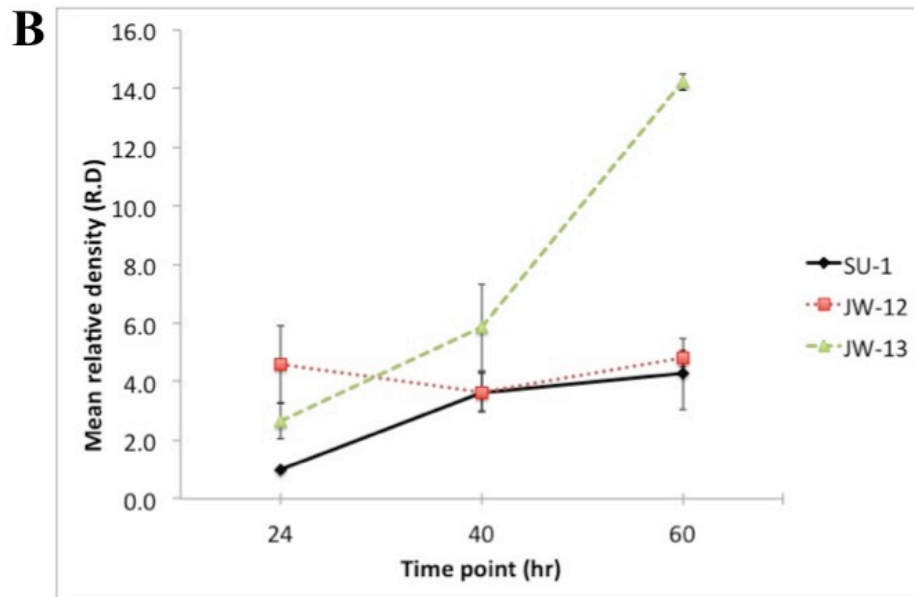
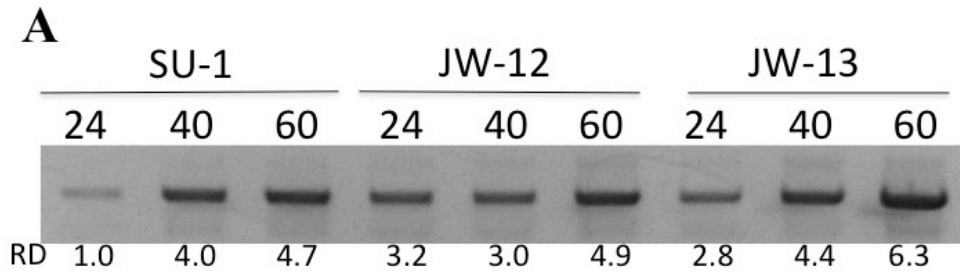
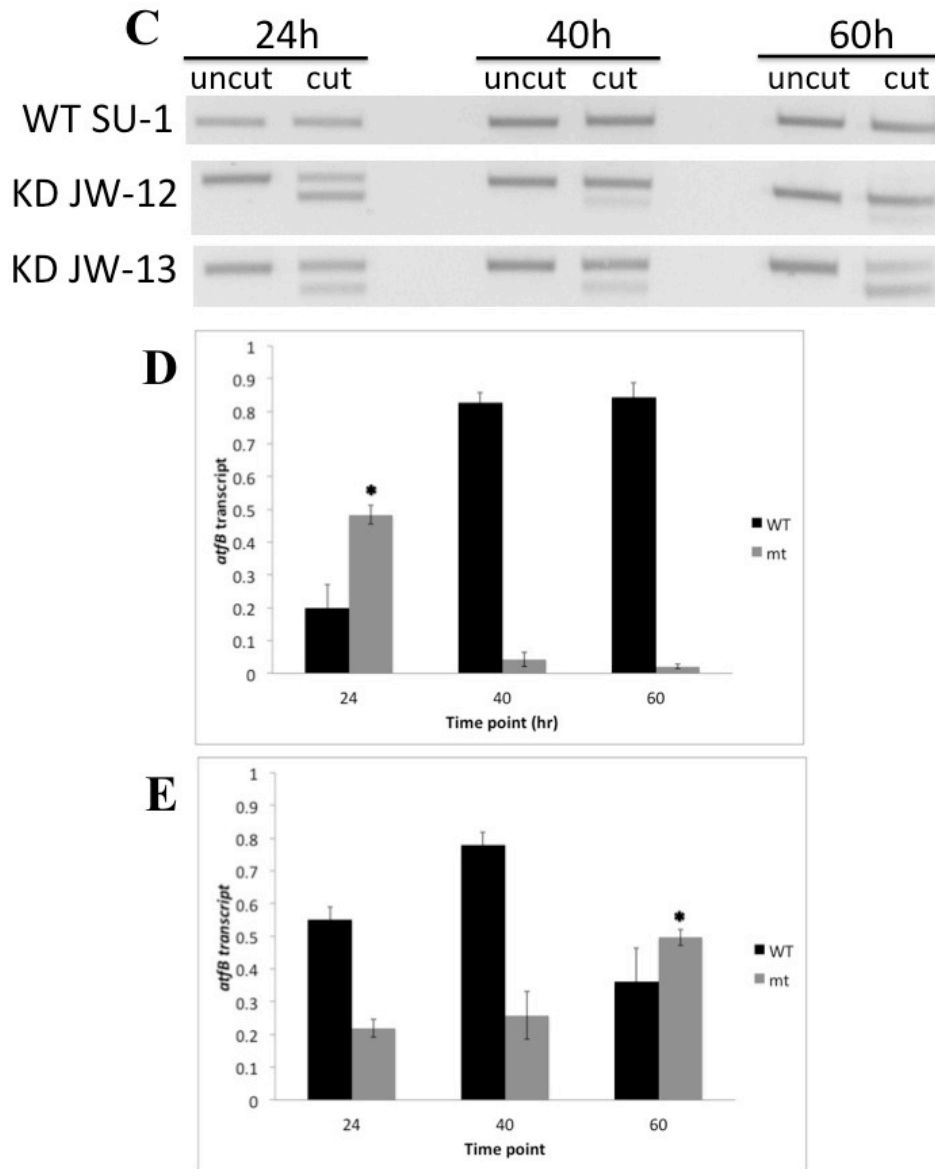


Figure 11 Analysis of *attB* transcript levels in strains SU-1, JW-12, and JW-13 using semi-quantitative real time PCR and a novel *HindIII* cutting assay

Strains SU-1, JW-12, and JW-13 were grown on aflatoxin inducing YES liquid medium for 24, 40, and 60 h and analyzed for *attB* transcripts as follows. **Panel A.** Total *attB* transcript in SU-1, JW-12 and JW-13 at 24 h, 40 h, and 60 h. Primers amplified the full length 957 bp *attB* transcript. R.D., relative density as measured by ImageJ densitometry software analysis¹⁰¹. **Panel B.** Graphical analysis of densitometry measurements from Panel A. Transcript levels are reported as the means \pm SEM for triplicate cultures conducted in a single biological replicate of the experiment. Two biological replicates were conducted with representative data shown in Panel B.

Figure 11 (cont'd)



Panel C. A *Hind*III-cutting assay (see **Methods**) was conducted on amplified full length *atfB* transcripts obtained from strains SU-1, JW-12, and JW-13 after 24, 40, and 60 h of growth (see **Methods**). **Panel D and E.** The ratio of WT *atfB* transcript (lane “cut”, top band in Panel C) to *atfB* disruption transcript (lane “cut”, bottom band in Panel C) was calculated based on densitometry (see **Methods**). WT: wild type *atfB* transcript, mt: *atfB* disruption transcript.

markedly decreased levels at 40 h in JW-12 and JW-13 (**Figure 12**). We were unable to detect the 34 kDa protein in JW-13 suggesting that constitutive expression levels of the MT transcript at 24, 40, and 60 h in JW-13 resulted in nearly a complete elimination of the AtfB protein. This is also supported by higher levels of mutant transcript expression in JW-13 compared to JW-12 (**Figure 11D and 11E**). In contrast, decreased expression of MT transcript at 40 and 60 h in JW-12 may have allowed some accumulation of the 34 KDa AtfB protein. So, the *atfB* transcript and AtfB protein data strongly support a direct association between the presence of the *atfB* disruption construct and aflatoxin synthesis and fungal growth.

Accumulation of aflatoxin enzymes is decreased in JW-12 and JW-13

We also analyzed protein levels of aflatoxin enzymes Nor-1, OmtA, and Ver-1 at 40 h of growth in aflatoxin-inducing medium by Western Blot using antibodies specific to Nor-1, OmtA, and Ver-1. We observed significantly lower levels of Nor-1, OmtA, and Ver-1 aflatoxin proteins in JW-12 and JW-13 compared to SU-1 (**Figure 13**). The pattern of aflatoxin enzyme accumulation closely mimics the pattern of AtfB protein accumulation in JW-12 and JW-13 (**Figure 12**).

AtfB protein levels impact expression of AtfB specific targets

Duplicate isolates of SU-1, JW-12, and JW-13 were grown under aflatoxin inducing conditions and RNA was purified from all 6 isolates and subjected to RNA Seq analysis. Of the approximately 14,000 total transcripts expressed and annotated in the disruption strains, 100 (JW-12) and 40 (JW-13) were differentially expressed at

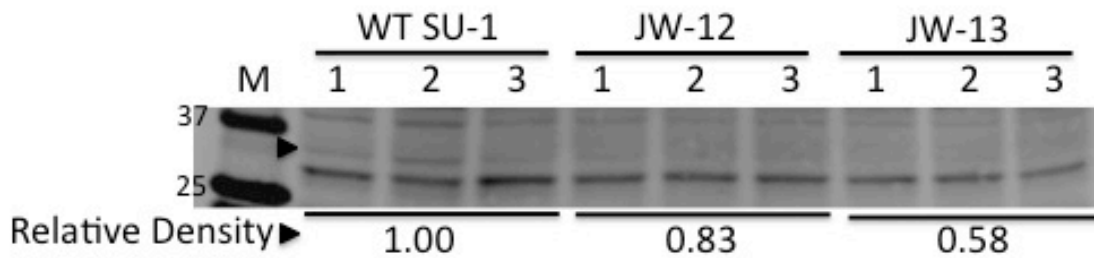


Figure 12 AtfB protein levels analyzed by Western blot analysis

Strains SU-1, JW-12, and JW-13 were grown for 40 h on YES liquid medium and proteins extracted for Western blot analysis (see **Methods**). *A. parasiticus* proteins were detected on membranes using a highly specific anti-AtfB polyclonal antibody⁵³. Total protein (100 µg) was loaded per lane. The 34 kDa AtfB protein (arrow head) was quantitated using densitometry and values expressed as relative density compared to wild type (SU-1). The molecular weight of AtfB was confirmed by an AtfB immunoprecipitation and a peptide competition analysis. The native AtfB protein was barely detectable in JW-12 and JW-13 but clearly detectable in the wild type strain SU-1 (control); this observation was supported by the densitometry data (arrow head).

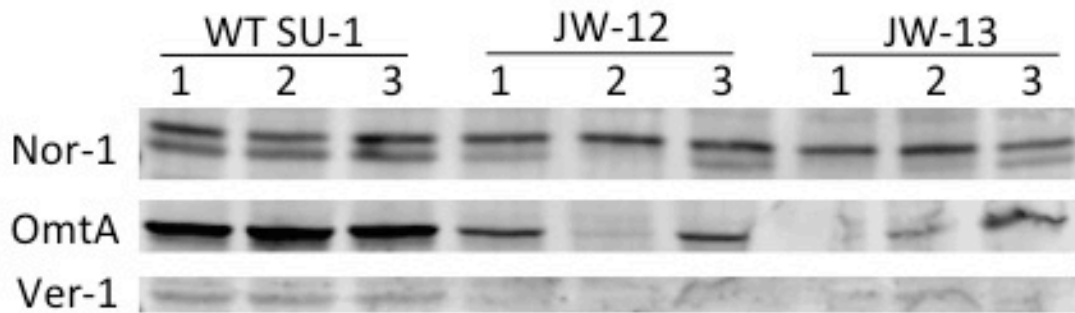


Figure 13 Aflatoxin enzyme accumulation shows similar pattern of expression to AtfB protein

Proteins were extracted from SU-1, JW-12, and JW-13 grown in aflatoxin inducing conditions for 40 h, resolved by SDS gel electrophoresis (4-12% gradient polyacrylamide gel), and transferred to PVDF membrane. Protein extracts were prepared from triplicate samples for each strain. Highly specific Nor-1, OmtA, and Ver-1 antibodies were used to conduct Western blot analysis as previously described^{79,80}. The presence of the *atfB* disruption construct and the expression of the mutant transcripts in JW-12 and JW-13 decreased accumulation of aflatoxin enzymes at 40 h which at least in part explains the decrease in aflatoxin levels measured in the growth medium in JW-12 and JW-13.

statistically significant levels of gene expression when compared to SU-1 during growth in YES medium at 40 h. Further analysis demonstrated that the majority of these gene targets are down-regulated (statistically significant, $q < 0.05$) in JW-12 and JW-13 (85 of 100 and 38 of 40, respectively; **Figure 14A** blue bar graph). Of particular importance, 38 of the 40 genes in JW-13 that were differentially expressed as compared to SU-1 were also among the 100 genes in JW-12 that were differentially expressed. These data strongly suggest that even though the disruption construct integrated at different ectopic sites and exhibited different patterns of expression of the MT transcript in JW-12 and JW-13, the net impact on down-regulation of AtfB on target genes in these two disruption strains was very similar (that is, they downregulated an overlapping subset of genes in *A. parasiticus*). This observation strongly supports a direct association between the presence of the disruption construct in JW-12 and JW-13, a decrease in AtfB protein levels and aflatoxin enzyme accumulation, and a decrease in expression of AtfB target genes.

At 40 h of growth in aflatoxin inducing conditions (YES medium), we observed that 20 out of 32 genes in the aflatoxin gene cluster are expressed at a minimum of 2-fold lower levels in JW-12 and JW-13 than in SU-1 (control) including *glcA*, *nadA*, *moxY*, *vbs*, *hypA*, *ordB*, *cypX*, *ordA*, *omtA*, *omtB*, *avfA*, *hypB*, *verB*, *hypD*, *fas-2*, *nor-1*, *hypC*, *afIT*, *cypA*, and *norB* (**Figure 14B**); these differences in expression were not statistically significant. In contrast, the gene encoding a Ser-Thr protein phosphatase, *afIYe* was slightly up regulated in both strains (not statistically significant) and *fas-1* was up-regulated in JW-12 but the transcript was not detected in JW-13. Expression of *afIR* was down regulated in JW-12 and up regulated in JW-13 suggesting that the AtfB regulation

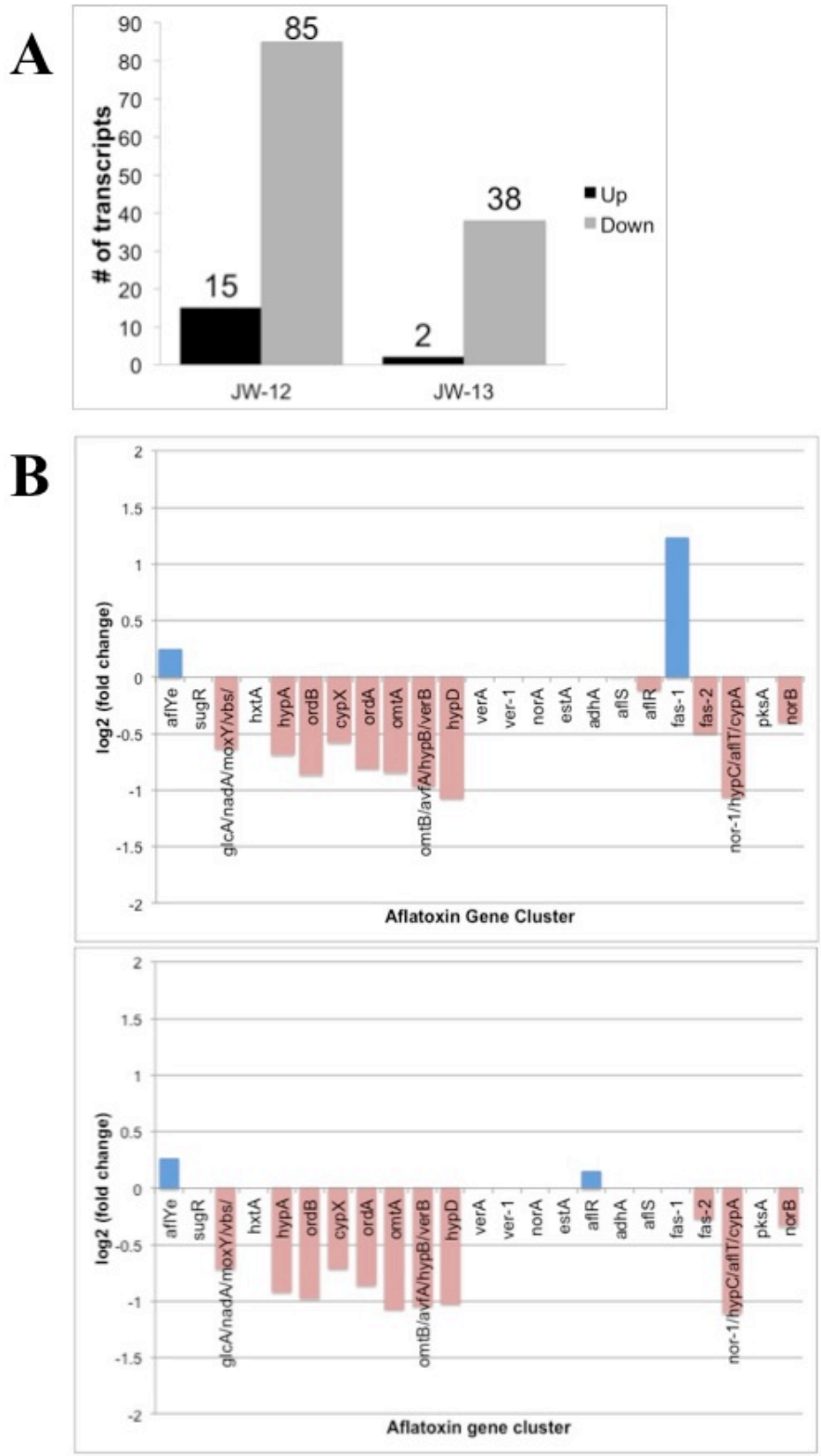


Figure 14 Comparison of the transcriptome in strains SU-1, JW-12 and JW-13 by RNA Seq analysis

Figure 14 (cont'd)

Strains SU-1, JW-12, and JW-13 were grown for 40 h in YES liquid medium, RNA extracted, and RNA Seq analysis performed on duplicate samples for each strain (see **Methods**). Only transcripts that were differentially expressed between JW-12 and SU-1 (**Panel A**, JW-12) or JW-13 and SU-1 (**Panel A**, JW-13) are shown (q-value cutoff < 0.05). The number of transcripts that are up-regulated or down-regulated are indicated by different colored bars (see legend, **Panel A**). Differential expression of transcripts encoded by genes in the aflatoxin cluster was also analyzed (**Panel B**). Top panel, genes differentially expressed between SU-1 and JW-12. Bottom panel, genes differentially expressed between SU-1 and JW-13. Differential expression was calculated and reported as log base 2 of the fold change in expression. Blue bars that extend above zero on the y-axis are up-regulated as compared to SU-1. Red bars that extend below zero on the y-axis are down-regulated. Common gene name(s) presented in the bar graphs (x-axis) are based on annotation of the *A. flavus* aflatoxin gene cluster (reference genome).

of *afIR* expression in JW-12 and JW-13 is different; these changes are relatively small and not statistically significant. Although expression of specific genes in the aflatoxin clusters in JW-12 and JW-13 was not significantly different from SU-1, most genes showed the same overall trend of down-regulation in both strains.

Down regulation of “sentinel” gene expression in JW-12 and JW-13

As part of the RNA Seq analysis, we were interested in sentinel virulence-associated genes regulated by AtfB (**Figure 15A**). We hypothesized that AtfB regulates expression of genes related to secondary metabolism, stress response, and conidiospore development. 100 (JW-12) and 40 (JW-13) transcripts expressed and annotated were differentially expressed at statistically significant ($q < 0.05$) levels of gene expression when compared to SU-1 during growth in aflatoxin inducing conditions (YES medium). Of particular importance is the subset of 40 overlapping genes identified in both JW-12 and JW-13. Two transcripts (AFLA_092830 and AFLA_107430) were up-regulated and 38 transcripts were down-regulated in both JW-12 and JW-13 (**Figure 15B**). We utilized RT-PCR analysis to validate expression of 8 candidate genes selected from 40 overlapping genes identified by RNA Seq analysis (**Figure 15C**). 4 genes (AFLA_074620 encodes a sodium/phosphate symporter, AFLA_096210 encodes a catalase, AFLA_037820 encodes a Hsp-30-like heat shock protein, AFLA_044790 encodes a conidiation-specific family protein) were down regulated in support of RNA Seq analysis. RT-PCR analysis detected no changes in expression observed for the 3 aflatoxin genes *afIJ*, *afID*, and *afIR* and AFLA_062510 which encodes a heavy chain myosin protein.

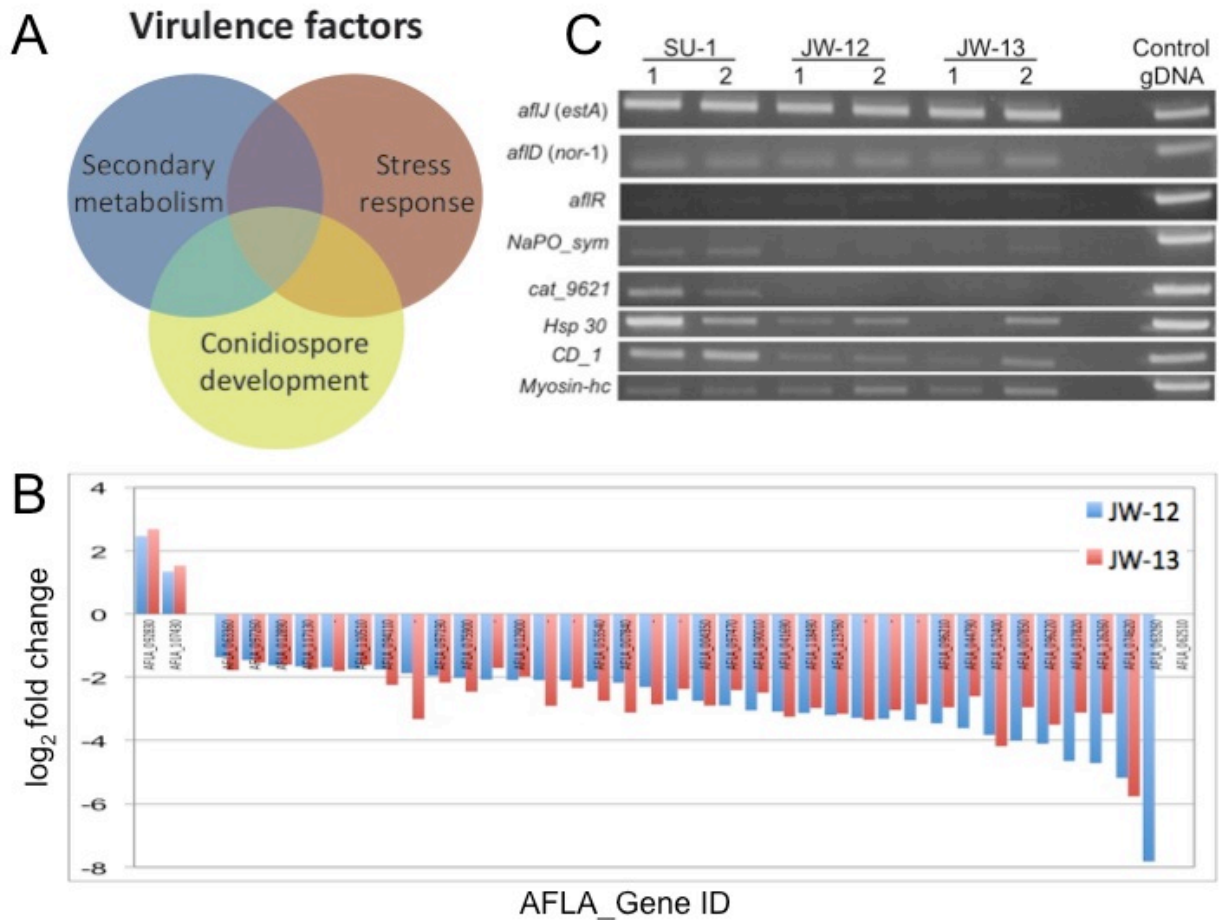


Figure 15 AtfB regulates expression of selected sentinel virulence-associated genes

Panel A. Proposed model for fungal virulence-associated cellular processes (virulence factors) integrating secondary metabolism (SM), stress response (SR), and conidiospore development (CD). **Panel B.** 40 overlapping differentially expressed genes (statistically significant, $q < 0.05$) were identified in JW-12 and JW-13 as compared to SU-1 grown under aflatoxin inducing conditions. Blue bars represent JW-12 and red bars represent JW-13. Two genes were up regulated and 38 genes were down regulated in JW-12 and JW-13 compared to SU-1 grown under the same conditions.

Figure 15 (cont'd)

The ratio of raw expression data for JW-12 (duplicate samples) and JW-13 (duplicate samples) grown for 40 h in YES were compared to SU-1 (duplicate samples). Differential expression was calculated and reported as log base 2 of the fold change in expression (y-axis). AFLA_gene designation is presented on the x-axis. The presence/expression of the *atfB* mutant transcript and loss of function of the AtfB protein caused a significant down-regulation of the same 38 transcripts in both strains. We conclude that AtfB regulates expression of important sentinel genes. **Panel C.** RT-PCR validation of 8 representative genes from RNA Seq analysis. Expression of four genes (a conidiation family protein, a heat shock protein 30, a putative catalase, and a sodium/phosphate symporter) as detected by RT-PCR supported trends of down-regulation observed by RNA Seq analysis and there were slight or non-detectable changes in gene expression detected for the three aflatoxin genes (*aflD*, *aflJ*, *aflR*) and a heavy chain myosin-related gene. Genomic DNA (50 ng) was used as a control.

The fungal AtfB regulatory networks extends beyond secondary metabolism, stress response, and development

The entire transcriptome of JW-12 and JW-13 was annotated and GO pathway terms were assigned based on the *Aspergillus fumigatus* GO/pathway database. *A. fumigatus* is an important human pathogen and secondary metabolism, stress response, and conidiospore development enhance disease capability of *A. fumigatus* in host tissue¹⁰⁴. To assess the potential relevance of interspecies functional networks, the differentially expressed genes in JW-12 vs. SU-1 and JW-13 vs. SU-1 were subjected to GO/pathway enrichment analysis. REViGO software was used to conduct GO-based visualization of enriched GO terms in a combined list of GO terms in disruption strains. Visualizations were then illustrated (**Figure 16**) as a graphical analysis in a semantic space with similar GO terms clustered together. “Biological processes in secondary metabolism” was the most over-represented GO-term followed by “actin cytoskeleton rearrangement/transport”. Other over-represented pathways in disruption strains compared to control are related to “oxidative stress response”, “pH regulation”, “mRNA function”, “glutathione synthesis”, and “vitamin B6 synthesis”. Taken together, network data analysis demonstrates that the regulation of fungal-specific AtfB extends beyond SM, SR, and CD (virulence-associated processes).

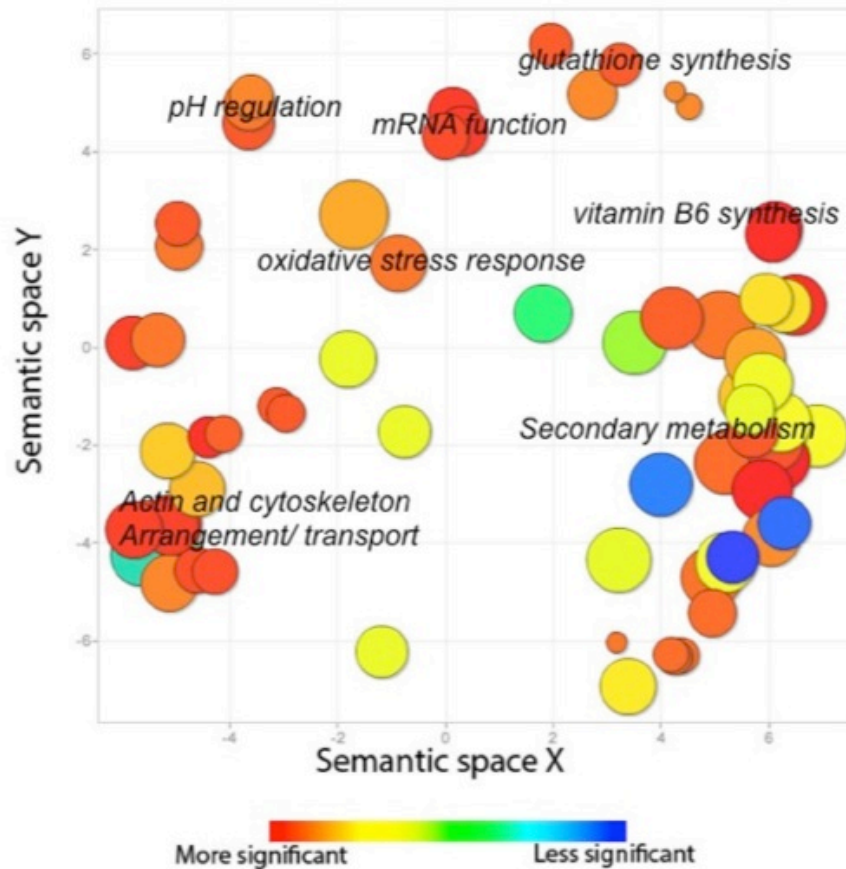


Figure 16 Gene ontology (GO) analysis of candidate genes in the AtfB regulatory network in JW-12 and JW-13

GO terms represented by circles are visualized in a semantic similarity-based scatter plot, where similar GO terms are close to each other (as determined using ReviGO software¹⁰³). The area of the circle is proportional to the significance of the over-representation of the GO term (-log base10 p-value). The color of the circles represents the statistical significance of the over-representation of the GO term as shown in the legend.

DISCUSSION

Our studies provide details of the mechanism by which AtfB is directly linked to co-regulation of aflatoxin biosynthesis, oxidative stress response, and fungal development. The current study shows that the time-dependent synthesis of the *atfB* disruption transcript (MT) correlates to the phenotype observed ('white fluffy' mycelial morphology, low levels of conidiospores formation, and low levels of aflatoxin) in disruption strains JW-12 and JW-13. There was a 100% correlation between these specific phenotypes and the presence of the gene disruption construct (that is, the presence/expression of the *atfB* disruption construct integrated at an ectopic site in the *A. parasiticus* genome and expressed at that location positively correlated with the occurrence of the phenotype). Of critical importance, we did not observe these changes in phenotype in any isolate that did not carry the *atfB* disruption construct (4 transformants analyzed; normal levels of conidiospores, aflatoxin +, PCR construct -), in the transformation control and host strain NR-1, or in the parent strain SU-1. Thus, we conclude that the presence of the disruption construct in JW-12 and JW-13 down regulated expression of the AtfB protein at 40 h resulting in the observed changes in phenotype reported above. This in turn resulted in down regulation of accumulation of at least 3 aflatoxin enzymes, Nor-1, Ver-1, and OmtA.

The use of this novel co-transformation method shows that ectopic integration of a disruption construct has the ability to regulate the timing and level of the MT transcript, subsequently regulating gene function and specific gene targets within a regulatory network. The unique temporal pattern of MT transcript expression argues that although the integration of the disruption construct occurred at different locations in JW-12 and

JW-13, this event resulted in varying degrees of the same phenotype and that the mechanism of down-regulation is targeted and specific. Although the mechanism that regulates the expression of MT transcript is unclear, we speculate that different promoters drive expression of MT transcript in JW-12 and JW-13 and this depends on the specific promoter adjacent to the site of ectopic integration. An alternative explanation is that MT transcripts are produced and processed by RNA binding proteins that control the rate of transcript turnover. *Erwinia carotovora* RsmA (repressor of secondary metabolism) functions as an RNA binding protein and is thought to modulate production of the quorum sensing molecule, N-acyl homoserine lactone (AHL) by limiting the levels of *hslI* transcripts (gene coding for the 3-oxo-C6-HSL synthase)¹⁰⁵. Preliminary analysis of RNA binding domain prediction in AtfB revealed 95 binding sites with high relative scores (80-100%) (Wee et al, unpublished data). In addition, mRNA stability could also explain the differences in MT transcript levels observed in JW-12 and JW-13. In JW-12, high levels of MT transcripts were produced at 24 h and this decreased by 40 h whereas MT transcripts in JW-13 were detected at highest levels at 60 h. In support of the utility of this novel gene disruption method, we recently conducted gene disruption analysis of Vps34, a gene encoding a vacuolar sorting protein using a similar co-transformation method (Wee et al. 2015, **Chapter 3**). In this study, high levels of MT transcripts expressed by the Vps34 disruption construct at 40 h down-regulated expression of WT transcripts at that time point. One focus for future work will be to characterize the site of disruption construct integration by inverse PCR analysis or next generation sequencing (NGS) to identify the promoter that drives expression of disruption (MT) transcripts.

One goal of the current work was to explain the mechanisms by which the presence of the disruption construct generated the observed decrease in AtfB protein levels at 40 h in JW-12 and JW-13. We observed statistically significant (q-value < 0.05) changes in the transcriptome of JW-12 and JW-13 by RNA Seq analysis at 40 h suggesting that the amount of MT transcript produced before 40 h was sufficient to alter changes in gene expression. The MT transcript is produced in a time-dependent pattern that is different in JW-12 (highest levels at 24 h) and JW-13 (relatively stable levels, highest levels at 60 h). Overall, mutant transcripts are expressed in higher levels in JW-13 than in JW-12. This could, at least in part, explain variation in the number of genes differentially expressed in JW-12 (100 genes) compared to JW-13 (40 genes). We also propose that accumulation of the *atfB* disruption transcript at 24 h has a greater overall impact on the transcriptome as compared to accumulation of this transcript at a later time point. Since aflatoxin gene expression is first detected between 24 and 30 h of growth under standard conditions⁶⁴, high levels of expression of the disruption construct at 24 h could either block expression of the wild type transcript prior to the onset of aflatoxin synthesis or block ribosome access to the wild type transcript. In contrast, accumulation of disruption transcript after aflatoxin gene expression has already initiated may minimize the impact on aflatoxin gene expression. Although it may be useful to characterize MT transcript accumulation prior to 24 h via RNA Seq analysis in disruption strains, focusing our efforts on analyzing specific subset of genes altered due to AtfB function will be of priority.

Unique expression patterns of the MT transcript resulted in strongly overlapping (38 out of 40 genes in JW-13 overlapped with specific genes in JW-12) subsets of

genes down-regulated in JW-12 and JW-13 providing a direct connection between expression of the *atfB* disruption construct, a decrease in AtfB function, a decrease in accumulation of aflatoxin enzymes, and down regulation of the specific target genes. These data strongly suggest that the overlapping subset of genes that were down regulated in both JW-12 and JW-13 are downstream targets of the AtfB regulatory network.

We observed that 20 genes in the aflatoxin gene cluster were down regulated in JW-12 and JW-13 as compared to SU-1. Although differences in the expression of these genes were not statistically significant, the overall trend of down regulation partially supports decreased levels in accumulation of aflatoxin enzymes, Nor-1, OmtA, and Ver-1. It is interesting to note that most genes in the 'middle' of the aflatoxin cluster are down regulated compared to 'early' and 'late' genes that flank this middle region (**Figure 14B**, page **69**). This observation may support a role for histone H4 acetylation in regulation of the aflatoxin cluster. In a previous study, we observed that the order of genes in the aflatoxin cluster determines the timing and level of transcriptional activation⁶⁴. In this study, we proposed that the number and location of CRE-binding sites in promoter regions of the aflatoxin genes enable AtfB to mediate localized unwinding of histones and location-specific initiation of gene expression.

REViGO is a free, rapid, and simple web-based server tool for characterization and visualization of enriched functional categories expressed as GO terms. Gene ontology or GO provides categories based on relationships of genes related to cellular component, molecular function, or biological processes. The REViGO software is a computer-based tool (algorithms based on a hierarchical clustering) that groups highly

similar GO terms while working to reduce redundancy within lists of such terms¹⁰³. The most prominent trend in our results is consistent with previous and current research, with genes involved in secondary metabolism and oxidative stress pathways being altered (statistically significant) in disruption strains JW-12 and JW-13 as compared to SU-1 (control). REViGO also revealed gene targets over-represented in novel pathways that could potentially be regulated by AtfB. This extends the role of AtfB regulation beyond aflatoxin synthesis, oxidative stress response, and development to other biological processes such as stress signaling (pH regulation), to other stress response networks (glutathione biosynthesis), and to intracellular transport machinery (actin rearrangement). Of particular interest, the actin cytoskeleton rearrangement and transport GO term is the second most represented category in this analysis. Analyzing AtfB function directly related to specific gene targets in this category will be one focus of future research.

Our current work demonstrates that the genetic alteration of AtfB function altered AtfB binding to promoters of target genes in regulatory networks involved in co-regulation of expression of the aflatoxin biosynthetic pathway, of oxidative stress-related enzymes, and of conidiospore development. The net result was a strong impact on the level of aflatoxin synthesis, conidiospore number/pigment, and fungal morphology (alterations in phenotype). We further suggest that AtfB represents a global, significant, and robust regulatory node in secondary metabolism (beyond aflatoxin), several cellular defense networks, and cytoskeleton arrangement and transport. Due to the low numbers of bZIP factors in the aspergilli genomes and the subset of fungal specific gene targets, the work with AtfB lays the groundwork to explore a unique target in

filamentous fungi for manipulation of beneficial and harmful secondary metabolites through transcriptional regulation.

CHAPTER 3: UTILIZING A CRISPR/CAS9-LIKE MECHANISM TO ELUCIDATE THE ROLE OF VPS34 IN AFLATOXIN SYNTHESIS

Data in this chapter will be included in a manuscript: **Wee J, Hong SY, Roze LV, Day DM, Chanda A, Linz JE (2015).**

ABSTRACT

The Class III phosphatidylinositol-3 kinase, Vps34 localizes to subcellular compartments and is involved in autophagy, protein trafficking, and endosome maturation in yeast. In this study, we show that in the filamentous fungus *Aspergillus parasiticus*, Vps34 plays a role in the synthesis, compartmentalization, and export of aflatoxin, one of the most potent naturally occurring carcinogens known. Here we show that a novel endogenous CRISPR/*cas9*-like system in *A. parasiticus* down regulates function of the fungal Vps34. We observed multiple tandem integration of the disruption construct at ectopic sites in the *A. parasiticus* genome. The efficacy of this method was assessed by correlating high levels of mutant *vps34* transcript (a decrease in wild type *vps34* transcript) to an increase in aflatoxin synthesis and export and alteration in fungal development. Disruption of Vps34 (encodes a lipid kinase known to regulate fusion of early endosomes to late endosomes in yeast) or treatment with 3-methyladenine (predominantly inhibits activity of Class III PI3Ks) increased aflatoxin synthesis and export. Finally, we propose that the cellular process of compartmentalization and export of secondary metabolites can be considered a virulence-associated process and contributes to virulence of *A. parasiticus*.

INTRODUCTION

Phosphatidylinositol 3-kinases (PI3K) are lipid kinases that have been implicated in a wide array of human diseases such as cancer, inflammation, and autoimmune dysfunction^{106–108}. Therefore, PI3Ks have been attractive cellular targets for drug development. Lipid products of these kinases act as key mediators of intracellular signaling pathways involved in growth, motility, survival, homeostasis, and protein trafficking^{109–113}. Defects in PI3K function and disruption in lipid product signaling have been associated with deficiencies in cellular metabolic functions and autophagy. In particular, the Class III PI3K vacuolar protein sorting-34 (Vps34) was shown to localize to specific sub-cellular compartments called endosomes in yeast^{113,114}. Vps34 in yeast is involved in the cellular processes of protein trafficking and autophagy, and more specifically in the maturation and fusion of early endosomes. We hypothesized that *A. parasiticus* Vps34 plays a key role in aflatoxin biosynthesis.

Aflatoxin biosynthesis is a tightly regulated process in *A. parasiticus*. Aflatoxin synthesis begins with the activation of specific genes clustered in a 70 kb region of chromosome 3¹⁷. Synthesis of this secondary metabolite also involves sequential, highly coordinated sub-cellular protein trafficking leading to the production of aflatoxisomes. These specialized endosomes have been shown to complete the final steps of the aflatoxin biosynthetic pathway and likely play a role in most, if not all, biosynthetic steps. We previously demonstrated that aflatoxin synthesis and export are mediated by aflatoxisomes and that aflatoxisomes carry proteins involved in the final steps of aflatoxin synthesis in *A. parasiticus*^{115,116}. Chanda et al. blocked endosome fusion to the vacuole by a genetic knockout of AvaA (encodes a late endosome GTPase known as

Ypt7 in yeast) or by an inhibitor of Vps16, called Sortin 3⁶². Ypt7 associates with the late endosome tethering complex called HOPS and Vps16 associates with HOPS and the early endosome tethering complex called CORVET. AvaA knockout and Sortin 3 treatment increased aflatoxin protein levels and increased the synthesis, storage, and export of aflatoxin. Thus, activation of aflatoxin export was associated with a down-regulation of the vacuole-targeting pathway and up-regulation of the endosome export pathway.

Previous work conducted in our laboratory indicated involvement of PI3Ks in regulation of aflatoxin biosynthesis⁸⁸. Wortmannin, an inhibitor of Class I and II PI3K down-regulated aflatoxin accumulation and aflatoxin gene expression through a cAMP-dependent PKA pathway. We proposed that a cytosolic wortmannin-sensitive cAMP-dependent PKA pathway participates in regulation of aflatoxin gene expression and aflatoxin production. Here, we utilized a novel endogenous CRISPR/*cas9*-like system in *A. parasiticus* to down regulate function of the fungal Class III PI3K called Vps34. In contrast to the cytosolic Class I and II PI3K, the Class III PI3K Vps34 localizes to early endosomes in yeast and helps mediate maturation of early endosomes and their fusion to form late endosomes. As expected, the endogenous CRISPR-like system did down regulate expression of *vps34*. Although the observed mechanism for down-regulation of the *vps34* transcript is not identical to a canonical CRISPR/*cas9* system, the fungal system does exhibit several key hallmarks of bacterial CRISPRs (see **Discussion**, page **108**).

Clustered interspaced short palindromic repeats (CRISPRs) are DNA loci found in up to 40% of sequenced eubacterial species and up to 90% of sequenced

archaea^{117,118}. CRISPRs provide prokaryotes with the ability to mount an “acquired immune response” (adaptive immunity) to viral infection and to the presence of foreign plasmids. As viral or plasmid DNA enters the cell, small portions of the DNA are replicated and the resulting “DNA spacers” are inserted in a set of repeated sequences adjacent to the CRISPR locus. The DNA region carrying the DNA spacers is expressed and the resulting transcript is processed by a zinc-finger *cas* (CRISPR associated sequence) endonuclease to generate crRNA (CRISPR RNA). Upon a new cycle of viral infection, another *cas* protein (Cas type III) forms a complex with crRNA and the viral genome and the *cas9* protein (a type II Cas) generates sequence specific breaks in the viral genome as directed by the ends of the crRNA sequence (also called guide RNA or gRNA).

We demonstrate that multiple copies of a the *vps34* knockdown construct integrate in tandem at an ectopic site and that expression of mutant transcripts is strongly associated with down-regulation of wild type *vps34* transcripts. The inverse relationship between wild type and mutant transcripts is reminiscent of RNAi and is particularly important because it correlates to a specific phenotype observed in mutant strains. JW-17, a representative strain that carries the *vps34* knockdown construct exhibited a 6-fold increase in aflatoxin production, increased growth, and increased conidiospore development. The phenotype observed after knockdown of the early endosome protein Vps34 is similar to the phenotype observed after disruption of the late endosome protein AvaA or after inhibition of the activity of Vps16, which is present in tethering complexes in early and late endosomes. Therefore, we propose that an endogenous CRISPR/*cas9*-like system that evolved in filamentous fungi is able to alter

'foreign DNA' entering the cell. To our knowledge, we are the first to show that this system exists in fungal cells and also the first to demonstrate a role for a Class III PI3K in secondary metabolite (aflatoxin) biosynthesis. We also propose that Vps34 encodes a protein that plays a key role in maturation and fusion of early endosomes in *A. parasiticus* and that downregulation of Vps34 downregulates endosome fusion and upregulates aflatoxin synthesis, storage, and export.

MATERIALS AND METHODS

Fungal strains, media, and growth conditions

A. parasiticus strain SU-1 (ATTC 56775) was the wild-type aflatoxin-producing strain used in this study. *A. parasiticus* NR-1 which harbors a non-functional gene encoding nitrate reductase (*niaD*) was derived from SU-1 and used as a recipient and control strain for co-transformation (for the purpose of clarity, we will refer to NR-1 as the host strain)⁹⁹.

YES liquid medium (2% yeast extract and 6% sucrose, pH 5.8) and a chemically defined GMS liquid medium (previously described in Roze et al. 2004) were used as aflatoxin-inducing growth media⁵⁵. Conidiospores from frozen mycelia stock solutions were inoculated into 100 mL liquid medium at a final concentration of 10^4 spores per mL; each flask contained five 6-mm glass beads (Sigma)⁴⁴. Cultures were incubated at 30°C with shaking at 150 rpm in the dark for designated time periods (standard conditions).

Potato dextrose agar (PDA; Becton Dickinson, Franklin Lakes, New Jersey) was used as an aflatoxin-inducing solid growth medium. 10^4 spores (10 μ l) were center-

inoculated onto the solid medium surface which was then incubated for 24 h to 120 h at 30°C in the dark.

3-methyladenine (3-MA) was obtained from Sigma Aldrich (St. Louis, MO).

Identification, cloning, and disruption of *A. parasiticus* Vps34

Vps34 was identified and designated AFLA_099880 (encodes a 902 amino acid protein, NCBI Accession EED46324.1) based on the published *A. flavus* genome database (<http://www.aspergillusflavus.org/>). *A. parasiticus* Vps34 sequence identity was confirmed by cloning, nucleotide sequence analysis, and comparison against the recently published *A. parasiticus* genome sequence available through the NCBI database (Accession: JMUG00000000) (<http://www.ncbi.nlm.nih.gov/>).

We amplified two fragments (Fragment 1, 5'- ATGGAGGCCTTCACATTCGC -3', forward primer, Fragment 1, 5'- ATCGATTAAGCTTCATTAGGGAGAATTTCCACTGCCTGA- 3', reverse primer; Fragment 2, 5'- CTAATGAAGCTTAATCGATTTCGCTGGCTAATTTCTT -3', forward primer, 5'- TCATGCTCTCCAACCCTGAA -3', reverse primer) from an ORF of 2,796 bp by PCR. Primers were used to create the two fragments for overlap extension PCR which in turn created a 200 bp deletion in the middle of the ORF and inserted an adjacent *HindIII*-site (**Figure 19B**). Integration of the knockout construct into the wild type Vps34 locus would in theory generate a frame shift and production of a truncated protein downstream of the 200 bp deletion. The Vps34-OE PCR product (2,528 bp) was cloned into a pGEMT easy vector, transformed into competent *E. coli* cells (Invitrogen) and confirmed by nucleotide sequence analysis (ABI robotic catalyst and 373A DNA

sequencer) at the Research Technology Support Facility Genomics Core, Michigan State University. Protoplasts were obtained as previously described from strain NR-1 (*niaD*⁻, aflatoxin +)⁹⁹. A circular and uncut plasmid pSL82 containing a 6.3-kb *Hind*III fragment with the selectable marker *niaD* was used together with a *Sac*I-linearized Vps34 disruption construct for co-transformation of strain NR-1. We also transformed the circular and uncut plasmid pSL82 alone into the host strain, NR-1 to serve as a transformation control.

Molecular analysis of transformants

84 *niaD*⁺ transformants were obtained from co-transformation of NR-1 with the Vps34 disruption construct and pSL82. 6 *niaD*⁺ transformants were chosen from transformation of NR-1 with pSL82 alone to serve as a control. Genomic DNA obtained from the combined 90 transformants was screened using the SIB-selection method by an initial PCR screen using primers 5'-TACTGTCGTACGAGCCAACG -3', forward primer; 5'- TGCTCAGGATGCACTTGTTTC -3', reverse primer, followed by isolation of individual strains within a SIB which resulted in identification of isolates JW-17, JW-39, and JW-54. Genomic DNA was isolated from frozen fungal mycelium using the phenol-chloroform method previously described⁴⁴. A 200 bp deletion within the Vps34 construct enabled identification of two fragments, a 600 bp wild type Vps34 fragment and a 400 bp mutant fragment. Transformants that carried the disruption construct were then subjected to two rounds of single spore isolation to obtain a genetically stable isolate.

Genomic DNA from *A. parasiticus* SU-1, *A. parasiticus* host strain NR-1, *A. flavus* NRRL3357 and transformant strain JW-17 was isolated from frozen fungal mycelium

using the phenol-chloroform method previously described⁴⁴. Southern hybridization analysis was performed as described in Chapter 2⁸². Briefly, 2.5 µg genomic DNA obtained from wild type *A. parasiticus* SU-1, host strain NR-1, and *A. flavus* NRRL 3357 was digested for 16 h with 20 U of *Bam*HI-HF and *Eco*RI-HF for the Southern blot control (NEB, Ipswich, MA). Genomic DNA obtained from SU-1 and JW-17 was digested with *Bam*HI-HF, *Eco*RI-HF, *Sac*I, and *Hind*III to test the presence of the *Vps34* disruption construct. Digested DNA was separated on a 0.8% agarose gel and transferred onto a Nytran® SuPerCharge membrane (Schleicher and Schell, Inc., Keene, NH) by capillary transfer. Membranes were UV cross-linked (120,000 uJ/cm²) in a UV Stratalinker 2400 (Stratagene, Inc., La Jolla, CA).

A 600 bp *vps34* probe was generated by PCR (5'-TACTGTCGTACGAGCCAACG -3', forward primer; 5'-TGCTCAGGATGCACTTGTTTC -3', reverse primer). PCR products were purified with a Qiagen Gel purification kit (Qiagen, Valencia, CA). Probe labeling, hybridization, and detection were performed using an Amersham Gene Images AlkPhos Direct Labeling and Detection System (GE Healthcare, Pittsburg, PA) according to manufacturer's instructions.

Aflatoxin measurements in strains SU-1, JW-17, and in 3-methyladenine experiments

Triplicate cultures of SU-1 and JW-17 were grown in YES liquid medium under standard conditions (see above) and harvested at designated time points (24 h, 40 h, 60 h). Aflatoxin B₁ concentration (µg) in the medium was quantified by ELISA using anti-

aflatoxin B₁ polyclonal antibodies (Sigma-Aldrich, St. Louis, MO) and normalized to mycelial dry weight (g) as previously described^{66,82}.

In two independent biological experiments (n=4 for each treatment), SU-1 was grown in GMS liquid medium under standard aflatoxin inducing conditions and treated with either DMSO (vehicle control) or 50 µM 3-MA and harvested at 72 h of growth. Aflatoxin B₁ levels in the medium were quantified by an ELISA method as described above.

Statistical analysis was performed with the use of SigmaPlot software, version 11 (Systat Software Inc., San Jose, CA). ELISA and dry weight measurements are presented as the means ± S.E., n=3, and were analyzed by the Student's t test. ELISA measurements obtained from 3-MA studies are presented as means ± S.E., n=4 (Grubb's test did not detect a significant outlier).

RNA isolation and transcript analysis

Triplicate cultures of SU-1 and JW-17 were grown in YES liquid medium under standard conditions, harvested at 24 h, 40 h, and 60 h and fungal cells disrupted using a mortar and pestle in the presence of liquid nitrogen. TRIzol® reagent (Invitrogen, Grand Island, NY) was used to extract total RNA from ground mycelium⁵³. An Agilent 2100 Bioanalyzer (Agilent Technologies, Santa Clara, CA) was used to assess RNA quality. Total RNA (1 µg) was reverse-transcribed into cDNA with the QuantiTect reverse transcription kit (Qiagen).

A 600 bp *vps34* transcript was amplified with *vps34* specific primers (5'-TACTGTCGTACGAGCCAACG -3', forward primer; 5'- TGCTCAGGATGCACTTGTTTC -

3', reverse primer) by RT PCR of cDNA prepared from cultures after 24 h, 40 h, and 60 h of growth. A 200 bp deletion within the Vps34 construct enabled identification of two fragments derived from the 600 bp wild type *vps34* transcript and the 400 bp mutant transcript to assess change in the ratio of wild type to mutant transcript over time. RT-PCR analysis of gene expression was performed as described in Chapter 2.

RESULTS

Key domains in fungal Vps34 are highly conserved across different species

To identify candidate genes that encode a Class III phosphatidylinositol-3 kinase in *A. parasiticus*, we searched the *A. flavus* genome database available at <http://www.aspergillusflavus.org/genomics/> using "Vps34" as a search landmark. The complete *A. flavus* and *A. parasiticus* genomes are now available (nucleotide accession number JMUG00000000). The search identified a single gene designated AFLA_099880 (NCBI amino acid sequence EED46324.1) encoding a putative phosphoinositide 3-kinase. Local NCBI BLAST and preliminary identification of conserved domains identified the resemblance of EED46324.1 to Class III PI3Ks. AFLA_099880 mapped to the left arm of Chromosome 6 in *A. flavus*. The nucleotide sequence and deduced amino acid sequence of Vps34 in *A. flavus* and *A. parasiticus* exhibited 98% identity.

The deduced amino acid sequence similarity is relatively high ranging from 85% to 99% within aspergilli species (BLAST results not presented). In contrast, *Aspergillus* Vps34 exhibit only approximately 40% identity to Vps34 in the baker's yeast, *Saccharomyces cerevisiae* and 42% identity to mouse and human Vps34.

AFLA_099880 encodes a 2,796 bp ORF in *A. flavus* that is 98% similar to *A. parasiticus*. We used the *A. flavus* AFLA_099880 sequence to help identify Vps34 in *A. parasiticus*. Based on the high degree of protein identity between *A. flavus* and *A. parasiticus* Vps34, we used the *A. flavus* amino acid sequence to identify conserved domains within the protein. We observed that Vps34 possesses an N-terminal lipid binding C2 domain, a PIK domain with unknown function, and a C-terminal ATP-binding catalytic domain. Based on protein sequence identity, these key regions are highly conserved among aspergilli (*A. flavus*, *A. fumigatus*, *A. nidulans*, *A. niger*, *A. oryzae*) and in yeast, mouse, and human Vps34 (**Figure 17**).

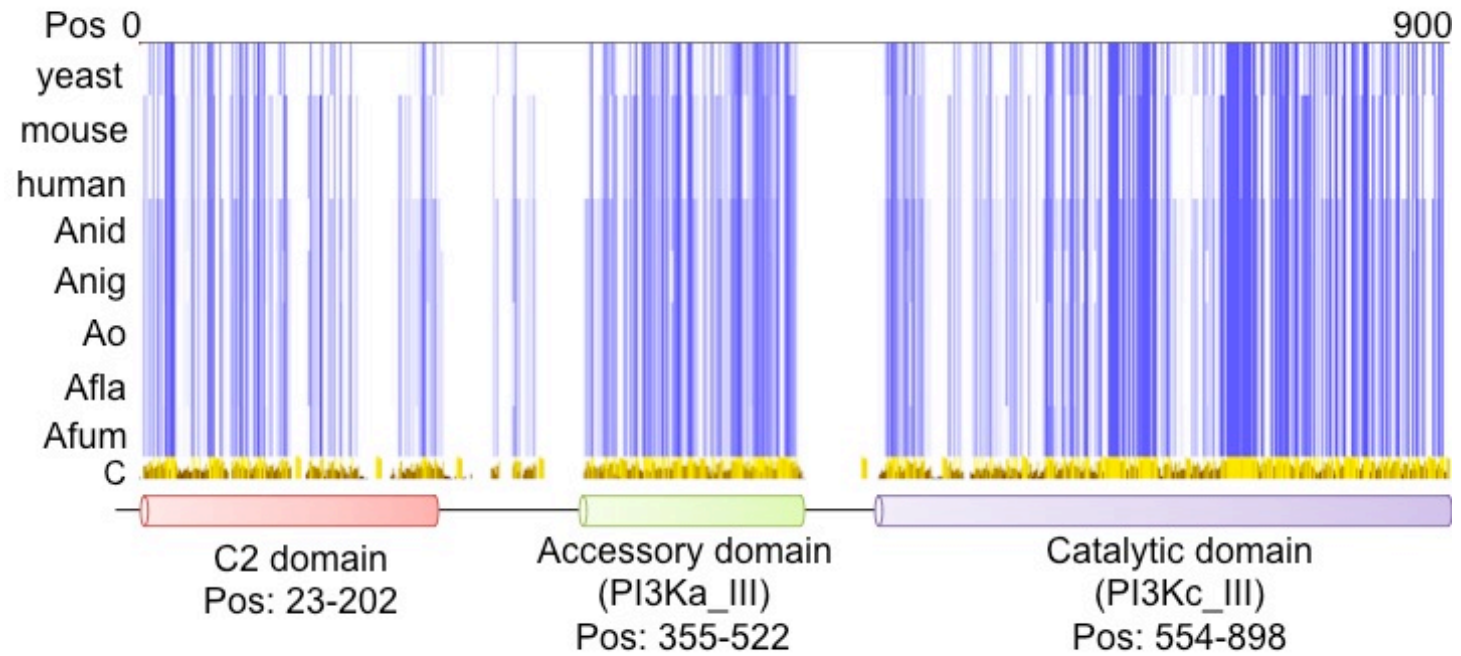


Figure 17 Alignment of Vps34 amino acid sequences from aspergilli, yeast, mouse and human

Figure 17 (cont'd)

The locus designated AFLA_099880 encodes a 902 amino acid protein that is highly conserved across different species. Multiple sequence alignment was performed by ClustalOmega (<http://www.ebi.ac.uk/Tools/msa/clustalo/>). A specific JAVA plugin was used to create similarity plot visualization. Gaps in the similarity plot represent regions of reduced sequence identity and the intensity of the blue bars indicates the percentage similarity (darker blue corresponds to higher similarity). All classes of PI3Ks (Class I, II, III) are known to possess three key regions essential for function; an N-terminal lipid binding C2 domain, a PIK domain with unknown function, and a C-terminal ATP-binding catalytic domain. Classes of PI3K are not only determined by their protein domain structures but by their substrate specificity and cellular regulation. The *A. flavus* Vps34 amino acid sequence was used as a reference to highlight specific amino acid positions corresponding to each domain. Abbreviations: Afla, *Aspergillus flavus*; Afum, *A. fumigatus*; Anid, *A. nidulans*; Anig, *A. niger*; Ao, *A. oryzae*; Pos, amino acid position; C, conservation plot highlighting regions of highest similarity depicted by yellow bars.

Vps34 mutant construct stability and potential loss of mutant phenotype

Initial PCR screening and preliminary characterization of Vps34 transformants were conducted as described in the Methods section. A collection of isolates was created from 90 transformants and genomic DNA was subsequently isolated by a sib-selection strategy¹¹⁹. Pooled gDNA from 15 SIBs ('siblings') was analyzed by PCR. Each SIB contained a gDNA pool of 6 isolates. SIB 15 contained 6 isolates from the pSL82 only transformation and served as a control (**Figure 18A**, last lane '15'). PCR analysis of gDNA obtained from SIB 4, 8, and 11 clearly indicated the presence of the Vps34 construct (600 bp native Vps34, 400 bp Vps34 disruption construct). Each isolate within SIB 4, 8, and 11 was grown and gDNA isolated for a follow up PCR. Transformants JW-17, JW-39, and JW-54 screened positive for the 400 bp Vps34 disruption construct (**Figure 18B**). JW-17, JW-39, and JW-54 also exhibited similar phenotype and were subjected to two rounds of single spore isolation. After one round of single spore isolation to obtain a genetically pure isolate, we observed the loss of phenotype due to construct instability. PCR analysis of JW-54 indicated the disappearance of the 400 bp fragment indicative of loss of the disruption construct (**Figure 18C**). JW-17 retained the construct after two rounds of single spore isolation (data not shown) and was used as a representative strain for further analysis.

Multiple tandem integration of *vps34* knockout construct into an ectopic site in the *A. parasiticus* genome

NR-1 (host strain) and JW-17 (one representative strain used for further analysis) were grown in aflatoxin inducing YES medium and the extracted gDNA was analyzed by

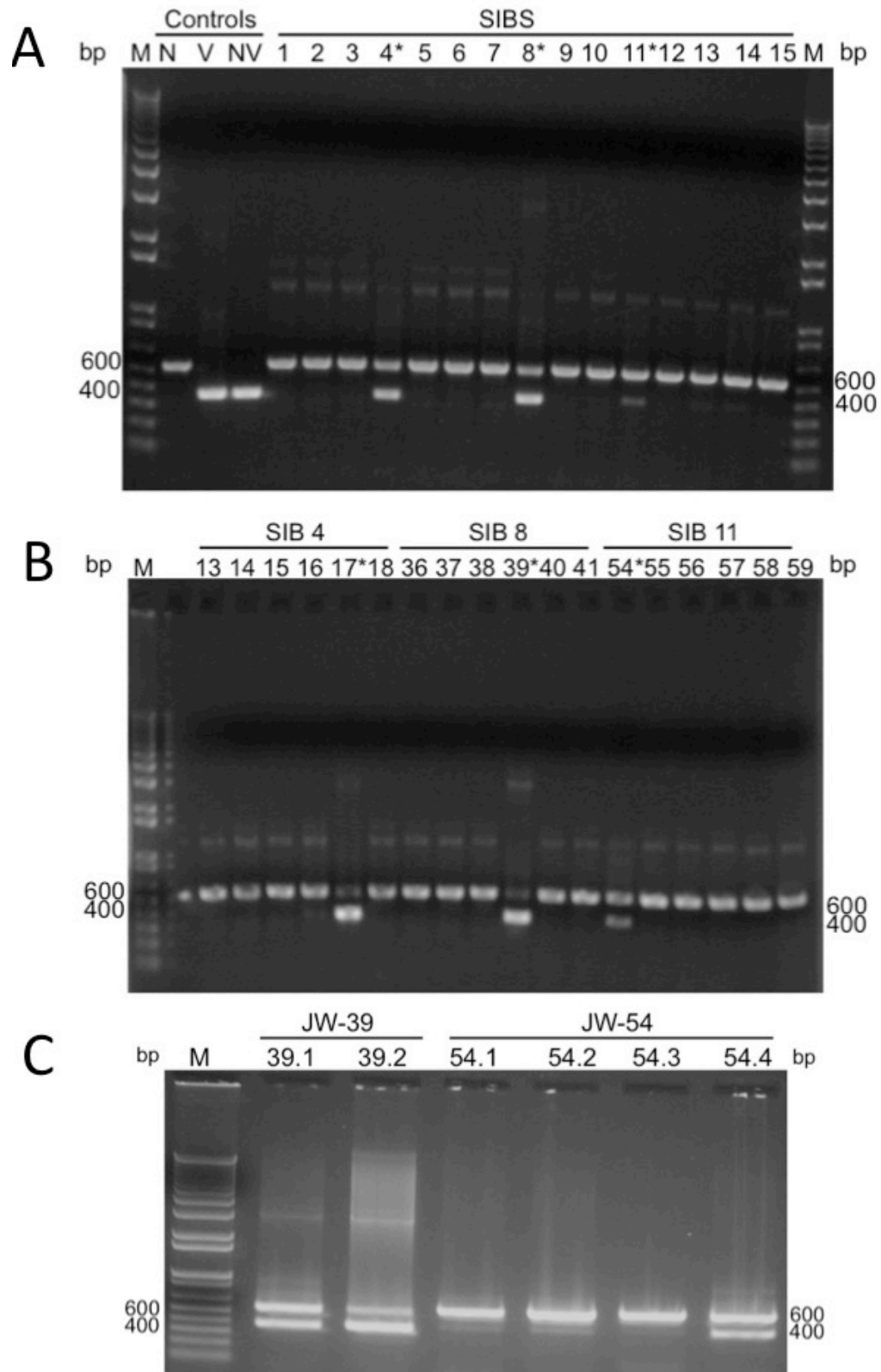


Figure 18 Molecular characterization of Vps34 transformants

Figure 18 (cont'd)

Molecular characterization of Vps34 transformants. **Panel A:** SIB-selection strategy for screening transformants by initial PCR screening. gDNA was obtained from 15 SIBs (6 isolates per SIB) and subjected to PCR analysis. SIB 15 contained 6 isolates from the pSL82 only transformation and served as a control. SIB 4, 8, and 11 screened positive for the 400 bp Vps34 disruption construct with the 600 bp native construct still present. PCR controls used, N: 50 ng gDNA obtained from host strain, NR-1; V: 50 ng OE-PCR Vps34 disruption construct used for co-transformation; NV: Vps34 disruption construct in the background of NR-1 gDNA. **Panel B:** PCR analysis of 6 isolates obtained from SIB 4, 8, and 11. Transformants 17, 39, and 54 screened positive for the 400 bp Vps34 disruption construct. The intensity of the 600 bp fragment as compared to the 400 bp fragment (ratio of band intensity) indicates varying number of copies of ectopic integration. **Panel C.** Supporting evidence for potential loss of knockdown construct after single spore isolation procedure. PCR analysis of gDNA obtained from JW-39 and JW-54 after one round of single spore isolation. The ratio of the 600 bp native Vps34 fragment to 400 bp mutant Vps34 fragment in JW-39 indicated higher amounts of the mutant construct (Panel B, lane labeled '39*'). After a single round of single spore isolation, PCR analysis indicates equal amounts of native and mutant fragments present in JW 39.1 and JW 39.2. The potential loss of construct is demonstrated by first round single spore isolates of the unstable strain JW-54 isolate 54.1, 54.2, and 54.3. Note the complete disappearance of the 400 bp mutant Vps34 fragment in JW 54.2. One potential weakness of this genetic system is construct stability, which may be influenced by the location of ectopic integration within the genome.

Southern blot analysis under high stringency conditions using a 600 bp DNA probe (see **Methods**). Genomic DNA isolated from NR-1 was digested with *Bam*HI or *Eco*RI, transferred to a solid Nytran support, and probed with the 600 bp fragment. The resulting pattern of fragments (a single fragment in each of the digests) suggested the presence of a single *vps34* copy present in *A. parasiticus* SU-1 (wild-type), *A. parasiticus* NR-1 (control and recipient host strain for co-transformation), and *A. flavus* wild-type strain NRRL3357 (closely related species) (**Figure 19C**). The 5.0 kb *Bam*HI- and 7.0 kb *Eco*RI bands observed in the host strain NR-1 appeared intact at the same location in JW-17 (**Figure 19D**) indicating that the wild-type *vps34* gene was not replaced by the *vps34* disruption construct by co-transformation. However, we did observe integration of multiple copies of the *vps34* construct at a different ectopic site in JW-17 (non-native recombination) (**Figure 19D**). This is supported by the observation of a “ladder effect” in lanes 2, 4, 6, and 8 (designated 17). Band intensity of the ectopically integrated construct is approximately 2-3 times higher than that of the native locus (**Figure 19D**, lane 1, 3, 5, 7 designated C) suggesting multiple copies of the *vps34* knockout construct integrated at a non-native locus. The presence of a *Hind*III-site within the *vps34* construct and the resulting restriction band patterns supported tandem integration of *vps34* constructs as observed by disappearance of high intensity bands in JW-17 *Hind*III-digested genomic DNA (**Figure 19D**, compare lane 8 to lane 2, 4, 6). Based on these analyses, we hypothesized that multiple tandem integration of the disruption construct at ectopic sites in JW-17 is associated with the modified phenotype observed in mutant strains JW 17, JW 39, and JW 54.

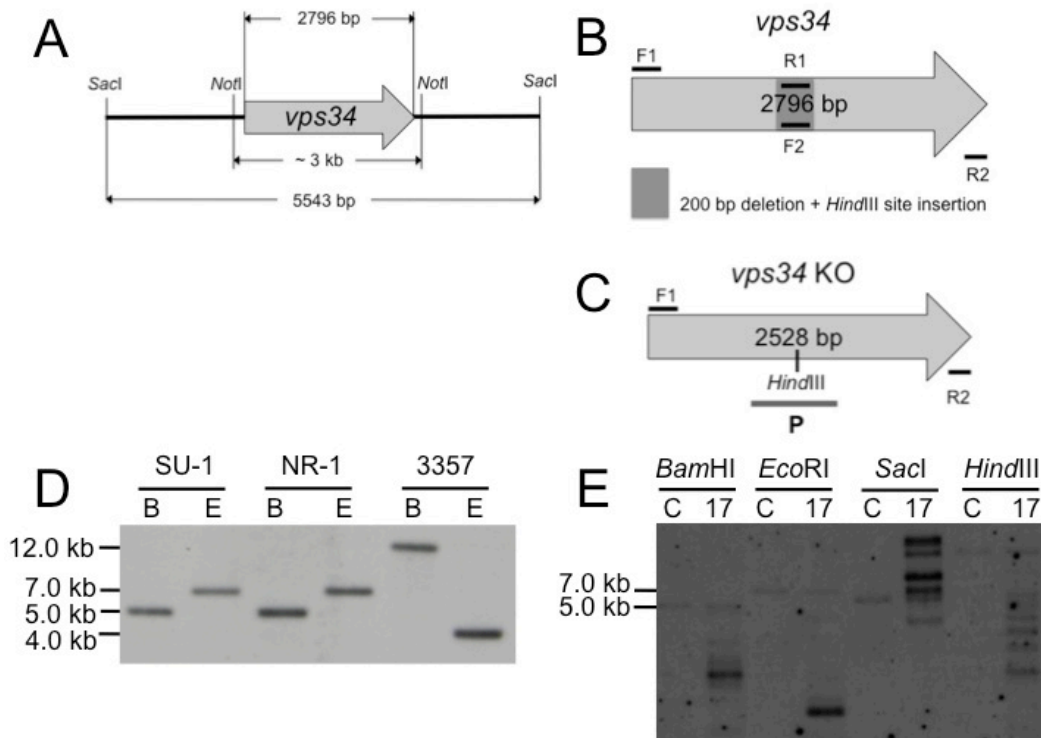


Figure 19 Disruption of Vps34 and Southern hybridization (blot) analysis

Panel A. *Vps34* encodes a 2796 bp ORF. **Panel B.** Primers F1 and R1 were used to generate Fragment 1 and primers F2 and R2 were used to generate Fragment 2. The resulting fragments were amplified by primers F1 and R2 to generate an overlap extension PCR (OE-PCR) product of 2528 bp. **Panel C.** The *vps34* OE-PCR product contained a 200 bp deletion with an adjacent *HindIII*-site. This construct was cloned into a pGEMTeasy vector and was used for co-transformation (see **Methods**). **Panel D.** Southern blot analysis of gDNA obtained from wild-type SU-1, the transformation control and host strain NR-1, and *A. flavus* NRRL3357 revealed a single copy of *Vps34* (B, *Bam*HI-digest; E, *Eco*RI-digest). **Panel E.** Southern blot analysis of control and host strain NR-1 (C) and representative *vps34* knockdown strain, JW-17 (designated 17). Multiple tandem integration of the *vps34* knockdown vector at a non-native locus can be observed in mutant strain JW-17 (Lanes 2, 4, 6, 8).

Presence of the *vps34* disruption construct is directly linked to increased aflatoxin synthesis and conidiospore development

On an aflatoxin-inducing solid growth medium (PDA), growth of strains SU-1 and JW-17 was observed for 24 h to 120 h. Although ectopic integration of the *vps34* construct did not alter fungal growth rate significantly on solid media, we did observe slight increases in conidiospore number and spore pigmentation by visual inspection at 48 h and 120 h by visual inspection (**Figure 20**).

Under standard aflatoxin inducing conditions, *A. parasiticus* initiates aflatoxin synthesis between 24 and 30 h, and maximum levels of synthesis occur by 40 h^{53,62}. Comparing aflatoxin levels produced by SU-1 and JW-17 in aflatoxin inducing YES medium, JW-17 produced 2-fold more aflatoxin at 40 h (not statistically significant, P=0.2) and 6-fold more aflatoxin at 60 h (statistically significant, P=0.01) when compared to SU-1 (**Figure 21B**). We also observed the development of cleistothecia (asexual survival structures) in JW-17 and not in SU-1. It was also interesting to note an increase in fungal growth in JW-17 compared to SU-1 (observable trend, not statistically significant) (**Figure 21A**). The presence of survival structures and the observed increases in growth support the proposed association between aflatoxin production and fungal fitness and these phenotypes also may contribute to ecological competitiveness between toxigenic strains and non-toxigenic strains of *A. parasiticus* in the soil environment.

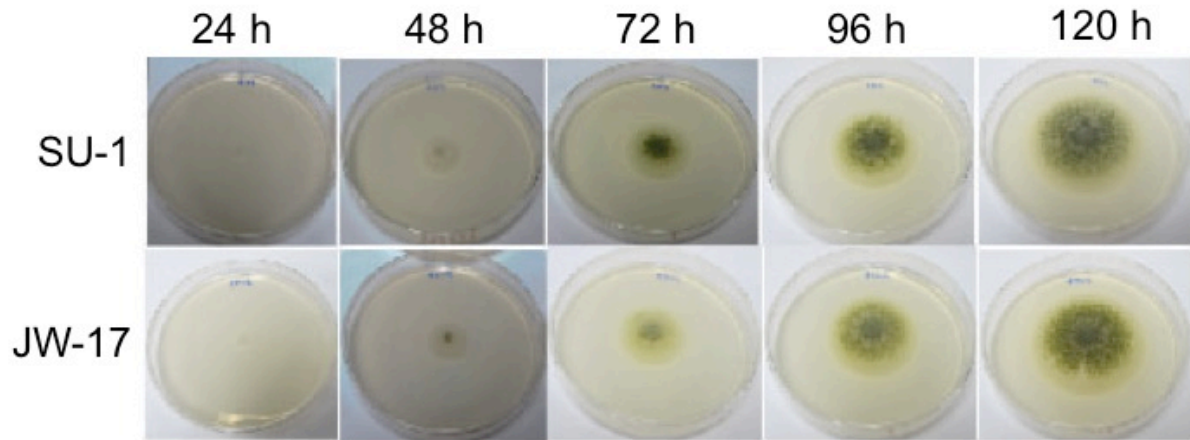


Figure 20 Characterization of fungal growth, conidiospore number and pigment, and aflatoxin production (phenotype) in strains SU-1 and JW-17

A. parasiticus strains were grown for 24, 48, 72, 96, and 120 h on aflatoxin inducing PDA agar and analyzed for growth and conidiospore number/pigment. We observed slight increases in conidiospore number and spore pigmentation at 48 h and 120 h by visual inspection but not at 72 h and 96 h.

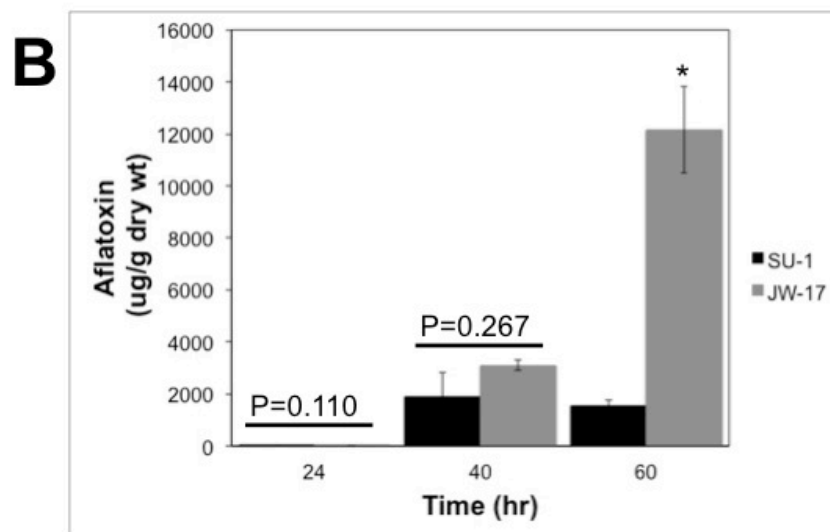
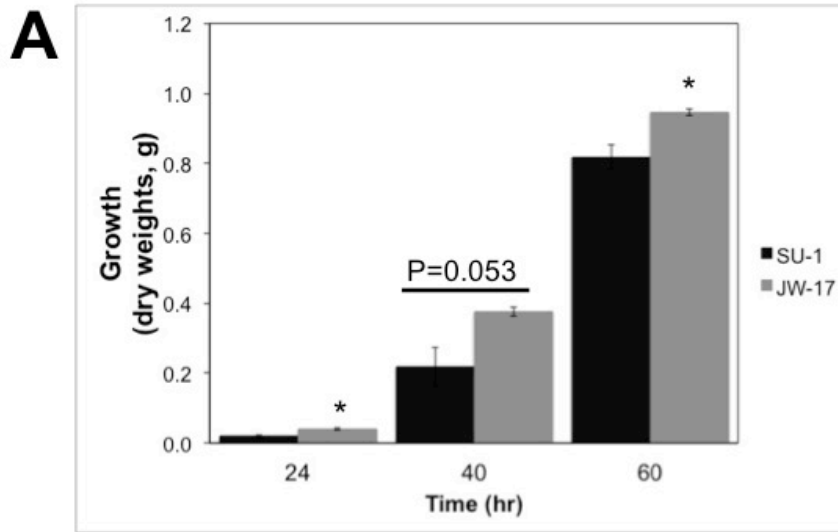


Figure 21 Aflatoxin levels and growth measurements in SU-1 and JW-17

Panel A: Dry weight comparison between SU-1 and JW-17 (a *vps34* knockdown strain) grown in YES medium for 24 h, 40 h, and 60 h. Dry weights are presented as the means \pm SEM; $n=3$ per strain per time point). Dry weight measurements indicate a statistically significant increase in growth at 24 h and 60 h ($p<0.05$) but not at 40 h ($P=0.053$) in JW-17 compared to the control SU-1.

Figure 21 (cont'd)

Black bars: wild type SU-1, grey bars: Vps34 disruption mutant JW-17. **Panel B:** Comparison of aflatoxin accumulated in the growth medium by SU-1 and JW-17. Aflatoxins in the medium were quantitated by ELISA (presented as means \pm SEM; triplicate samples, n=3 per time point per strain) and normalized to dry weight of the mycelium. Aflatoxin accumulation in the medium indicated a 6-fold increase in aflatoxin levels (statistically significant, $p < 0.01$) at 60 h in JW-17 compared to SU-1. Aflatoxin accumulation in JW-17 at 24 h and 40 h showed increased levels when compared to SU-1, although this difference was not statistically significant (p-values presented above bar graphs). Differences in aflatoxin at 60 h were statistically significant.

Taken together, these data support a direct association between the presence of the *Vps34* disruption construct in the *A. parasiticus* genome with the occurrence of increased growth, increased conidiospore development and higher aflatoxin production in JW-17.

***Vps34* mutant transcript expression levels increase over time**

We amplified a 600 bp fragment of the *vps34* transcript by semi-quantitative PCR (RT PCR) from cDNA obtained from SU-1 and JW-17 after 24 h, 40 h, and 60 h of growth. Due to the presence of a 200 bp deletion in the *vps34* disruption construct, we were able to resolve two fragments (600 bp corresponding to wild type *vps34* and 400 bp corresponding to the knockout construct) in cDNA populations prepared from JW-17 subsequently allowing the assessment of the ratio of wild type *vps34* transcript to mutant *vps34*. The quantity of mutant *vps34* transcript produced by integration of the *vps34* knockout construct showed a significant increase over time (**Figure 22**) strongly suggesting that the disruption construct is expressed at the transcript level. We also observed time-dependent differential expression when comparing *vps34* mutant transcript levels at 24 h in JW-17 as compared to 40 h and 60 h. These data suggest that the inverse relationship between mutant and wild type *vps34* transcript (down-regulation of wild type *vps34* transcripts and increase in mutant transcripts) is associated with the altered phenotype observed in mutant strains JW-17, JW-39, and JW-54.

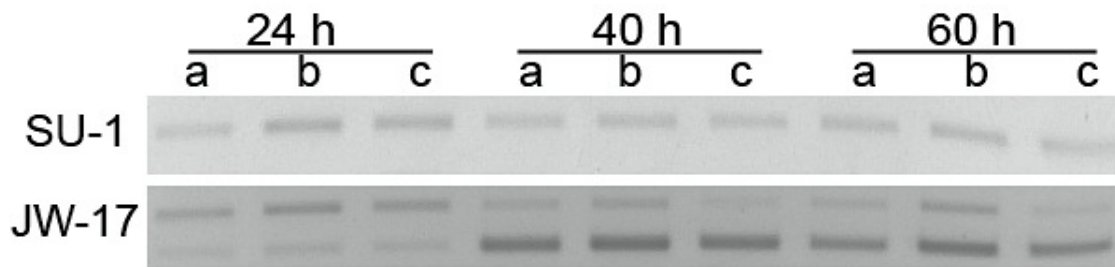


Figure 22 Mutant *vps34* transcript levels are up-regulated in JW-17

We exploited the endogenous CRISPR/*cas9*-like system to knock down Vps34 in *A. parasiticus* NR-1 using the same strategy as for AtfB (Chapter 2). Vps34 encodes a Class III PI3K that positively regulates early endosome maturation and fusion. Vps34 mutant strain JW-17 exhibited increased aflatoxin synthesis, growth, and conidiospore development. We conducted RT-PCR analysis of expression of the wild-type and mutant *vps34* transcript. The larger fragment (600 bp) in JW-17 represents the wild-type *vps34* transcript and the smaller fragment (400 bp) is the mutant *vps34* transcript (see **Methods**). Expression of the mutant transcript significantly down-regulated expression of the wild-type *vps34* transcript in strain JW-17. Each sample was conducted in triplicate (n=3) per time point per strain. **Figure 19** represents one of two independent biological replicate experiments. This genetic system for gene knockdown in *A. parasiticus* exhibits several key hallmarks of CRISPR/*cas9* system observed in prokaryotes.

3-methyladenine increases aflatoxin synthesis in wild-type strain SU-1

Previous work conducted in our laboratory indicated involvement of PI3Ks in regulation of aflatoxin biosynthesis⁸⁸. The discovery that PI3Ks are involved in multiple protein sorting and trafficking endocytic events and also in fusion of vesicles with the plasma membrane in yeast prompted us to investigate the effect of 3-MA, a selective inhibitor of predominantly Class III PI3K activity, on aflatoxin production^{120,121}. Treatment of wild-type SU-1 with 3-MA increased aflatoxin levels up to 10-fold in a chemically defined aflatoxin inducing GMS medium detected in the culture medium at 72 h of growth (**Figure 23**). The increased levels of aflatoxin accumulation observed in 3-MA treated fungal cultures suggest that a 3-MA sensitive PI3K plays a role in aflatoxin synthesis and export.

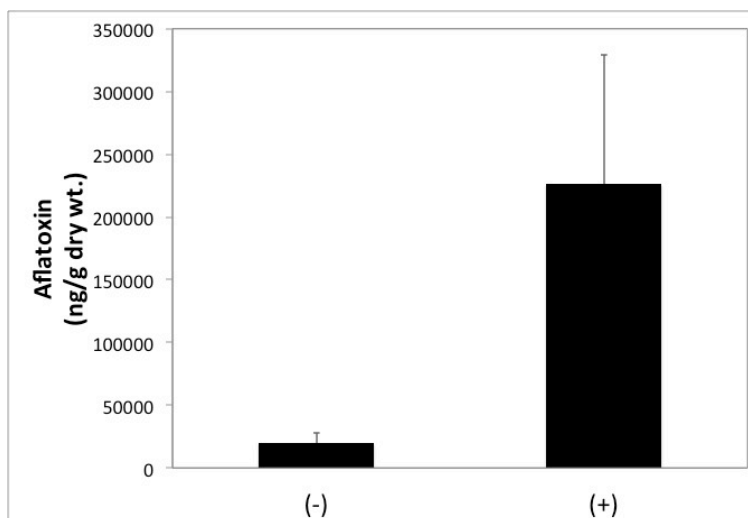


Figure 23 3-methyladenine increases aflatoxin levels in wild-type SU-1 under aflatoxin inducing GMS liquid medium

Comparison of aflatoxin accumulated in the media in the presence (+) and absence (-) of 3-MA after 72 h of growth in an aflatoxin inducing, chemically defined GMS medium. Aflatoxin levels were measured by ELISA and are presented as the mean \pm SEM (n=4 for each condition, DMSO vehicle control or 3-MA treatment) normalized to dry weights. 50 μ M 3-MA treatment up-regulated aflatoxin accumulation up to 10-fold (not statistically significant based on Student's t-test, $p=0.094$). Growth was not significantly affected at this concentration; however, we observed that 1 mM 3-MA inhibited growth of *A. parasiticus* when added to GMS medium.

DISCUSSION

Aflatoxin biosynthesis is a tightly regulated, non-growth related process. As part of transcriptional regulation, aflatoxin synthesis starts with the activation of specific genes clustered in a 70 kb region of chromosome 3 in *A. parasiticus*. Aflatoxin biosynthesis is triggered by environmental signals (such as absence of light, nutrient limitation, oxidative stress, and pH) that are sensed by a cAMP/PKA signaling pathway. The cAMP/PKA pathway activates specific transcription factors in the cytoplasm to translocate into the nucleus, bind to promoters of specific genes, and initiates gene expression. *A. parasiticus* begins aflatoxin synthesis between 24 h and 30 h, and maximal levels of toxin synthesis is observed by 40 h under standard aflatoxin inducing growth conditions (YES liquid medium). Between 30 h and 40 h, accumulation of aflatoxin transcripts and enzymes roughly correlate to the pattern of aflatoxin synthesis.

The activation of aflatoxin export is associated with down-regulation of the cytoplasm to vacuole-targeting pathway. A middle aflatoxin structural gene *ver-1*, encodes a NADPH dependent reductase that is responsible for the conversion of versicolorin A to demethylsterigmatocystin. Analysis of a strain B3-15 that expresses GFP-tagged Ver-1 protein demonstrated that at least part of Ver-1 is transported from the cytoplasm to the vacuole likely for protein turnover or degradation⁸¹. The prototypical yeast Class III PI3K Vps34 is involved in transport of proteins from the Golgi to the vacuole. It is likely that early endosomes carrying proteins such as Ver-1 depend on signaling by lipid products of Vps34 (PIP3) for protein turnover (vacuole) or fusion with late endosomes.

Chanda et al. (2009) demonstrated that blocking of endosome fusion to the vacuole by a genetic knockout of *AvaA* (encodes a late endosome GTPase known as Ypt7 in yeast) or by treatment with a small molecular weight inhibitor, Sortin 3 (inhibits a Vps16 activity; Vps16 is a protein associated with the endosome tethering complexes CORVET and HOPS) increased aflatoxin protein levels and increased export of aflatoxin⁶². Vps34, a Class III PI3-kinase and key component of the yeast early endosome membrane, is known to activate the small GTPase protein Ypt7 (Rab7, *AvaA*) [43], a component of the HOPS tethering complex. Vps34 in yeast was also reported to recruit the CORVET tethering complex, which mediates fusion of early endosomes to late endosomes. The phenotype of the Vps34 knockdown strains was nearly identical to the *avaA* knockout strains and to the phenotype of cells treated with Sortin 3 as previously described⁶². Together, these data argue that blocking HOPS and/or CORVET tethering complex activity in *A. parasiticus* down-regulates endosome maturation and fusion. This increases endosome accumulation, aflatoxin synthesis, and aflatoxin export.

Aflatoxins belong to a group of fungal secondary metabolites collectively known as mycotoxins. Mycotoxins are produced by *A. parasiticus*, *A. flavus*, and *A. fumigatus* as they colonize a host plant or as they establish human infection¹²². Aspergilli are important fungal pathogens of plants, animal, and humans. We previously proposed that secondary metabolism (SM), stress response (SR), and conidiospore development (CD) are important virulence-associated processes in aspergilli. In the current study, we exploited a novel and endogenous fungal CRISPR/*cas9*-like system to characterize the role of Vps34 in subcellular localization and export of aflatoxin, a potent carcinogen

associated with liver and lung cancer. Based on this analysis, we now propose that the sub-cellular compartmentalization and export of secondary metabolites can be considered a virulence-associated process in *A. parasiticus*.

Previous work identified a fungal-specific bZIP transcription factor called AtfB that controls virulence-associated processes SM, SR, and CD in *A. parasiticus*. We currently have generated knockdown strains of two independent gene targets, AtfB and Vps34 that control SM, SR, and CD and therefore are proposed to control fungal virulence. The advantage of an endogenous CRISPR-like system to control *Aspergillus* virulence is that one must only supply a synthetic gene sequence to alter expression of selected gene targets and control associated regulatory networks. In addition, another potential advantage of this approach is that construct design, the selectable marker (*niaD*), and the transformation/initial screening protocols are identical to knockdown (RNAi type procedures) and traditional knockout procedures. The major difference is that 1 out of every 3 transformants screened positive for the construct so use of the endogenous CRISPR like system requires screening of fewer transformants saving time and money. One potential weakness of this approach is construct stability. One potential weakness of this approach is construct stability. In order to obtain single spore isolates of mutant strains, two rounds of single spore isolation are necessary to obtain a genetically pure culture. We have observed instances where the mutant strains could revert back to the wild type phenotype after being subjected to single spore isolation (see **Figure 18C**). However, this drawback could also serve as an advantage of using these particular isolates as potential “natural complement” strains in complementation studies. The benefit of studying a parallel loss of knockdown construct and loss of phenotype in

unstable strains (“natural complement”) enables one to study the direct link between the loss of gene function and a particular phenotype instead of conducting genetic complementation studies.

To our knowledge, we are the first to provide preliminary evidence that a CRISPR/*cas9*-like system exists in filamentous fungi. Although the specific mechanism involved in down-regulation of native *vps34* transcript is not identical to the CRISPR/*cas9* system described in eubacteria, specific hallmarks observed in our studies demonstrate close resemblance to the CRISPR/*cas9* in prokaryotes^{117,118}. Similarities between CRISPRs and fungal knockdown include: (1) multiple copies of knockdown construct integrate in tandem; (2) the integrated copies are expressed at the transcript level; (3) there is an inverse relationship between expression of the knockdown transcript and accumulation of the wild type transcript; and (4) downregulation of the wild type transcript alters phenotype in the treated cell. Important differences appear to be related to the fact that the knockdown construct does not integrate at the same specific CRISPR locus in *A. parasiticus* and that the CRISPR RNA (cRNA) in *A. parasiticus* represent the full length native transcript of the target gene. Future work will be directed at understanding the molecular mechanisms of the fungal CRISPR/*cas9* system and characteristics of specific CRISPR DNA sequences and *cas9* endonucleases within filamentous fungi.

CHAPTER 4: *A. PARASITICUS* GENOME SEQUENCE, PREDICTED CHROMOSOME STRUCTURE, AND DIFFERENTIAL GENE EXPRESSION

This chapter has been published by: Linz JE, **Wee J***, and Roze LV (2014) in *Eukaryotic Cell*. J.E.L. and J.W.* contributed equally to this article and are co-first authors.

ABSTRACT

The filamentous fungi *Aspergillus parasiticus* and *A. flavus* produce the carcinogenic secondary metabolite aflatoxin on susceptible crops. These species differ in the quantity of aflatoxins B₁, B₂, G₁, and G₂ produced in culture, in the ability to produce the mycotoxin cyclopiazonic acid, as well in morphology of mycelia and conidiospores. To understand the genetic basis for differences in biochemistry and morphology, we conducted next generation sequence (NGS) analysis of the *A. parasiticus* strain SU-1 genome and comparative gene expression (RNA Seq) analysis of *A. parasiticus* SU-1 and *A. flavus* 3357 grown under aflatoxin inducing and non-inducing culture conditions. Although *A. parasiticus* SU-1 and *A. flavus* 3357 are highly similar in genome structure and gene organization, we observed differences in the presence of specific mycotoxin gene clusters and differential expression of specific mycotoxin genes and gene clusters that help explain differences in the type and quantity of mycotoxins synthesized. Using computer aided analysis of secondary metabolite clusters (antiSMASH), we demonstrated that *A. parasiticus* SU-1 and *A. flavus* 3357 may carry up to 93 secondary metabolite gene clusters and, surprisingly, up to 10% of the genome appears to be dedicated to secondary metabolite synthesis. The data also suggest that fungal-specific zinc binuclear cluster (C6) transcription factors play an important role in regulation of

secondary metabolite cluster expression. Finally, we identified uniquely expressed genes in *A. parasiticus* SU-1 that encode C6 transcription factors as well as genes involved in secondary metabolism and stress response/cellular defense. Future work will focus on these differentially expressed *A. parasiticus* SU-1 loci to reveal their role in determining distinct species characteristics.

INTRODUCTION

Aspergillus parasiticus and *A. flavus* are the predominant aflatoxin producers on susceptible crops¹¹. The *A. flavus* NRRL 3357 complete genome sequence is available (<http://www.aspergillusflavus.org/genomics/>) and the sequence and location of the aflatoxin biosynthetic gene cluster was determined as part of this analysis. The nucleotide sequence of the *A. parasiticus* SU-1 aflatoxin biosynthetic gene cluster is also available⁴⁷ and *A. flavus* 3357 and *A. parasiticus* SU-1 exhibit a high degree of sequence identity between the aflatoxin genes as well as between other genes that have been sequenced in both organisms.

Although it is clear that *A. flavus* and *A. parasiticus* are closely related species, several phenotypic characteristics have been used to differentiate these species including the quantity and type of mycotoxins synthesized in culture and on plants. For example, *A. flavus* strains synthesize predominantly B aflatoxins while *A. parasiticus* strains produce both B and G type aflatoxins^{11,15}. Less than 50% of *A. flavus* isolates are reported to produce aflatoxins while almost all strains of *A. parasiticus* are toxigenic¹²³. *A. parasiticus* strains generally synthesize greater quantities of aflatoxin

than *A. flavus*^{11,15}. *A. flavus* strains are also reported to synthesize cyclopiazonic acid (CPA) while *A. parasiticus* strains are not known to synthesize this mycotoxin¹¹.

A. parasiticus and *A. flavus* also exhibit morphological differences and gross mycelial structure and conidiospore morphology have been used to help assign species designations to isolates in the genus *Aspergillus*¹²⁴. *A. flavus* and *A. parasiticus* can grow and produce aflatoxin on a wide variety of susceptible crops. *A. flavus* is the most widely reported fungus associated with food and it appears to have a broader host range because it is strongly associated with contamination of corn, cotton, peanuts, and tree nuts while *A. parasiticus* primarily is associated with contamination of peanuts¹²³. Both species share an ecological niche in the soil but it is not clear how well these organisms compete there.

To identify the genetic basis for reported differences in species morphology and biochemistry, we conducted Illumina next generation sequence (NGS) analysis on the *A. parasiticus* SU-1 genome. We compared the *A. parasiticus* SU-1 genome sequence and predicted chromosome structure with the available *A. flavus* 3357 genome and compared expression (RNA Seq) of all detectable *A. parasiticus* SU-1 and *A. flavus* 3357 genes under identical aflatoxin inducing (YES growth medium, 40 h of growth; standard conditions, see **Methods**) and aflatoxin non-inducing (YEP medium, 40 h) growth conditions. We observed that the genome sequences of *A. parasiticus* SU-1 and *A. flavus* 3357 exhibit a high degree of identity and the chromosome structure and gene distribution are predicted to be similar. Despite these similarities, we observed significant differences in the presence of specific secondary metabolism genes and entire gene clusters as well as differential expression of secondary metabolism and

other genes between the 2 species that may contribute to species differences in phenotype. In addition we identified 3 sets of uniquely expressed genes in *A. parasiticus* that encode C6 fungal-specific transcription factors as well as enzymes involved in secondary metabolism and stress response/cellular defense. Identification of these differentially expressed genes prompts further study of the genetic basis for unique phenotypes observed in these closely related fungal species.

MATERIALS AND METHODS

Microorganisms and culture conditions

Aspergillus parasiticus strain SU-1 (ATCC 56775) and *A. flavus* strain NRRL 3357 were used as the wild type aflatoxin producing strains. YES liquid medium (2% yeast extract, 6% sucrose, pH 5.8)¹²⁵ was used as an aflatoxin inducing rich growth medium and YEP liquid medium (2% yeast extract; 6% peptone, pH 5.8; 7) was used as an aflatoxin non-inducing medium. An aliquot of frozen conidiospores from each strain was used to inoculate 100 ml of these growth media (250 ml Ehrlenmeyer flask carrying 5, 6mm glass beads) at 10^4 spores per ml and these cultures were incubated for 40 h in the dark at 30C with shaking (150 RPM) as described previously (standard growth conditions)⁵³.

DNA preparation and Illumina next generation sequence (NGS) analysis

Genomic DNA was prepared from *A. parasiticus* SU-1 grown for 44 h in YES medium under standard conditions using a method described by Cihlar and Sypherd¹²⁶ as modified by Horng et al.¹²⁷. Genomic DNA was subjected to Illumina next generation

sequence (NGS) analysis by Functional Biosciences (Madison, WI) and bioinformatics analysis was conducted by ContigExpress LLC (New York, NY). Quality control checks on the raw sequencing data (80 million reads in the forward and reverse directions) were performed using FastQC version 0.10.1. K-mer error correction was performed on the raw reads using Quake version 0.3.4. Paired-end reads were extracted from the corrected read pool and the remaining reads were deposited as single-end reads. Both paired-end and single-end reads were used in *de novo* genome assembly. SOAPDenovo version 1.05 was used to perform assembly of the error corrected reads. Standard parameters for paired-end reads were used. The K-mer which generated scaffold sequences with a maximal N50 was 67. The resulting scaffolds were gap-filled using corrected paired-end reads. The final scaffold sequences consisted of 375 gap-filled scaffold sequences larger than 1 kb.

Comparison of chromosome structure and gene distribution in *A. parasiticus* SU-1 and *A. flavus* 3357

The 31 largest scaffolds from the *A. parasiticus* SU-1 *de novo* genome sequence assembly were compared to the 16 largest *A. flavus* 3357 scaffolds that composed the arms of the eight chromosomes in this filamentous fungus (<http://www.aspergillusflavus.org/genomics/>). The relative position of each of the 31 *A. parasiticus* SU-1 scaffolds was assigned by direct sequence comparison using the 16 largest *A. flavus* 3357 scaffolds as reference. These position assignments were supported by examination of the relative location of 43 secondary metabolite gene clusters that were shared by *A. flavus* 3357 and *A. parasiticus* SU-1. The location of *A.*

parasiticus SU-1 open reading frames on *A. parasiticus* SU-1 scaffolds and chromosomes also was completed based on direct sequence comparison of the largest *A. flavus* 3357 and *A. parasiticus* SU-1 scaffolds.

antiSMASH (antibiotics and Secondary Metabolite Analysis Shell) software was used to identify secondary metabolite loci within the *A. flavus* 3357 and *A. parasiticus* SU-1 genomes⁹⁶. FASTA formatted files of the *A. flavus* 3357 genome sequence (NCBI accession number AAIH000000000) and the *A. parasiticus* SU-1 *de novo* genome assembly were uploaded onto the web version of antiSMASH (<http://antismash.secondarymetabolites.org/>) with default settings. antiSMASH output displays a list of identified clusters based on the chemical backbones of their predicted products.

Predicted function of the uniquely expressed genes was determined by ContigExpress.LLC, New York, NY. Raw FASTA reads of 213 uniquely expressed transcripts in *A. parasiticus* SU-1 were translated in six frames and submitted as BLAST queries using NCBI non redundant protein sequences. Function and Gene Ontology (GO) assignment was conducted using BLAST2GO. A subsequent BLAST of the translated transcript sequences was compared against a KEGG database and assigned KEGG ID and pathway analysis using KOBAS. Function, GO, and functional pathway analysis were compiled in an Excel File.

RNA preparation and RNA sequence (RNA Seq) analysis

Total RNA was isolated from 2 biological replicates of *A. parasiticus* SU-1 and 2 biological replicates of *A. flavus* NRRL 3357 grown under standard conditions in YES

for 40 h using the TRIzol method (TRIzol reagent; Invitrogen, Carlsbad, CA) as described by the manufacturer. Total RNA was also isolated from a single sample of *A. parasiticus* SU-1 grown in YEP under standard conditions for 40 h. The integrity and purity of the RNA samples was assessed using an Agilent 2200 TapeStation Bioanalyzer System (Agilent, Santa Clara, CA). All samples had an RNA Integrity Number (RIN) of 9.0 or higher with an OD_{260/280} between 1.78 – 1.80. Illumina RNA sequence analysis was conducted on purified total RNA samples by Orogenetics (Norcross, GA) and bioinformatics analysis of the resulting data was conducted by ContigExpress, LLC (New York, NY).

cDNA library construction was conducted as follows: 100 ng of total RNA was reverse transcribed into cDNA using Clontech SmartPCR cDNA kit (Clontech, Mountain View, CA). Fragment AnalyzerTM (AATI, Ames, IA) and Qubit® (Life Technologies, Grand Island, NY) were used to assess cDNA quality. Restriction enzyme digestion end repair was conducted by removing adaptor sequences and fragmentation of the resulting cDNA was conducted using a Covaris M220 focused-ultrasonicator (Woburn, MA). Fragmented cDNA was subjected to Illumina library preparation with NEBNext-based reagents (NEB, Ipswich, MA). The quality, quantity, and size distribution of Illumina libraries were determined using an Agilent Bioanalyzer 2100. cDNA clusters were generated on a cBot automated station and the Illumina libraries were submitted for Illumina HiSeq2000 2x100 bp Paired-End sequencing (Illumina, San Diego, CA).

Data analysis workflow was developed by ContigExpress LLC (New York, NY). FASTQC (Babraham Institute, Cambridge, UK) was used to assess quality of paired-end 2x100bp Illumina raw sequence reads. The number of raw reads per RNA sample

were as follows: SU-1 in YES, replicate 1 (35,870,008); SU-1 in YES, replicate 2 (23,352,926); 3357 in YES, replicate 1 (21,887,760); 3357 in YES, replicate 2 (28,694,452); SU-1 in YEP (22,730,224). Processed reads were then mapped to the *de novo* scaffold sequences of the *A. parasiticus* SU-1 genome with paired-end configuration using Bowtie2, version 2.0.0-beta7¹²⁸. The *A. flavus* 3357 genome (<http://www.aspergillusflavus.org/genomics/>) was used to obtain *A. flavus* cDNA gene designations which were compared to the scaffold sequences using BLAST, version 2.2.24+¹²⁹. The matched scaffold region of the top hit of each *A. flavus* gene, when available, was used to annotate that region with an *A. flavus* gene ID. The annotation information was assembled in the GTF format for downstream analysis. The mapping files of 3 *A. parasiticus* samples and 2 *A. flavus* samples were used to assemble the master gene annotations. The BLAST-based gene annotation was submitted to Cufflinks (version 2.0.2) as the reference annotation¹³⁰. Differential gene expression analysis was performed with the master gene annotations using Cufflinks.

Identification and function of “uniquely expressed loci” in *A. parasiticus*

We compared the level of gene expression in the 2 *A. flavus* 3357 biological replicates grown for 40 h on YES under standard conditions versus the 2 *A. parasiticus* SU-1 biological replicates grown for 40 h under the same conditions. We compiled a list of 1409 genes that exhibited significant levels of differential expression between the 2 fungal species grown for 40 h on YES (q value < 0.05). Of these 1409 genes, 318 were not identified in the *A. flavus* 3357 genome (<http://www.aspergillusflavus.org/genomics/>). We hypothesized that either these genes were truly absent in *A.*

flavus 3357, or they were omitted due to gaps in coverage in the *A. flavus* 3357 genome sequence. We also observed that of the 318 genes not present in the *A. flavus* 3357 genome, 213 were expressed at significant levels in *A. parasiticus* SU-1 but the transcript was not detected in *A. flavus* 3357. Because these 213 genes and their transcript were absent in *A. flavus* 3357 but present in *A. parasiticus* SU-1, we propose that they represent genes that are uniquely expressed in *A. parasiticus* SU-1 (as compared to *A. flavus* 3357). For the remaining 105 genes, transcripts were detected in *A. flavus* 3357 suggesting that they were not identified previously due to gaps in construction of the genome sequence.

RESULTS

***A. parasiticus* SU-1 genome sequence and predicted chromosome structure**

As part of bioinformatics analysis, contigs from Illumina sequence analysis of the *A. parasiticus* SU-1 genome were assembled into 375 scaffolds greater than 1 kb in size. The resulting scaffolds then were listed by decreasing length. The top 31 *A. parasiticus* SU-1 scaffolds by length represented approximately 95% of the predicted SU-1 genome (**Table 2**). The location of all 375 *A. parasiticus* SU-1 scaffolds was assigned based on direct sequence comparison with 16 *A. flavus* 3357 scaffolds presented in the *A. flavus* 3357 genome browser (<http://www.aspergillusflavus.org/genomics/>). The location of the top 31 *A. parasiticus* SU-1 scaffolds by length was assigned to *A. flavus* 3357 chromosomes by similar analysis and these data were used to construct a schematic of the *A. parasiticus* SU-1 genome (**Figure 24A**). We observed that the predicted chromosome structures of the *A.*

parasiticus SU-1 and *A. flavus* 3357 genomes are quite similar (**Figure 24A and 24B**). The *A. parasiticus* SU-1 genome is predicted to consist of 8 chromosomes that are of similar size to the 8 homologous *A. flavus* 3357 chromosomes. A total of 13,290 *A. parasiticus* SU-1 genes were identified based on the *A. flavus* 3357 genome annotation (carries 13,487 genes) and the relative location of these loci was assigned to *A. parasiticus* SU-1 scaffolds and chromosomes by direct sequence comparison to homolog in *A. flavus* 3357 scaffolds and chromosomes.

A. parasiticus SU-1 genes were provided *A. flavus* 3357 gene designations based on identity and these were located on the *A. parasiticus* SU-1 scaffolds and chromosomes using the *A. flavus* 3357 genome as a template. We observed that 96% of *A. flavus* 3357 ORFs have at least one homolog in the *A. parasiticus* SU-1 genome and 4% the *A. flavus* 3357 ORFs have no detectable homolog in the *A. parasiticus* SU-1 genome (**Figure 25A**). *A. parasiticus* SU-1 and *A. flavus* 3357 share greater than 90% sequence identity over greater than 90% of genome sequence (**Figure 25B**).

Table 2 Top 31 *A. parasiticus* SU-1 scaffolds by length

| <i>A. parasiticus</i> scaffold no. | Scaffold length (bp) | Scaffold location ^a |
|------------------------------------|----------------------|--------------------------------|
| 35 | 3001269 | C2R |
| 222 | 2822244 | C4L |
| 310 | 2638474 | C7L |
| 77 | 2214935 | C3R |
| 311 | 2173408 | C2L |
| 32 | 2057647 | C1R |
| 44 | 1914451 | C4R |
| 26 | 1893530 | C1L |
| 30 | 1776511 | C6R |
| 139 | 1659146 | C5R |
| 129 | 1552207 | C3L |
| 64 | 1506959 | C1R |
| 18 | 1451838 | C5L |
| 69 | 1326957 | C8R |
| 29 | 1267361 | C2R |
| 123 | 1129355 | C3L |
| 25 | 1079114 | C5L |
| 309 | 793882 | C8L |
| 8 | 646144 | C8R |
| 22 | 639763 | C1R |
| 17 | 564883 | C6L |
| 28 | 492974 | C6L |
| 46 | 434019 | C6R |
| 11 | 433510 | C8L |
| 308 | 340505 | C6L |
| 126 | 338060 | C6L |
| 208 | 319820 | C7R |
| 253 | 225885 | C5R |
| 215 | 179257 | C6L |
| 307 | 169918 | C1R |
| 76 | 154073 | C3R |

37198099

^a The location of the scaffold on the chromosome is shown as follows: the chromosome number is shown first and then the arm (e.g., C2R is chromosome 2, right arm, and C4L is chromosome 4, left arm).

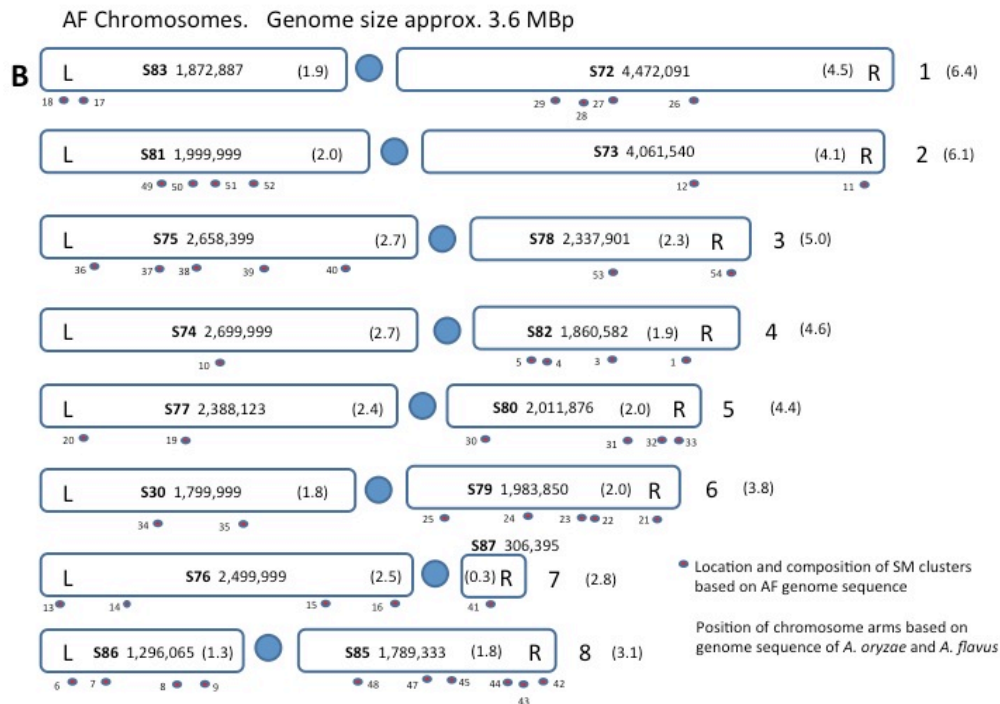
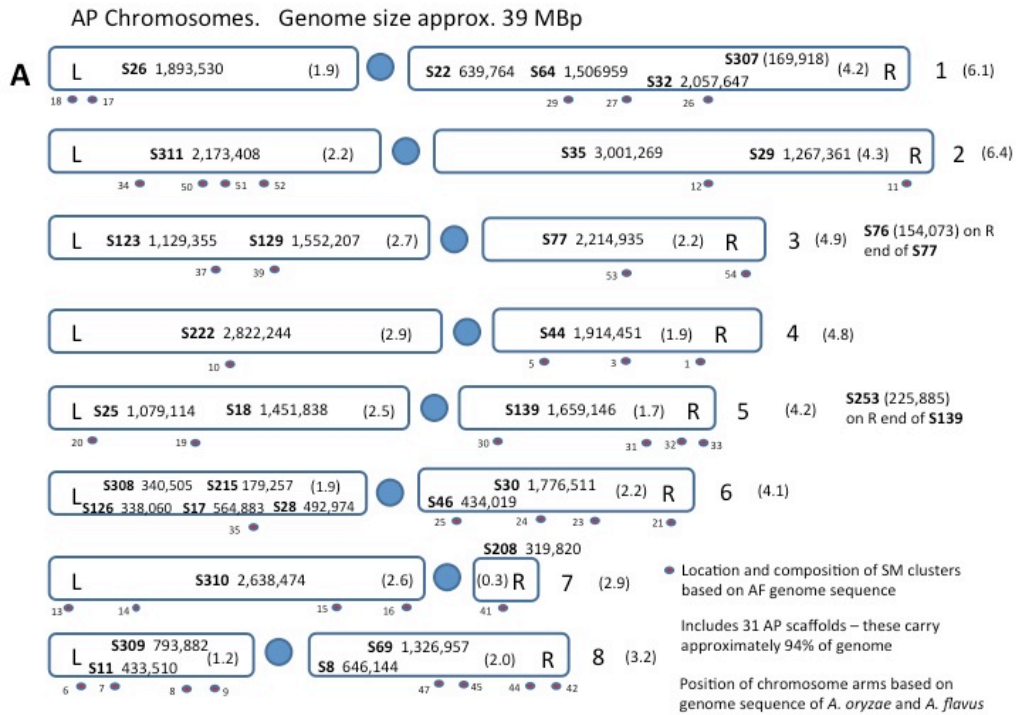


Figure 24 Predicted chromosome structure of *A. parasiticus* SU-1 and *A. flavus*

3357

Figure 24 (cont'd)

Panel A. The *A. parasiticus* SU-1 genome sequence was assembled into scaffolds and the position of the largest 31 scaffolds (S) was located on the left arm (L) or right arm (R) of 8 chromosomes as described in Methods. The number next to scaffold numbers indicates its length in Bp. Chromosome number appears in bold adjacent to the right arm of each chromosome and the size of the entire chromosome (MBp) is included in parentheses next to chromosome number. The relative location and size (Bp) of the largest 31 *A. parasiticus* SU-1 scaffolds (ie. **S26**, **S22**, **S64**) appears within each chromosome arm and the size of each arm (MBp) appears near the right hand end in parentheses. The location of 44 secondary metabolism gene clusters is indicated by small blue ellipses (filled with red) placed just below the chromosome arms – cluster numbers correspond to the gene cluster designations in the *A. flavus* genome browser cited in the text. **Panel B.** Predicted *A. flavus* 3357 chromosome structure based on the genome browser. Eleven secondary metabolite clusters present in 3357 (Clusters 4, 22, 28, 33, 36, 38, 40, 45, 48, 49, and 55) were not identified in SU-1 based on manual analysis for a single key cluster gene. Cluster 36 was also located to different chromosomes in SU-1 and 3357.

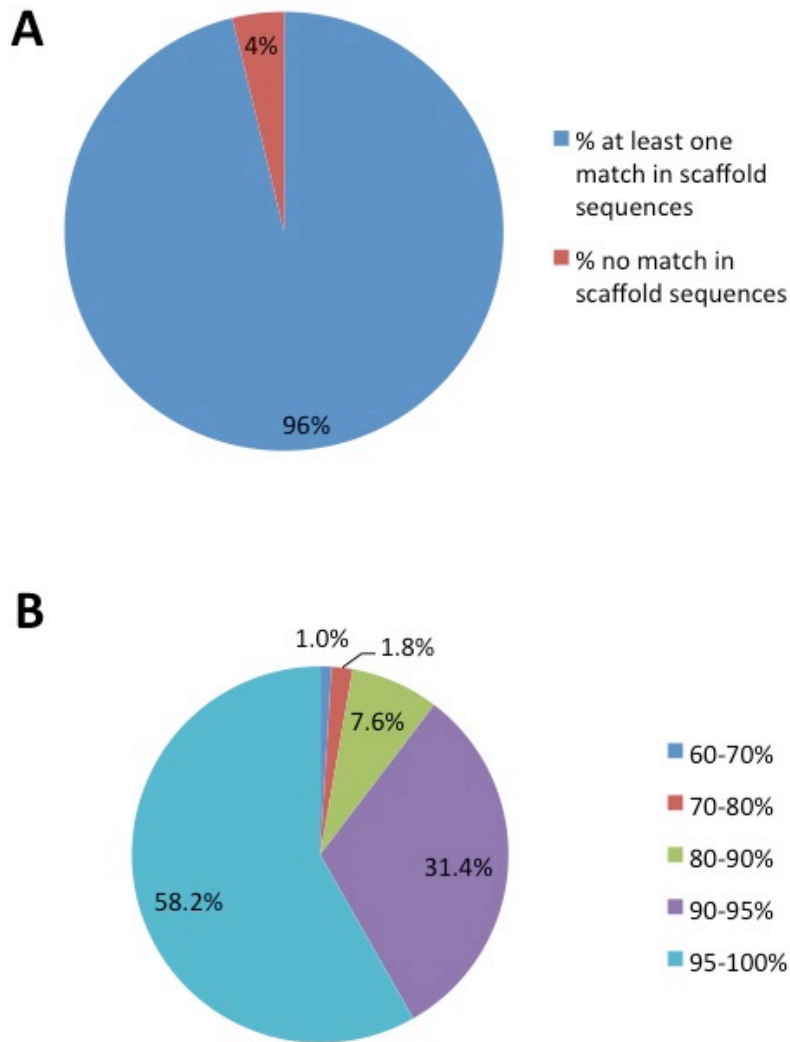


Figure 25 Analysis of genome identity between *A. parasiticus* SU-1 and *A. flavus* 3357

Panel A. Percent of *A. flavus* 3357 open reading frames with at least one homolog in *A. parasiticus* SU-1. **Panel B.** Distribution of identity over the *A. parasiticus* SU-1 genome sequence. Percent in pie chart represents the fraction of the genome that carries identity levels as indicated by color.

Fifty-five secondary metabolite gene clusters were identified and located to *A. flavus* 3357 chromosomes as part of the original sequence analysis of the *A. flavus* 3357 genome. We screened for these secondary metabolism gene clusters in the *A. parasiticus* SU-1 genome by BLAST analysis using one key gene in each cluster as the query sequence and the *A. parasiticus* scaffolds as the subject sequence. We detected the key gene from 44 of the *A. flavus* 3357 secondary metabolite gene clusters in *A. parasiticus* SU-1 and these clusters were found in similar locations on the *A. parasiticus* SU-1 chromosomes (**Figure 24, Table 3**). The exception is Cluster 34 which appears to be located on the left arm of chromosome 2 (C2L) rather than the left arm of chromosome 6 (C6L). Based on this labor-intensive manual analysis, we noted that *A. parasiticus* SU-1 lacks 11 of the secondary metabolite clusters observed in *A. flavus* 3357 including Clusters 4, 22, 28, 33, 36, 38, 40, 45, 48, 49, and Cluster 55 which mediates synthesis of cyclopiazonic acid (CPA) (**Table 3**).

In contrast to manual analysis, antiSMASH software (default parameters) detected 93 secondary metabolite clusters in *A. parasiticus* SU-1 including 30 PKS clusters, 22 NRPS clusters, 14 terpene clusters, 2 siderophore clusters, and 25 clusters designated 'putative' or 'other'. antiSMASH detected 87 secondary metabolite clusters in *A. flavus* 3357 including 28 PKS clusters, 22 NRPS clusters, 22 terpene clusters, 1 siderophore cluster, and 14 clusters designated 'other'. We recently expanded this analysis to perform direct sequence comparison at the individual cluster level (Wee et al., manuscript in preparation). Bioinformatics analysis support our initial observation that the proportion of the genome devoted to secondary metabolism is highly similar in *A. parasiticus* SU-1 and *A. flavus* 3357.

Table 3 Secondary metabolism gene clusters in the *A. parasiticus* SU-1 genome screened by BLAST analysis^a

| SM cluster no. ^b | AFLA gene no. ^c | Location of the SM gene cluster | | Chromosomal location of the SM gene cluster ^d | Location on <i>A. flavus</i> scaffold | Gene size (bp) | Location on <i>A. parasiticus</i> scaffold ^e | Level of expression ^f | | |
|-----------------------------|----------------------------|----------------------------------|---------------------------------------|--|---------------------------------------|----------------|---|----------------------------------|--------------------|----------------|
| | | Scaffold no. in <i>A. flavus</i> | Scaffold no. in <i>A. parasiticus</i> | | | | | SU-1 YES/ YEP | 3357 YES/ SU-1 YEP | 3357/ SU-1 YES |
| 18 | NRPS 5427 | 83 | 26 | C1L | 1,804,577 | 1,951 | 110,065 | 0, 0 no | 0, 0 no | 0, 0 no |
| 17 | PKS 5287 | 83 | 26 | C1L | 1,688,441 | 9,065 | 223,202 | 87, 113 no | 83, 113 no | 91, 83 no |
| 29 | C6TF 8409 | 72 | 64 | C1R | 3,179,694 | 2,056 | 962,759 | 0.1, 0 no | 1.6, 0 yes | 1.6, 0.1 no* |
| 28 | NRPS 8248 | 72 | None | C1R | 2,730,816 | 1,252 | None | | | |
| 27 | PKS 8215 | 72 | 64 | C1R | 2,646,293 | 6,545 | 426,236 | 0, 0 no | 0, 0 no | 0, 0 no |
| 26 | NRPS 7940 | 72 | 32 | C1R | 1,901,221 | 3,837 | 322,378 | 0.7, 0.9 no | 1.2, 0.8 no | 1.2, 0.7 no |
| 49 | PKS 12564 | 81 | None | C2L | 627,318 | 2,487 | None | 0.7, 0 no* | 0, 0 no | 0.7, 0 no* |
| 50 | PKS 12671 | 81 | 311 | C2L | 927,088 | 8,259 | 1,067,728 | 0, 0 no | 0, 0 no | 0, 0 no |
| 51 | PKS 12709 | 81 | 311 | C2L | 1,031,825 | 7,872 | 1,189,154 | 0, 0 no | 0, 0 no | 0, 0 no |
| 52 | PKS 12806 | 81 | 311 | C2L | 1,314,426 | 8,574 | 1,475,006 | 0, 0 no | 0, 0 no | 0, 0 no |
| 12 | NRPS 2872 | 73 | 35 | C2R | 1,592,347 | 3,036 | 2,557,918 | 0.8, 0 no* | 0, 0 no | 0, 0.8 no |
| 11 | NRPS 2302 | 73 | 29 | C2R | 34,356 | 3,066 | 1,177,535 | 0, 0.4 no | 0, 0.4 no | 0, 0 no |
| 36 | PKS 10425 | 75 | None | C3L | 24,095 | 2,355 | None | | | |

(continued on following page)

Table 3 (cont'd)

| SM cluster no. ^b | AFLA gene no. ^c | Location of the SM gene cluster | | Chromosomal location of the SM gene cluster ^d | Location on <i>A. flavus</i> scaffold | Gene size (bp) | Location on <i>A. parasiticus</i> scaffold ^e | Level of expression ^f | | |
|-----------------------------|----------------------------|----------------------------------|---------------------------------------|--|---------------------------------------|----------------|---|----------------------------------|--------------------|--------------------|
| | | Scaffold no. in <i>A. flavus</i> | Scaffold no. in <i>A. parasiticus</i> | | | | | SU-1 YES/ YEP | 3357 YES/ SU-1 YEP | 3357/ SU-1 YES |
| 37 | NRPS 10519 | 75 | 123 | C3L | 272,459 | 3,327 | 324,910 | 14, 0.1 yes | 0.6, 0.1 no* | 0.6, 14; +23 yes |
| 38 | PKS 10545 | 75 | None | C3L | 336,845 | 8,232 | None | 0.5, 0.3 no | 1.0, 0.3 no* | 1.0, 0.5 no * |
| 39 | PKS 10855 | 75 | 129 | C3L | 1,144,762 | 5,446 | 1,471,691 | 0.1, 0 no | 0, 0 no | 0, 0.1 no |
| 40 | PKS 284 | 75 | None | C3L | 2,307,795 | 7,005 | None | 18, 19 no | 130, 19 yes | 130, 19; - 6.8 yes |
| 53 | NRPS 13549 | 78 | 77 | C3R | 1,209,037 | 3,216 | 1,030,927 | 0, 0 no | 0, 0 no | 0, 0 no |
| 54 | OmtA 13,921 | 78 | 77 | C3R | 2,199,609 | 1,634 | 15,777 | 300, 0 yes | 78, 0 yes | 78, 300 no* |
| 54 | PksA 13941 | 78 | 76 | C3R | 2,239,960 | 6,624 | 135,232 | 0, 0 no | 0, 0 no | 0, 0 no |
| 10 | Arp1 1614 | 74 | 222 | C4L | 901,342 | 462 | 959,335 | 70, 132 yes | 0, 133 yes | 0, 70; + >100 yes |
| 5 | PksP 617 | 82 | 44 | C4R | 1,664,602 | 6,651 | 228,115 | 0, 0 no | 0, 0 no | 0, 0 no |

(continued on following page)

Table 3 (cont'd)

| SM cluster no. ^b | AFLA gene no. ^c | Location of the SM gene cluster | | Chromosomal location of the SM gene cluster ^d | Location on <i>A. flavus</i> scaffold | Gene size (bp) | Location on <i>A. parasiticus</i> scaffold ^e | Level of expression ^f | | |
|-----------------------------|----------------------------|----------------------------------|---------------------------------------|--|---------------------------------------|----------------|---|----------------------------------|--------------------|----------------|
| | | Scaffold no. in <i>A. flavus</i> | Scaffold no. in <i>A. parasiticus</i> | | | | | SU-1 YES/ YEP | 3357 YES/ SU-1 YEP | 3357/ SU-1 YES |
| 4 | NRPS 544 | 82 | None | C4R | 1,442,264 | 7,962 | None | 0, 0 no | 0.2, 2.2 no* | 0.2, 0 no |
| 3 | NRPS 445 | 82 | 44 | C4R | 1,115,175 | 16,528 | 780,095 | 0.1, 0 no | 1.5, 0.1 no* | 1.5, 0.1 no* |
| 1 | PKS 290 | 82 | 44 | C4R | 639,511 | 7,320 | 1,256,446 | 2.9, 1.1 no* | 2.2, 1.1 no* | 2.2, 2.9 no |
| 20 | PKS 6282 | 77 | 25 | C5L | 2,153,493 | 7,923 | 854,574 | 0, 0 no | 0, 0 no | 0, 0 no |
| 19 | MDR 6084 | 77 | 25 | C5L | 1,624,541 | 1,020 | 238,387 | 0.2, 0 no | 0, 0 no | 0, 0.2 no |
| 30 | NRPS 9020 | 80 | 139 | C5R | 302,181 | 5,256 | 1,501,541 | 0, 0 no | 0, 0 no | 0, 0 no |
| 31 | NRPS 9504 | 80 | 139 | C5R | 1,615,340 | 1,453 | 160,038 | 0, 0 no | 0, 0 no | 0, 0 no |
| 32 | C6TF 9637 | 80 | 253 | C5R | 1,928,138 | 2,531 | 126,829 | 0.2, 0.1 no* | 0.4, 0.1 no* | 0.4, 0.2 no* |
| 33 | PKS 9677 | 80 | None | C5R | 2,022,113 | 3,034 | None | | | |
| 34 | NRPS 10034 | 84 | 311 | C6L | 862,490 | 3,678 | 717,616 | 0, 0 no | 0, 0 no | 0, 0 no |
| 35 | NRPS 10170 | 84 | 215 | C6L | 1,198,962 | 3,129 | 115,582 | 0.1, 0.2 no* | 0.6, 0.2 no* | 0.6, 0.1 no* |

(continued on following page)

Table 3 (cont'd)

| SM cluster no. ^b | AFLA gene no. ^c | Location of the SM gene cluster | | Chromosomal location of the SM gene cluster ^d | Location on <i>A. flavus</i> scaffold | Gene size (bp) | Location on <i>A. parasiticus</i> scaffold ^e | Level of expression ^f | | |
|-----------------------------|----------------------------|----------------------------------|---------------------------------------|--|---------------------------------------|----------------|---|----------------------------------|--------------------|----------------|
| | | Scaffold no. in <i>A. flavus</i> | Scaffold no. in <i>A. parasiticus</i> | | | | | SU-1 YES/ YEP | 3357 YES/ SU-1 YEP | 3357/ SU-1 YES |
| 25 | ACV syn. 7086 | 79 | 46 | C6R | 1,819,006 | 11,325 | 173,928 | 0.1, 0.2 no* | 0.3, 0.2 no | 0.3, 0.1 no* |
| 24 | NRPS 6933 | 79 | 30 | C6R | 1,362,826 | 15,949 | 343,560 | 2.7, 1.0 no* | 5.5, 1.0 no* | 5.5, 2.7 no* |
| 23 | PKS/NRPS 6684 | 79 | 30 | C6R | 704,693 | 11,841 | 984,638 | 0,0 no | 0.3, 0 no | 0.3, 0 no |
| 22 | NRPS 6672 | 79 | None | C6R | 655,460 | 16,343 | None | | | |
| 21 | Gliotoxin 6442 | 79 | 30 | C6R | 77,944 | 461 | 1,686,932 | 2.6, 0 no* | 1.6, 0 no* | 1.6, 2.6 no |
| 13 | NRPS 3860 | 76 | 310 | C7L | 151,540 | 9,107 | 171,936 | 0, 0.1 no | 0, 0.1 no | 0, 0 no |
| 14 | IroE 4105 | 76 | 310 | C7L | 763,148 | 1,046 | 805,511 | 0, 0.5 no | 0, 0.5 no | 0, 0 no |
| 15 | DMAT 4549 | 76 | 310 | C7L | 1,948,240 | 1,375 | 2,001,813 | 0, 0 no | 0, 0 no | 0, 0 no |
| 16 | SidA 4719 | 76 | 310 | C7L | 2,481,875 | 1,575 | 2,561,114 | 22, 83 yes | 21, 83 yes | 21, 22 no |
| 41 | PKS 11482 | 87 | 208 | C7R | 153,643 | 5,571 | 123,539 | 0, 1 no* | 0.7, 0.9 no | 0.7, 0 no |
| 6 | NRPS 877 | 86 | 11 | C8L | 33,887 | 15,692 | 147,010 | 0, 0 no | 0, 0 no | 0, 0 no |

(continued on following page)

Table 3 (cont'd)

| SM cluster no. ^b | AFLA gene no. ^c | Location of the SM gene cluster | | Chromosomal location of the SM gene cluster ^d | Location on <i>A. flavus</i> scaffold | Gene size (bp) | Location on <i>A. parasiticus</i> scaffold ^e | Level of expression ^f | | |
|-----------------------------|----------------------------|----------------------------------|---------------------------------------|--|---------------------------------------|----------------|---|----------------------------------|--------------------|-------------------|
| | | Scaffold no. in <i>A. flavus</i> | Scaffold no. in <i>A. parasiticus</i> | | | | | SU-1 YES/ YEP | 3357 YES/ SU-1 YEP | 3357/ SU-1 YES |
| 7 | PKS 914 | 86 | 11 | C8L | 459,100 | 1,463 | 44,826 | 0.2, 0 no | 0.8, 0.1 no* | 0.8, 0.2 no * |
| 8 | PKS/NRPS 1000 | 86 | 309 | C8L | 687,862 | 5,998 | 178,580 | 0.8, 0.5 no | 0.1, 0.5 no* | 0.1, 0.8 no * |
| 9 | NRPS 1058 | 86 | 309 | C8L | 815,096 | 23,346 | 313,447 | 0.1, 0.1 no | 0.2, 0.2 no | 0.2, 0.1 no * |
| 48 | NRPS 12152 | 85 | None | C8R | 1,479,298 | 3,093 | None | | | |
| 47 | NRPS 119111 | 85 | 69 | C8R | 896,447 | 3,314 | 1,018,151 | 0, 0 no | 0, 0 no | 0, 0 no |
| 45 | NRPS 11844 | 85 | 69 | C8R | 710,225 | 3,304 | 774,162 | 6, 0 yes | 1.1, 0 no* | 1.1, 6.0; + 5 yes |
| 44 | PKS 11689 | 85 | 69 | C8R | 296,613 | 7,791 | 328,410 | 0.2, 0.1 no* | 0.1, 0.1 no | 0.2, 0.2 no * |
| 43 | PKS 11650 | 85 | None | C8R | 188,716 | 1,505 | None | 0, 0 no | 0, 0 no | 0, 0-no |
| 42 | PKS 11622 | 85 | 69 | C8R | 121,844 | 6,466 | 153,847 | 0, 0 no | 0, 0 no | 0, 0 no |

(continued on following page)

Table 3 (cont'd)

^aA single key gene in each of 55 secondary metabolite gene clusters identified previously in the *A. flavus* 3357 genome sequence (online) was used as a search query to analyze the *A. parasiticus* SU-1 scaffold sequences. The two species studied were *A. flavus* 3357 and *A. parasiticus* SU-1.

^bThe secondary metabolite (SM) cluster column shows the *A. flavus* gene cluster numbers.

^cThe AFLA gene no. column shows the predicted gene function and *A. flavus* gene designation for the key cluster gene. Abbreviations: NRPS, nonribosomal peptide; PKS, polyketide synthetase; DMAT, dimethylallyl tryptophan synthetase; C6TF, zinc binuclear cluster transcription factor; ACV syn., alpha amino adipylcysteinyl valine synthase.

^dThe chromosome number and arm (left [L] or right [R]) in *A. flavus* 3357 and *A. parasiticus* SU-1 is shown.

^eThe key gene in 11 of 3,357 secondary metabolite clusters was not identified in *A. parasiticus* SU-1 and is shown as None.

^fRNA Seq analysis was conducted on duplicate samples of *A. parasiticus* SU-1 and *A. flavus* 3357 grown for 40 h in YES medium and on a single isolate of SU-1 grown on YEP medium. The level of expression of each of the key genes is shown in the three columns. *A. parasiticus* SU-1 grown on YES medium compared to *A. parasiticus* SU-1 grown on YEP medium (SU1 YES/YEP), *A. flavus* 3357 grown on YES medium compared to *A. parasiticus* SU-1 grown on YEP medium (3357 YES/SU-1 YEP), and *A. flavus* 3357 grown on YES medium compared to *A. parasiticus* SU-1 grown on YES medium (SU-1/3357 YES) are shown. The first value represents the expression level of the first member of the comparison pair, and the second number represents the expression level of the second member of the comparison pair. If the difference in expression between the first and second member of the pair is statistically significant, “yes” follows the values (based on the q value). If the difference in expression is not statistically significant, “no” follows the values. In some cases, the differences in expression were at least 2-fold, but this was not statistically significant; in this case, “no*” follows the values.+, up-regulation; -, down-regulation.

Comparison of *A. parasiticus* SU-1 and *A. flavus* 3357 gene expression under aflatoxin inducing conditions

The level of differential expression during growth on YES (40 h) was calculated for all genes in the *A. parasiticus* SU-1 genome. Of 13,290 total transcripts expressed by *A. parasiticus* SU-1, 1408 (11%) exhibited significantly different levels of gene expression between *A. parasiticus* SU-1 and *A. flavus* 3357 during growth in YES medium at 40 h. This medium induces aflatoxin gene expression in both species and aflatoxin gene expression increases at maximum rates between 30 and 40 h in YES⁶². The number of genes exhibiting statistically significant differences in expression are much lower between 2 biological replicates of *A. flavus* 3357 (63 genes) or 2 biological replicates of *A. parasiticus* SU-1 (34 genes) analyzed in this study suggesting that the observed differences in expression between *A. parasiticus* SU-1 and *A. flavus* 3357 are not due to variability in gene expression between biological replicates.

Six aflatoxin genes (*cypA*, *afIT*, *nor-1*, *estA*, *hypC*, and *ordA*) and one additional secondary metabolism gene (*aroM*) are expressed at significantly higher levels (YES, at 40 h) in *A. parasiticus* SU-1 than in *A. flavus* 3357 (**Table 4**). In support of this observation, 13 additional genes in the aflatoxin gene cluster (Cluster 54) are expressed at a minimum of 2 fold higher levels in *A. parasiticus* SU-1 than in *A. flavus* 3357 including *fas-2*, a conserved hypothetical protein, *omtB*, *avfA*, *hypB*, *verB*, *avnA*, *hypE*, *ordB*, *omtA*, *vbs*, *cypX*, and *moxY* (**Table 4, Figure 26**); these differences in expression were not statistically significant. In contrast, the gene encoding the hybrid polyketide synthase/non ribosomal peptide synthase (PKS/NRPS) in the CPA gene Cluster 55 and 3 stress response genes (Hsp70, MnSOD, and xylulose reductase) are expressed at

significantly higher levels in *A. flavus* 3357 than in *A. parasiticus* SU-1. These data may help explain differences in the quantity of aflatoxin synthesized by the 2 species under our laboratory conditions (**Figure 27**) and differences in CPA produced by *A. flavus* 3357. In support of these data, we did not detect the CPA NRPS/PKS (gene designation AFLA_13949) in the *A. parasiticus de novo* genome sequence. We also did not detect transcripts for *adhA* and, *aflS* (in Cluster 54) as well as MFS multidrug transporter, FAD dependent oxidoreductase, and dimethylallyl tryptophan synthase (in Cluster 55, the CPA cluster) in *A. parasiticus* SU-1.

Of the 44 secondary metabolite gene clusters detected manually in *A. parasiticus*, 26 were not expressed in either *A. flavus* 3357 or *A. parasiticus* SU-1 under the aflatoxin inducing or non-inducing conditions utilized in this study (**Table 3**) suggesting that these gene clusters are either not expressed at significant levels or are expressed under growth conditions that these fungi encounter in the wild. The NRPS in Clusters 37 and 45 as well as Arp1 in Cluster 10 were expressed at significantly higher levels at 40 h of growth of *A. parasiticus* SU-1 in YES medium while the PKS in Cluster 40 was expressed at significantly higher levels in *A. flavus* 3357 under these same conditions (**Figure 26, Table 4**). We also observed at least 2 fold differences in expression levels between *A. parasiticus* SU-1 and *A. flavus* 3357 in 13 additional secondary metabolism gene clusters (**Table 4**) providing evidence that these species differ greatly in the type and quantity of secondary metabolites synthesized under the specified growth conditions.

Table 4 Expression of selected genes involved in secondary metabolism, stress response, and development

| Gene group | Gene or protein name(s) | AFLA gene designation | Ratio of expression ^a | | Level of expression (SU-1/3357 YES) ^b |
|------------|-------------------------|-----------------------|----------------------------------|-------------------|--|
| | | | SU-1 YES/YEP | 3357 YES/SU-1 YEP | |
| Aflatoxin | aflF, norB | 13944 | + > 100 * | | |
| | aflU, cypA | 13943 | 528 | 89 | 2600, 357; + 7.3 |
| | aflT | 13942 | 528 | 89 | 2600, 357; + 7.3 |
| | hypC | 13940 | 528 | 89 | 2600, 357; + 7.3 |
| | aflD, nor-1 | 13939 | 528 | 89 | 2600, 357; + 7.3 |
| | aflA, fas-2 | 13938 | 10 | 8 | |
| | aflB, fas-1 | 13937 | + > 10 * | | |
| | aflR | 13936 | 1.8 | 3 | |
| | aflJ, estA | 13932 | 1671 | 960 | 664, 288; + 2.3 |
| | hypE | 13929 | 7361 | 960 | |
| | hypD | 13927 | | 70 | |
| | aflG, avnA | 13926 | 7361 | 960 | |
| | aflL, verB | 13925 | 7361 | 960 | |
| | hypB | 13924 | 7361 | 960 | |
| | aflI, avfA | 13923 | 7361 | 960 | |
| | aflO, omtB | 13922 | 7361 | 960 | |
| | aflP, omtA | 13921 | + > 1000 | + > 1000 | |
| | aflQ, ordA | 13920 | + > 1000 | + > 1000 | 106, 22; + 4.8 |
| | aflK, vbs | 13919 | 346 | 100 | |
| | aflV, cypX | 13918 | + > 1000 | + > 1000* | |
| | aflW, moxY | 13917 | 346 | 100 | |
| | aflX, ordB | 13916 | + > 1000 * | + > 1000 * | |
| | aflY, hypA | 13915 | + > 1000 * | + > 1000 * | |
| | nadA | 13914 | 346 | 100 | |
| | hxtA | 13913 | - 10 * | + > 100 * | |
| | glcA | 13912 | 346 | 100 | |

(continued on the next page)

Table 4 (cont'd)

| Gene group | Gene or protein name(s) | AFLA gene designation | Ratio of expression ^a | | Level of expression (SU-1/3357 YES) ^b |
|-----------------------------|-------------------------|-----------------------|----------------------------------|-------------------|--|
| | | | SU-1 YES/YEP | 3357 YES/SU-1 YEP | |
| Aflatoxin | sugR | 13911 | - 10 * | | |
| Stress response | Mn SOD | 3342 | 129 | 700 | 167, 775: - 4.6 |
| | Hsp70 | 849 | | | 11, 24: - 2.2 |
| | Xylulose reductase | 1558 | | 2.5 | 132, 282; - 2.1 |
| Conidiation | Medusa | 13641 | + > 100 * | + > 100 * | |
| | RosA | 2193 | | | |
| | AbaA | 2962 | | + 3 * | |
| | BrlA | 8285 | | + > 100 * | |
| Secondary metabolism | AroM | 1768 | 2 | | 16, 7; + 2.3 |
| | PKS_NRPS (CPA) | 13949 | | + > 100 | 0.1, 17; - 170 |
| C6 transcription factors | AflR | 13936 | | 3 | |
| | Unknown | 6437 | | - 3 * | - > 10 * |
| | Unknown | 4737 | | - 2 * | |
| | Cluster 29 | 8409 | | + > 10 * | + > 100 |
| | Cluster 11 | 2304 | | -5 | -10 |
| Other transcription factors | AtfB | 9401 | | 4 | |
| Housekeeping genes | Citrate synthase | 4929 | -25 | -40 | |

(continued on next page)

Table 4 (cont'd)

^a The ratios of raw expression data of *A. parasiticus* SU-1 grown for 40 h in YES medium to strain SU-1 grown for 40 h in YEP medium (SU-1 YES/YEP) and *A. flavus* 3357 grown for 40 h in YES medium to *A. parasiticus* SU-1 grown for 40 h in YEP medium (3357 YES/SU-1 YEP) are shown. All values reported in these two columns are significant ($q < 0.05$) except for the values with asterisks. The values with asterisks display trends in differential expression, but they are not statistically significant ($q > 0.05$). Symbols; +, upregulated in YES or YEP medium; -, downregulated in YES or YEP medium.

^b The level of expression of *A. parasiticus* SU-1 grown for 40 h in YES medium and the level of expression of *A. flavus* 3357 grown for 40 h in YES medium (SU-1/3357 YES) are shown. The first value represents the raw expression data for strain SU-1 grown in YES medium at 40 h, and the second value represents the raw expression data for strain 3357 grown in YES medium for 40 h. The ratio of these values determines the fold upregulation (+) or downregulation (-), which is shown after the first two values. All values reported in this column are statistically significant.

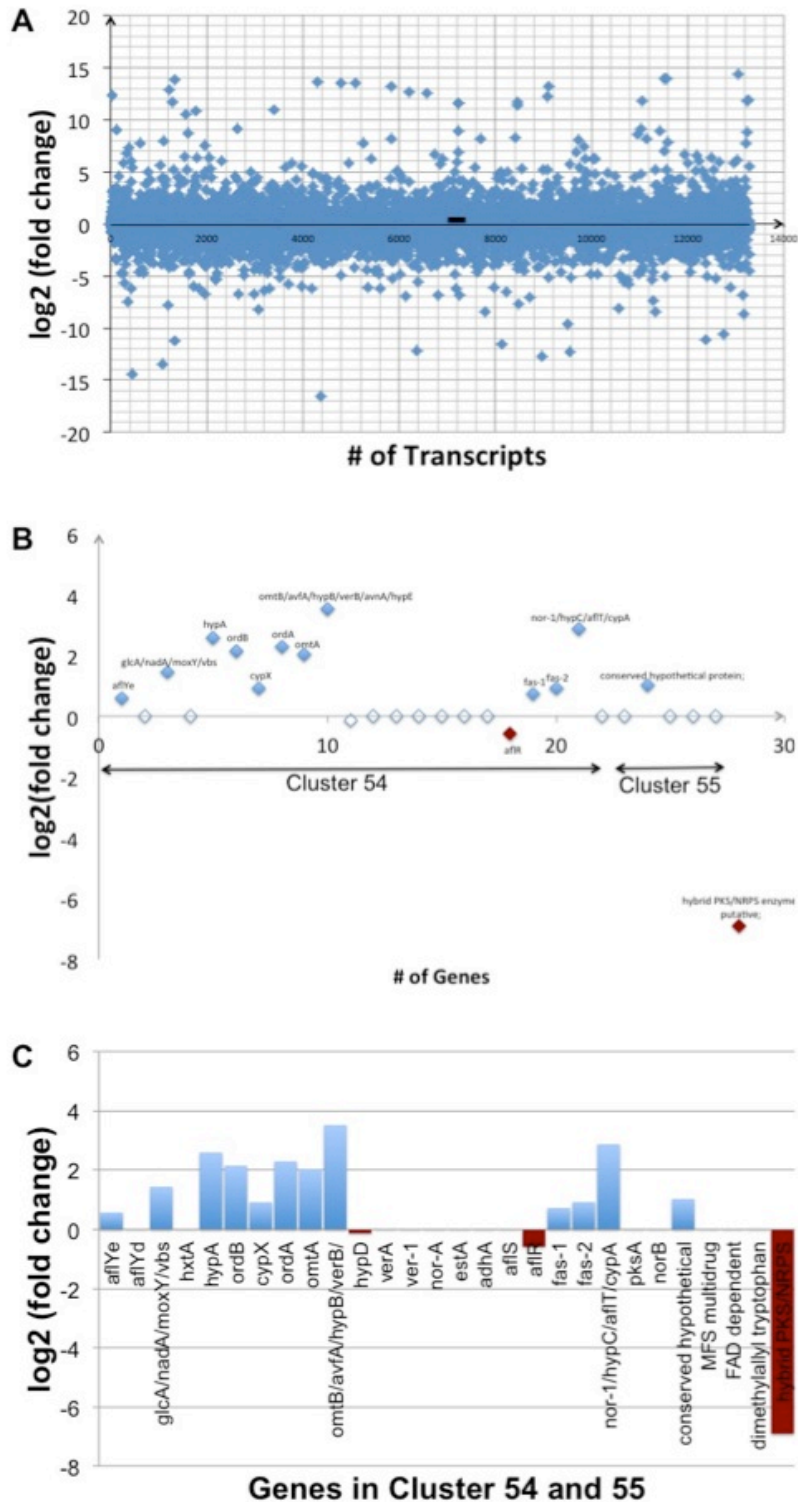


Figure 26 RNA Seq analysis of gene expression in secondary metabolite Clusters 54 and 55 in *A. parasticus* SU-1 and *A. flavus* 3357

Figure 26 (cont'd)

Panel A. Differential expression of specific genes in Cluster 54 and 55. Genes that are up-regulated are designated in blue diamonds and genes that are down-regulated are designated with red diamonds. Common gene names are presented next to the colored diamond and are based on the *A. flavus* genome browser. The relative level of differential expression (log base 2) between *A. parasiticus* SU-1 relative to *A. flavus* 3357 is indicated by the distance above (up-regulation) and below (down-regulation) the zero difference horizontal line. In specific cases, RNA SEQ analysis presented aggregate expression data for closely spaced genes within Cluster 54 (eg. *omtB/avfA/hypB/verB/avnA/hypE*). Genes included within these aggregates are closely spaced and encoded on the same strand of DNA. Presumably RNA SEQ was unable to resolve independent data for these groups of genes. **Panel B.** Bar graph presentation of differential expression data.

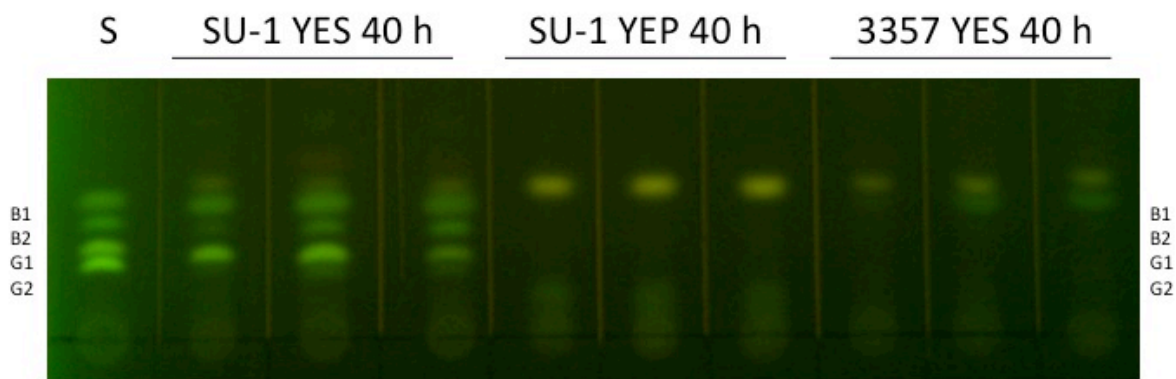


Figure 27 Aflatoxin accumulation in *A. parasiticus* SU-1 and *A. flavus* 3357 grown in culture

A. parasiticus SU-1 and *A. flavus* 3357 were grown in triplicate under standard aflatoxin inducing (YES 40 h) and aflatoxin non-inducing (YEP 40 h) culture conditions as described in Methods. Total aflatoxin was extracted from cultures and analyzed by thin layer chromatography as described in methods. Lane S illustrates migration of aflatoxin standards B₁, B₂, G₁, and G₂. An unidentified metabolite appears in all cultures above the aflatoxin spots.

Gene expression in *A. parasiticus* SU-1 and *A. flavus* 3357 was also compared during growth in YES (aflatoxin inducing growth conditions) and YEP (aflatoxin non-inducing growth conditions) with a focus on aflatoxin, secondary metabolism, and cellular defense/stress response genes (**Table 4**). 1284 *A. parasiticus* SU-1 genes and 1802 *A. flavus* 3357 genes exhibited significant differences in gene expression between YES and YEP at 40 h. We only analyzed a single biological replicate of SU-1 on YEP for these comparisons so these data are preliminary in nature. However, most genes within the aflatoxin gene cluster are up-regulated in YES as expected for both *A. flavus* 3357 and *A. parasiticus* SU-1 (**Figure 26, Table 4**) so it is likely that these trends in expression will be confirmed upon further analysis.

Identification of “uniquely expressed genes” in *A. parasiticus*

We observed that 860 *A. parasiticus* SU-1 loci have no homologue in the *A. flavus* 3357 genome sequence based on direct DNA sequence comparison between the genomes and RNA Seq analysis of gene expression on YES and/or YEP. The lack of these loci in the *A. flavus* 3357 genome may imply that these loci are unique *A. parasiticus* SU-1 gene sequences. Alternatively these loci may be located within gaps in the *A. flavus* 3357 genome sequence. Of these 860 loci, the difference in the level of expression between *A. flavus* 3357 and *A. parasiticus* SU-1 for 318 of these loci is statistically significant. For 213 of these loci, RNA transcripts (expression) could not be detected in *A. flavus* 3357 while transcripts were detectable at significant levels in *A. parasiticus* SU-1 (**Figure 28, Table 5**). We identified gene function for 68 of these genes by BLAST analysis of the translated protein products and then assigned predicted function

by KOBAS GO analysis. Of particular importance to the current study, we identified 9 fungal specific transcription factors, 4 enzymes involved in secondary metabolism, and 14 enzymes involved in stress response/cellular defense that are unique to *A. parasiticus* SU-1 and likely contribute to phenotypic and biochemical differences observed between the 2 species. Surprisingly, no known function was assigned to 145 of the 213 uniquely expressed genes (68%) based on BLAST analysis of the NCBI database (**Figure 28**) suggesting that they may contribute unique functions in the biology of *A. parasiticus* SU-1.

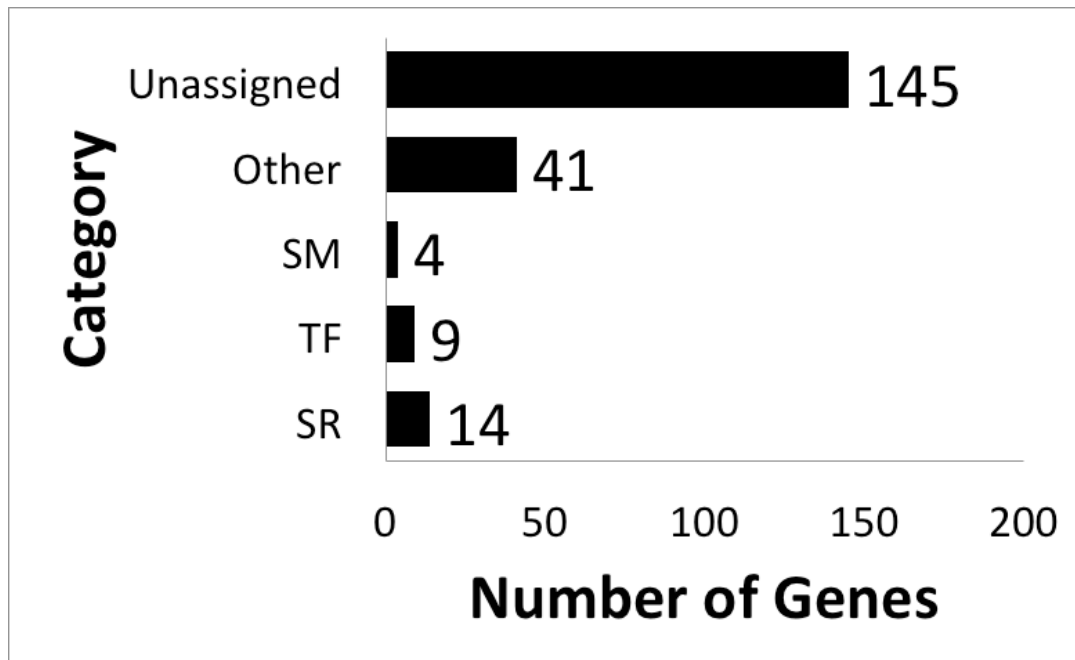


Figure 28 KOBAS GO pathway analysis of uniquely expressed genes in *A. parasiticus* SU-1

Of 213 uniquely expressed *A. parasiticus* SU-1 genes, we were unable to assign predicted functions for 145 (68%) based on BLAST analysis of the NCBI genome database. The remaining 68 genes were assigned predicted functions and assigned to functional groups. Functional group annotations appear on the Y-axis as follows: SM, secondary metabolism; TF, transcription factors; SR, oxidative stress response; Unassigned, transcripts with no known or assigned function; Other, transcripts with predicted functions other than SR, TF, and SM. Bars represent the number of genes in each functional group.

Table 5 Predicted function of selected proteins by functional category

| Gene_ID^a | Protein function | Category^b |
|----------------------------|--|-----------------------------|
| XLOC_003627 | 3-hydroxybenzoate 6-hydroxylase 1 | SR |
| XLOC_001416 | acyl- oxidase | SR |
| XLOC_010908 | acyl- oxidase | SR |
| XLOC_011069 | acyl- oxidase | SR |
| XLOC_006050 | aldo keto reductase | SR |
| XLOC_004307 | cytochrome p450 | SR |
| XLOC_013229 | cytochrome p450 alkane | SR |
| XLOC_013253 | glyoxalase bleomycin resistance protein dioxygenase | SR |
| XLOC_001771 | phytanoyl- dioxygenase family protein | SR |
| XLOC_011364 | salicylate hydroxylase | SR |
| XLOC_003035 | short-chain dehydrogenase | SR |
| XLOC_008563 | short-chain dehydrogenase reductase family | SR |
| XLOC_009101 | zinc-type alcohol dehydrogenase-like protein | SR |
| XLOC_000430 | dimeric dihydrodiol dehydrogenase | SR |
| XLOC_001156 | c6 finger domain | TF |
| XLOC_011187 | c6 transcription | TF |
| XLOC_008080 | c6 transcription factor | TF |
| XLOC_010864 | c6 transcription factor | TF |
| XLOC_000259 | c6 zinc finger domain-containing protein | TF |
| XLOC_000432 | fungal specific transcription | TF |
| XLOC_013226 | fungal specific transcription | TF |
| XLOC_006054 | fungal specific transcription factor domain-containing protein | TF |
| XLOC_010866 | zn-c6 fungal-type dna-binding domain | TF |
| XLOC_004365 | ent-kaurene synthase | SM |
| XLOC_013227 | nrps-like enzyme | SM |
| XLOC_003657 | o-methyltransferase involved in polyketide biosynthesis | SM |
| XLOC_008561 | polyketide synthase | SM |

^aXLOC, *A. parasiticus* SU-1 gene designation.

^bSR, stress response; TF, transcription factor; SM, secondary metabolism.

DISCUSSION

The focus of this ongoing work was to identify the genetic basis for the observed species differences between *A. parasiticus* SU-1 and *A. flavus* 3357. Overall the number of genes identified in our analysis of the *A. parasiticus* SU-1 genome (13,290) was similar to that identified in *A. flavus* 3357 (13,487). Even though their genome sequences and chromosome structure are similar, we observed statistically significant levels of differential expression between *A. flavus* 3357 and *A. parasiticus* SU-1 during growth in YES at 40 h and during growth on YES or YEP at 40h. Furthermore, expression of 2,930 *A. parasiticus* SU-1 genes could not be detected in YES and expression of 3,836 genes could not be detected on YEP growth medium. Since we only analyzed a single strain of each species, the results we present provide a starting point for a broader analysis of many different strains of each species to determine if differences we observed in the current work extend beyond the 2 strains we analyzed.

One short-term goal of the current work was to explain specific species differences in mycotoxin biosynthesis including the quantity and type of aflatoxin produced in culture as well as the synthesis of cyclopiazonic acid (CPA). We observed significantly higher levels of expression of 6 key genes (*cypA*, *aflT*, *nor-1*, *estA*, *hypC*, *ordA*) in *A. parasiticus* SU-1 as well as a minimum 2 fold increase in expression of 13 other aflatoxin genes that could in part explain species differences in aflatoxin biosynthesis and future work can focus on expanding focus of this analysis to additional strains of *A. flavus* and *A. parasiticus*. Up-regulation of all 19 of these aflatoxin genes in *A. parasiticus* SU-1 could account for higher levels of aflatoxin synthesized by this species while higher levels of *ordA* and *cypA* specifically (which mediate conversion of

B aflatoxins to the corresponding G aflatoxins) could explain why most strains of *A. parasiticus* synthesize both B and G aflatoxins while most strains of *A. flavus* synthesize predominantly B aflatoxins. We also detected significantly higher expression of the hybrid PKS/NRPS in *A. flavus* 3357 that catalyzes the initial steps in the synthesis of CPA in many *A. flavus* strains. The CPA PKS/NRPS was expressed at up to 100 fold higher levels in *A. flavus* 3357 than in *A. parasiticus* SU-1. In support of this observation, this hybrid gene and 3 other genes in Cluster 55 were not detected in the assembled *A. parasiticus* SU-1 genome.

We also compared the presence and location of 55 secondary metabolism clusters present in the *A. flavus* 3357 genome. While 43 of these clusters were detected in both organisms at the same approximate location, 1 cluster was present on a different chromosome perhaps providing evidence for intragenomic recombination leading to translocation of this cluster. During analysis of the 318 loci that were present in the *A. parasiticus* SU-1 genome but not *A. flavus* 3357 we detected additional PKS and NRPS like enzymes so it appears that both species are able to synthesize unique secondary metabolites. Further analysis of the *A. flavus* 3357 genome must be conducted to determine if these genes were simply present but detected as part of the original sequence analysis or if they are indeed unique to *A. parasiticus* SU-1.

antiSMASH is a simple and rapid bioinformatics analysis for identification and functional annotation for secondary metabolite gene clusters in bacterial and fungal genome sequences⁹⁶. antiSMASH algorithms are based on specific hallmarks (functional motifs) and sequence identity in clusters of secondary metabolism Clusters of Orthologous Groups (smCOGs). This software was reported to have a 97% reliability

when it was used to compare 484 cloned fungal and bacterial secondary metabolism gene clusters in the Genbank database. While we manually detected 44 clusters based on a single key enzyme present in a specific pathway, antiSMASH expanded upon this analysis and detected 93 clusters based on a collection of enzymes present in the same cluster. antiSMASH detected a similar number of PKS and NRPS in *A. parasiticus* SU-1 (30 PKS, 22 NRPS) and *A. flavus* 3357 (28 PKS, 22 NRPS) and approximately 60% of the secondary metabolite clusters are committed to synthesis of PKS and NRPS in both species. Of particular interest, there was a clear difference in the number of terpene clusters in *A. parasiticus* SU-1 (14 clusters) and *A. flavus* 3357 (22 clusters). Analyzing how the observed differences in the number and predicted function of terpene and siderophore clusters impact species phenotype will be one focus of future research.

Finally, we detected 213 genes that appear to be “uniquely expressed” in *A. parasiticus* SU-1. These genes and their transcripts were not identified in *A. flavus* 3357 as part of the current study or in the *A. flavus* 3357 genome available online. KOBAS GO Pathway analysis enabled us to place 27 of these 213 genes into functional groups including secondary metabolism (4 genes), cellular defense/stress response (14 genes), and C6 (zinc binuclear cluster) transcription factors (9 genes)^{131,132}.

Members of the C6 transcription factor family are particularly interesting because they are specific to fungi and are strongly associated with many secondary metabolism gene clusters in both *A. flavus* and *A. parasiticus*. In the current study, we manually identified 13 different C6 transcription factors associated with secondary metabolite gene clusters in both 3357 and SU-1. AflR, one of those 13 C6 factors, is a key positive regulator of expression of most of the aflatoxin genes¹³³; *aflR* is clustered with the other

aflatoxin genes on Chromosome 3 in *A. parasiticus* SU-1 and *A. flavus* 3357. In parallel studies, we used ChIP Seq analysis to demonstrate that the bZIP transcription factor AtfB interacts with promoters of several different C6 transcription factors in *A. flavus* 3357 suggesting that AtfB plays a direct role in regulation of secondary metabolism via activation of expression of C6 transcription factors (Wee et al., in preparation). We previously demonstrated that AtfB and AflR physically interact suggesting that AtfB may help recruit the C6 transcription factors to promoters of secondary metabolism genes. Yin et al. (2012) demonstrated that another bZIP designated RsmA, binds to 2 sites in the AflR promoter helping to activate its expression in *A. nidulans*³⁷. These observations suggest that the C6 transcription factors play an important role in regulating secondary metabolism and that we could target them to modulate secondary metabolite expression without affecting the host plant or humans that consume crops associated with mycotoxins. .

The 27 “uniquely expressed” genes and their functional networks described briefly above will be the focus of future efforts in analysis of the genetic basis for biochemical and morphological differences between these closely related species.

CHAPTER 5: PROPOSED FUTURE STUDIES

A. Studies to explore newly identified AtfB networks in detail

At the end of Chapter 2 in this dissertation, we concluded our discussion proposing that AtfB could mediate novel cellular processes involved in actin cytoskeleton arrangement/transport and other targets in cellular defense. We propose that AtfB could be a negative regulator of endosome biogenesis and of aflatoxin export. We know that *Velvet* (VeA), a global regulator of *Aspergillus* secondary metabolism regulates endosome development and aflatoxin gene expression, and we now have some evidence that AtfB could be a master regulator of *Aspergillus* secondary metabolism and could be the “key coordinator” between aflatoxisome development and aflatoxin gene expression. Real time fluorescence microscopy (for example, fluorescent antibodies against myosin/dynamin or fluorescent dyes such FM464 and Cell Tracker Blue (CMAC)) coupled with time course AtfB promoter binding studies in AtfB disruption strains (JW-12 and JW-13) will be very helpful to understand the correlation between the expression pattern of sentinel genes and endosome/vacuole ratio.

B. Studies to understand details in the involvement of Vps34 in early endosome maturation, fusion, and export

Our studies linked aflatoxin biosynthesis to an early endosome-associated lipid kinase, Vps34. We propose that blocking late endosome to vacuole fusion and/or early endosome to late endosome maturation and fusion facilitates accumulation of aflatoxisomes carrying functional aflatoxin enzymes resulting in increased aflatoxin accumulation. Studies focusing on identifying signals that activate early to late

endosome maturation (either chemically or genetically) could provide novel targets to manipulate secondary metabolism at the cellular level. PIP3, a lipid product of Vps34 is thought to facilitate maturation of early to late endosomes. A time course purification of the vesicle/vacuole fraction followed by measurement of PIP3 levels by mass spectrometry will be helpful to characterize this process.

C. Studies to explain the mechanism driving the endogenous CRISPR/*cas9* system for genome editing in filamentous fungi

Studies focused on identification of a CRISPR-like locus within *A. parasiticus* and/or proteins that encode a Cas9-like endonuclease will be the first step to understand this mechanism. Alternatively, the *Aspergillus* genome editing system could be a hybrid between an RNAi-mechanism (accumulation of mutant transcripts down-regulate native transcripts) and a CRISPR/*cas9* system in eubacteria.

D. Studies to investigate 213 “uniquely expressed” genes in *A. parasiticus*

KOBAS GO pathway analysis placed 27 of these 213 genes into functional groups, including secondary metabolism (4 genes), cellular defense/stress response (14 genes), and C6 (zinc binuclear cluster) transcription factors (9 genes). Members of the C6 transcription factor family are particularly interesting because they are specific to fungi and are strongly associated with many secondary metabolism gene clusters (cluster-specific transcription factors). To understand the genetic basis for biochemical and morphological differences between closely related species, the 27 unique genes and characterization of their function will be the focus in upcoming studies.

APPENDICES

APPENDIX A:
COMPUTER-AIDED ALGORITHMS REVEAL NOVEL CIS-REGULATORY
ELEMENTS IN AFLATOXIN BIOSYNTHESIS

INCLUDED AS PART OF:

Roze, L. V., Chanda, A., **Wee, J.**, Awad, D. & Linz, J. E. Stress-related Transcription Factor AtfB Integrates Secondary Metabolism with Oxidative Stress Response in *Aspergilli*. *Journal of Biological Chemistry* **286**, 35137–35148 (2011).

BACKGROUND

Approximately 10% of the *A. parasiticus* and *A. flavus* genome appears to be dedicated to secondary metabolite synthesis. This percentage only includes structural genes and key enzymes present in specific pathways without taking into account other genes that are responsible for the regulation of secondary metabolism. Using computer-aided software analysis of secondary metabolite clusters (anti-SMASH), we demonstrated that *A. parasiticus* SU-1 and *A. flavus* NRRL 3357 may carry up to 93 secondary metabolite gene clusters. Approximately 60% of the secondary metabolite clusters are committed to the synthesis of PKS and NRPS in both *A. parasiticus* (30 PKS and 22 NRPS) and *A. flavus* (28 PKS and 22 NRPS). From an evolutionary standpoint, why is such a large percentage of the genome dedicated to the synthesis of secondary metabolites?

Sequence Analysis of Aflatoxin Gene Promoters

Several lines of evidence presented above indicated that aflatoxin gene promoters contain AtfB-binding sites. We applied MEME motif-based sequence analysis (available at: <http://meme.nbcr.net/meme/>)¹³⁴ to search for random 8-mer motif pattern occurrence within the 500-bp promoter regions upstream from the translation initiation codon (ATG) in 17 aflatoxin genes (*pksA*, *nor-1*, *fas-2*, *fas-1*, *aflR*, *aflJ*, *adhA*, *estA*, *ver-1*, *verA*, *avnA*, *verB*, *avfA*, *omtB*, *omtA*, *ordA*, and *vbs*) and *laeA*. Exceptions included *avnA* and *avfA*, whose entire intergenic regions (367 and 173 bp correspondingly) were used for the analysis. A conserved motif AGCC(G/C)T(G/C)(A/G) (with the second highest frequency occurrence) was found 11 times in eight promoters (**Figure 29**). Six of the eight promoters possessed only one motif. Promoters of divergently transcribed genes (*fas-2/fas-1* and *aflR/aflJ*) shared the only motif that was located in the corresponding intergenic region. Two promoters contained multiple octamer motifs: *pksA* carried two motifs and *verA* possessed three motifs. Five of these eight promoters exhibited AtfB binding in ChIP analysis: *nor-1*, *fas-1*, *fas-2*, *pksA*, and *aflR*. The conserved octamer motif was not observed in the *vbs* promoter that also did not bind AtfB in ChIP analysis. In the *nor-1* promoter, the motif was found one time and included a portion of the CRE1 site identified previously in the *nor-1* promoter, TGACATAA (**Figure 29**). Interestingly, the five nucleotides immediately upstream from TGACATAA were highly conserved in all eight promoters, suggesting that they may contribute to AtfB binding.

Novel Predicted Motif in Aflatoxin Gene Promoters Overlaps CRE1

MEME motif-based sequence analysis of aflatoxin gene promoter regions revealed one novel motif AGCCG/CTG/CA/G that was highly conserved in eight aflatoxin promoters that belong to early (*pksA*, *nor-1*, *fas-2*, *fas-1*, and *aflR*) and middle (*aflJ*, *estA*, and *verA*) genes in the aflatoxin pathway. Importantly, in the *nor-1* promoter this motif overlapped the CRE1 site. The discovery of five conserved nucleotides AGCCG immediately upstream from CRE1 suggests that the functional AtfB-binding site in aflatoxin promoters may consist of 13 or more nucleotides, which agrees with our EMSA data. Future studies are necessary to clarify the functional role of this novel motif.

Our observations support the idea that the *in vivo* interaction of AtfB with the aflatoxin promoters occurs at the extended recognition sites containing CRE motifs of variable sequence. An analogous phenomenon was noticed in *S. cerevisiae* during the study of *in vivo* binding of the transcription factor Sko1 (an ortholog of AtfA) to the target gene promoters in response to osmotic stress. In this study the authors observed that the 15 Sko1 target promoters contain 47 CRE motifs with a variable near-consensus sequence, whereas only one motif was identical to the consensus. Moreover, the evolutionarily conserved CRE motifs also possess 2–5 flanking nucleotides upstream and/or downstream from the CRE site, and these nucleotides were conserved among the sensu stricto yeast species.

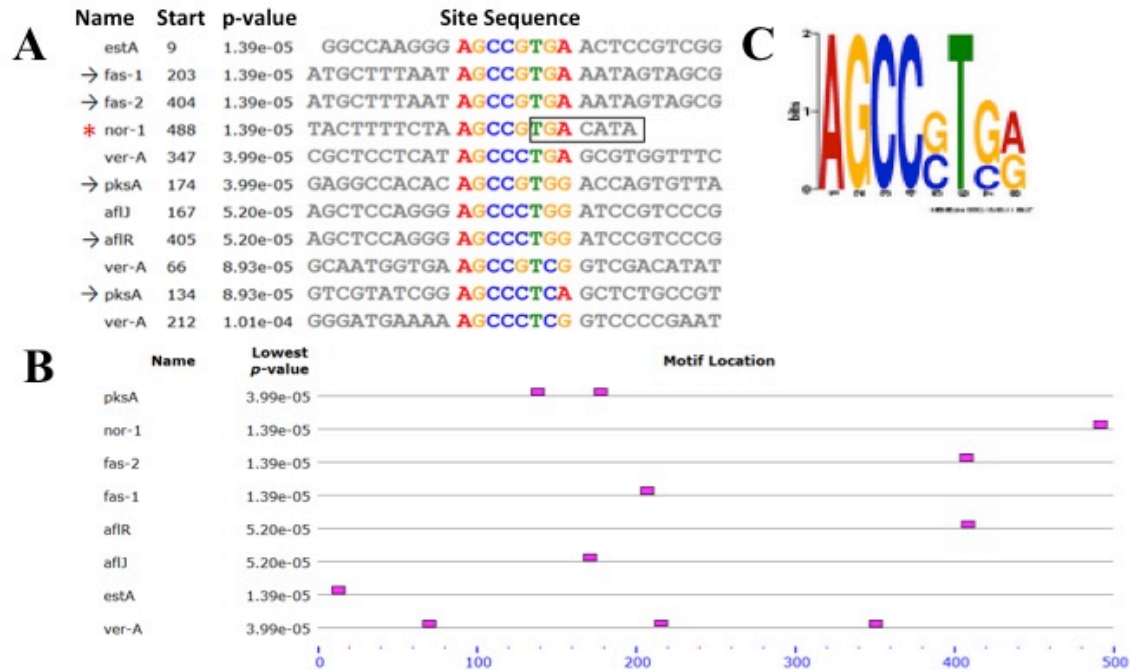


Figure 29 Sequence analysis of aflatoxin gene promoters using MEME

500-bp promoter regions upstream from ATG in 17 aflatoxin genes and *laeA* were analyzed for 8-mer motif pattern occurrence using MEME motif-based sequence analysis. The motif AGCC(G/C)T(G/C)(A/G) (second highest frequency occurrence) was found a total of 11 times within eight promoters. **Panel A**, sites carrying the motif in eight promoters; *, the *nor-1* promoter contained a functional CRE1 motif; 3, promoters analyzed by ChIP. **Panel B**, occurrence and location of the motif relative to the translation initiation codon (ATG-denoted at the end of the scale). Divergently transcribed *fas-2/fas-1* and *aflR/aflJ* share the only motif located in the corresponding intergenic region. **Panel C**, sequence logo of the motif, which contains partial a CRE1 site represented by position-specific probability matrices on the positive strand.

PRELIMINARY STUDIES

Based on our previous work, we expanded upon the current MEME analysis to include two additional features, (1) expanding the size of the motif from an 8-mer motif to a range of 7-12 bp sequence and (2) extracting the entire promoter region within the aflatoxin gene cluster. For the purpose of this study and in the context of aflatoxin biosynthesis, we define a 'promoter' region as sequences upstream of the ATG translation initiation codon. There are two reasons why we expanded this analysis. In the human genome, promoter regions typically range from 500 bp to 2 kb in length¹³⁵. In the case of the *nor-1* promoter in aflatoxin biosynthesis, the 8-mer binding site of AtfB (CRE1bp) overlaps with the transcriptional start site. By setting a range of 7-12 bp motif, we were able to expand the length of the motif to include regions that could be highly conserved beyond the 8-mer motif.

```

>norB-cypA
TGTGTGGATTCGTGAGTGTCTTTAGGGGTCGGATCGATGAACATTAGGTTTCGCTGCCAGACTGTAGTTTATC/TATCATAAAAA
GTGACCATCCAGCAG
CTTCGGCCACCGAAGGTCGGGTTCCGCTCCAGGGAAGTGACAGGGACTGGCCAGTTTCGATACCCCCACCCAAGCCAGGGATAA
GTAGCAGTAAAATGGT
AAATGGCCCTTATAAAGAGGAGTGGCCACATACGTTTCGACAGGAATCGTATCGTCTCCTTTAACCAACATTGGCCACC

>pksA-nor1
TGTGGGATAGGGTATGAGATTGTTGAAACTGGATGGAAGCAGGTCGCCCCCCGAGGAGCTATAGGAAGCTATATCAGTATTTGAA
AACTACACTTCGAGAT
ACTTCGTCGTTGACCGATGAGCTGAGTCTGATCGGAGCCCTCAGCTCTGCCGTCAGGTTACCAAGAGGCCACACAGCCGTGGA
CCAGTGTACTTCCCG
AAAAATGAGACCATGGTATATGCTTATTGACCATGTGGCCATCGAAGAGACTCAGCTTAGGACTACACGTCTAGCATCCGTTT
CCCCGGTCAGCAAGAG
GAGCCTTCAGCCATTCGATGTGACAAAGGCCTCCTATAATCATGTCCGATGTGATCGCATTAGACTTTTCTTCGGCAAGGAGA
GCCGTGACGATCTCCA
TGACAGTATATGGAGGATCTCCGTGACCTTTCTCCGAGGATCTGCGTGTGTAGCTCGCTTCCGACACGGCCTTTACCACCC
CAATCTCCCTCGCGTA
CCCGACACAGACCGATTGTGACCGCTCTTAGACAAAGCAGAGGGGCGAAAGAAGAAATTAAGAGCGTGTTCCTCCTTGACAGC
GGGAGTTGGCTGTCC
ACGCCTCTTTCAGTCGCATATACACCAGAAGAACAACAAGATGGGCACCGAATATGTGGCCGTCCTCACGGGGTCTTTTGA
CGGTATCTTCCCATC
TCTACACCCATTGAAGTTTGGTAAGCACCTAATCAGATGCAGGAGCCATGATGAACCTCCACCTGCTCACCATTCCCATTCTT
ATCGAGACCACCCGAC
AGCCAGCCAGTTGGTGCACCAATGGAGCCGATTTTCTACAGCGGCCATCGTAAAGGTCTGGAATCGCCTTGGTGACGGGTG
CCCTATACGGATATGC
GGCGTGGGCAAGTACTCTGTCCGTGAGCCTTGGCATCACTGGATGGTCCGCGCGTACGACGGTGTAGCATGGTGCCTTACAC
ATGGATGTTTCATGAAC
GCTACGAACACCGCCCTCTTCCACGCCGAGGATCAGTTCGAGAAAGGGGGCGTGAATAGCTTTCAGGAGAGCGTGAGGTTG
GTAGGAAGTGGGATTTG
GCTCAACACTGTGCGGAGCGCTCTTTCACCTGGCGGGCTCGGTGATGGGGATGCTGGGAGTGTGCGGCGTGGTGCCTTACTGATG
GTGATGGTCTTGACCA
TGCAGAGCTAAGGGAGATGCCGGCCCGTATTACTCAGATGTTTTATGGATGTAAC TAGTAGTAAATTCGGACTGACCAAAACGTC
TGTCACTTGTGAGTTG
CAACCTAATGCAAGAACCTAGCGGTCAGCGAATGTTAAGTCGAGCGGACATGGCCACGCATGTCCGTCCTGCTATGGTGACCT
ATTGCTAGTAGAGGCC
ACATAGGCTACTCAAATTTGACATGAGCAGATCTCTGCTATTAAGTCGGTGATTAGCGTGTGATGCGCGAATATCATTAGAT
ATGCCTTTTCTTTCTT
TTCTTTTAAATTTCTTTTGGGGGCCAGCAGCGGAGATCGAATTTGTTGGCATAACCATCAAATGCCTGCCACCCAACCGCCC
AATCGGCCAGCGACC
AACACACCGCCATATATAGTGGGATACGATCATGGGCTTTTGGTGGTTTCAACATTTCTTGAGTACTTTTCTAAGCCGTGACAT
A

>fas2-fas1
GCCTCGCACCGCTTTTGGGCCATGTCCGTCAGGATGCTGGACGGACCCAGCTCGACGTAGCGTTGAACAGCATTCTGTTGACC
GATTAATATGTTCCCTGC
GTGTCGACCCTGAGTCGATGTCTGGTAAATATGTCCTCCACGTTGAAGCGTTACAGTTGATGGAGTGTATCAGAGTCTCACC
AGCGGACAGGGAAATGC
TAAATGATGTCTGTACGAAGGTGAGATTAGCTGGCCATCGGTTGCAGTATACTAAGAAAGGGGCTGGAGTTATTACGCAAGGAG
CTCGACCAATAGTTGA
TGTGCAATATATTGATCATCCATGGCTTCTGGTCTCATATCGATACTCCGTTTTAGACACGAGCTGCGCGATCCGCCGTGGAA
TAAGATAGGAATGCTT
TAATAGCCGTGAAATAGTAGCGCTCATATAAATTAGTATCGGTTCAATGCTCGAACACCTAAGTTGATCACCGGCAATGATAC
TTTGCAGCCCGAACCC
CGAATCCCAGACTCTCGTGTGAGGTGAAAGGAAGACGCTCGGCTTGTCAAGAATGGCAGCCAGGCTGTGCACCAGACAGACT
AGGCCAAGGTTGGAG
GCCTCAAAATCTCTTTTCTTCTCCCTTGCTCGTAAAGTTTACATACTCCCTTTAACTACTACAGCTTTACTCTAAGGTG
ATTGTTTGGCTCTAAG
G

>af1R-af1J
CGTGGAGGTGAGGAAGGAATTCAGGAATCTCAATTGAAAGCGGGAAAGAAAACACACAAGGTGAAGGCTTGCTCCGGGAGAGT
AGCCGGCCCTTTTCGT
TGCTTCGCCTTAGGCCTAAATGTATGTACTCCTGTACCAGCTGAGGGGTTCTGACTTGCCCAAGGATTGTCTAGCTGTG
CGTTCCTTGTTTACGT
ACCGAGGCTGAAACCGGGTGACCAGAGAACTGCGTGATCGGTTTAAACGAAGCAAACCAAGCAACAAATAATGTTTCAGCTAGC
TGGCCCGCCTGCATGC
ATGCCTCGGGCTCAAGATAACGTAGTCCGTCATGGCGGGCTGAGAACCAGAAAAGACTTGTTCCTCGAAGCTAGATCTTTA
GCACCTGCGTGAGCTC
CAGGAGCCCTGGATCCGTCGCCGTTGCGAGTGTGAGATACCACCTGCGAACGTAATCTAAGAAATGGGACATAGATATGCCTGC
CGGGCTAACGATGCTG
ACGAAAGATAAAAAGTACGAGCCGGCAGATAGTACTCGGCTTGACAGATCAGCACTCCTTGACGCAGAGAAAGGATTACTGCTGGT
CAGATCCAAAACCTCT
TCAGATCACCTGTATTCTCAGCGACTTTTAAATCCAATGGGACGTTTCAGTAGCTCTCCTTGACCCGCACGGGATTTGCCGGT

```

Figure 30 Example image of input .txt. format of promoter regions

MEME Submission Information (job appMEME_4.10.01426530693384-1391171042)

meme@nbcrc.net

To: wee, josephine

Monday, March 16, 2015 2:31 PM



MEME

Multiple Em for Motif Elicitation

This is an auto-generated response to your job submission.

Your job ID is: **appMEME_4.10.01426530693384-1391171042**

You can view your job results at: http://nbcrc-222.ucsd.edu/meme_4.10.0/info/status?service=MEME&id=appMEME_4.10.01426530693384-1391171042

Job Details

| | |
|--------------------------|--|
| Submitted | Mon Mar 16 11:31:33 PDT 2015 |
| Expires | Fri Mar 20 11:31:33 PDT 2015 |
| Description | Graduate student |
| Sequences | A set of 18 DNA sequences, between 173 and 1685 in length (average length 753.6), from the file <code>Pafl_cluster (1).txt</code> which was renamed to <code>Pafl_cluster_1.txt</code> . |
| Background | A order-0 background generated from the supplied sequences. |
| Site Distribution | Any number of repetitions (of a contributing motif site per sequence) |
| Motif Count | Searching for 30 motifs. |
| Motif Width | Between 7 wide and 12 wide (inclusive). |

Figure 31 Screenshot view of MEME job submission

MEME analysis is available at <http://meme.nbcrc.net/meme/tools/meme>.

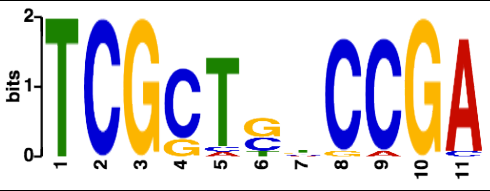



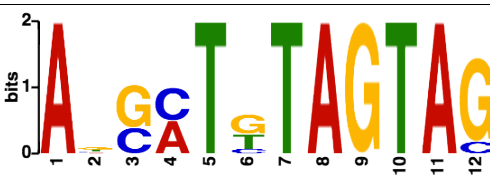

| Motif Logo | E-value | Sites | Motif Width |
|---|----------|-------|-------------|
|  | 3.3e-012 | 20 | 11 |
|  | 8.4e+005 | 11 | 12 |
|  | 1.5e+006 | 10 | 12 |
|  | 2.5e+006 | 9 | 9 |
|  | 1.7e+006 | 8 | 12 |
|  | 8.3e+005 | 8 | 9 |

Figure 32 Six highest reoccurring motifs based on preliminary analysis

The first two motifs are known to play a functional role in aflatoxin biosynthesis, the AfIR-site (occurring 20 times within promoters in the aflatoxin gene cluster and the AtfB-site (occurring 11 times within promoters). There are 4 other novel *cis*-regulatory regions present within promoters that could potentially play a functional role in transcriptional regulation of aflatoxin biosynthesis.

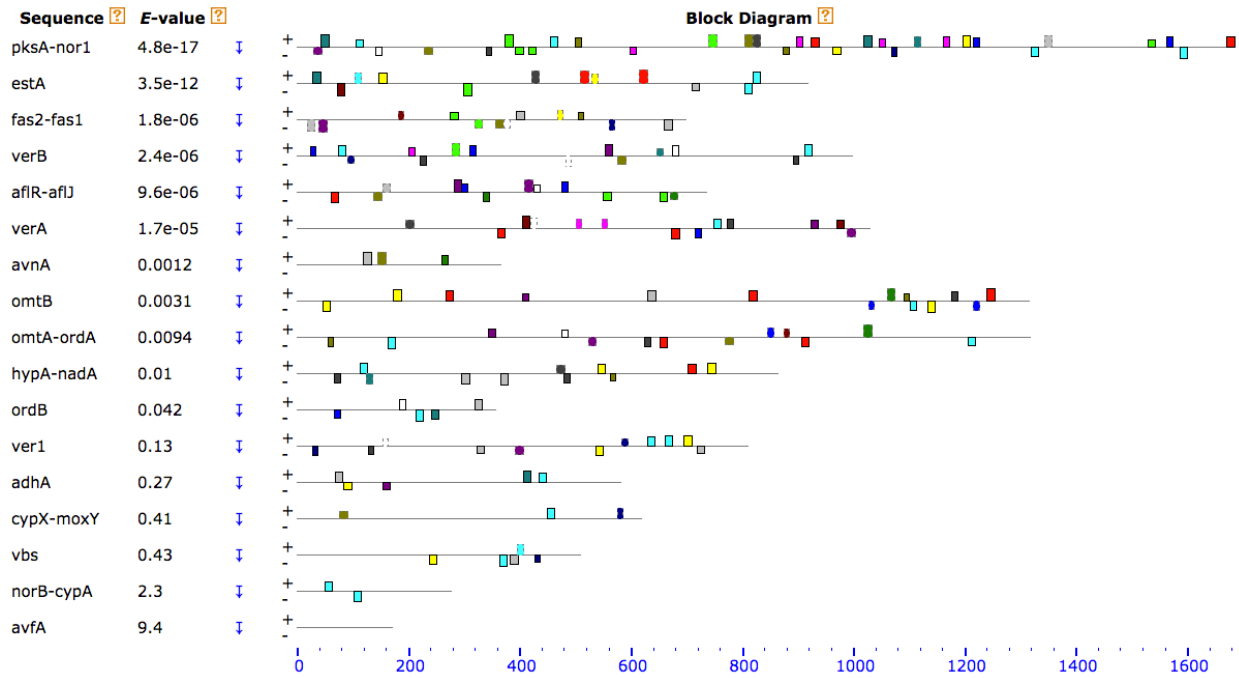


Figure 33 Location and distribution of 30 motifs

FUTURE STUDIES

Research questions

1. What are the cis-regulatory regions that control transcriptional regulation of genes co-regulated by and with aflatoxin biosynthesis?
2. Are there overlapping motifs present within promoters of the AtfB network (see AtfB paper 2015) linked to actin cytoskeleton rearrangement and transport?
3. Can we categorize and characterize 'master or major' cis-regulatory elements that are essential to drive expression of functional networks involved in virulence-associated processes (SM, SR, CD)?
4. Are elements of cis-regulatory regions specific for NRPS, PKS, terpenes, and siderophores or do they overlap between these functional groups of genes? Is transcription of genes within these groups driven by the same or different transcription factors?

APPENDIX B:

BIOCHEMICAL COMPOUNDS THAT TARGET AFLATOXIN BIOSYNTHESIS

BACKGROUND

Our laboratory has focused extensive research effort on identifying and characterizing compounds that inhibit aflatoxin biosynthesis. Initially, my research efforts were focused on characterizing the effect of a PI3K inhibitor, wortmannin on a cAMP/PKA signaling pathway. Wortmannin was previously shown to inhibit aflatoxin synthesis and decrease aflatoxin gene expression⁸⁸. My interest in PI3Ks led to the pursuit of another biochemical compound, 3-methyladenine that selectively inhibits Class III PI3K associated with endosomes and autophagosomes (**Chapter 3**, page **82**). Thus, we hypothesized that PI3Ks may play a dual signaling role (PI3K/cAMP/PKA pathway and vacuole biogenesis) in aflatoxin biosynthesis.

In 2007, our laboratory showed that the initiation and pattern of histone H4 acetylation in aflatoxin promoters correlated with the onset of accumulation of aflatoxin proteins and subsequently, aflatoxin production⁶⁴. The data supported the role of epigenetic regulation in aflatoxin synthesis. Our work suggested that the order of genes within the aflatoxin gene cluster determines the timing and order of transcriptional activation, and that the site of initiation and spread of histone H4 acetylation mediate this process. As part of this study, we were interested in biochemical compounds that target epigenetic regulation in aflatoxin synthesis. Specifically, we were interested in the function of two enzymes, histone acetyltransferases (HAT) and histone deacetylases (HDAC). HATs are responsible for the addition of an acetyl-group to conserved lysine

residues on histones where as HDACs remove acetyl-groups from these lysine residues. The opposing function of HATs and HDACs determines how tightly DNA wraps around histones, consequently influencing exposure of DNA to factors that increase or decrease the level of gene expression.

Zinc is required for the production of aflatoxin. Between the 1960s and 1980s, several studies described a stimulatory effect of zinc on aflatoxin biosynthesis in *Aspergillus parasiticus* and *A. flavus*^{136–139}. Our preliminary observations suggest that a zinc chelator, TPEN reduces aflatoxin levels in *A. parasiticus* (Day, unpublished). 100 μ M TPEN decreased aflatoxin levels produced by SU-1 grown on PDA solid media and 200 μ M TPEN decreased aflatoxin levels produced by SU-1 grown on a minimal media, GMS (**Figure 34** and **35**).

PRELIMINARY STUDIES

Table 6 highlights some potential compounds that target aflatoxin biosynthesis in *A. parasiticus*. The compounds are categorized by their effect on PI3Ks, histone acetylation/de-acetylation, and zinc regulation. These are preliminary observations and lack quantitative data because aflatoxin levels were measured by TLC. Although each treatment was conducted in triplicate cultures, some data collected were part of a single experiment (no biological repetitions). Nonetheless, I choose to present these data as they represent potential avenues to pursue based on preliminary data collected.

Table 6 Potential compounds to control toxic secondary metabolite synthesis by *A. parasiticus*

| Cellular target/ signalling pathway | Biochemical compound (known function) | Preliminary observations |
|--|--|---|
| Class I/II PI3K (cAMP/PKA) | Wortmannin | YES, YEG solid media (no change in aflatoxin levels produced) GMS, SMS solid media (inhibitory effect) Effects of different sugars (glucose, sucrose) on inhibitory effect of wortmannin (Figure 36) |
| | GSK 1059615 | On-going experiments |
| | NVP-BEZ235 | On-going experiments |
| Class III PI3K (Vacuole biogenesis) | 3-MA | Inhibitory effect on GMS liquid media (Chapter 3, page 107) |
| | PIT-1 | Inhibition of aflatoxin production in B62 strain grown on solid GMS media |
| Epigenetic regulation (HAT/HDAC) | Curcumin | Inhibition of aflatoxin levels produced by SU-1 grown in YES liquid media for 72 h in the presence of 1 μ M, 10 μ M, and 100 μ M curcumin observed by ELISA |
| | Anacardic acid (HAT inhibitor) | No inhibition on aflatoxin levels produced by SU-1 grown in YES liquid media for 72 h in the presence of 15 μ M and 50 μ M anacardic acid observed by TLC |
| | Garcinol (HAT inhibitor) | Approximately 2-fold reduction of aflatoxin levels produced by SU-1 grown in YES liquid media for 72 h in the presence of 10 μ M garcinol (changes in mycelial morphology and structure observed) |
| | Trichostatin A (HDAC inhibitor) | No observed changes in aflatoxin levels observed by SU-1 grown in YES liquid media for 72 h in the presence of 1 μ M Trichostatin A |

Table 6 (cont'd)

| Cellular target/ signaling pathway | Biochemical compound (known function) | Preliminary observations |
|---|--|--|
| Zinc chelators | TPEN | Reduction/inhibition of aflatoxin production in SU-1 and B62 strains grown on PDA and GMS solid media; 500 μ M TPEN completely inhibits fungal growth on PDA and GMS (Figure 34 and 35) |
| | DMPS | On-going experiments |

TPEN: N,N,N',N'-Tetrakis(2-pyridylmethyl)ethylenediamine, DMPS: 2,3-Dimercapto-1-propanesulfonic acid, HAT: histone acetyltransferase, HDAC: histone deacetylase

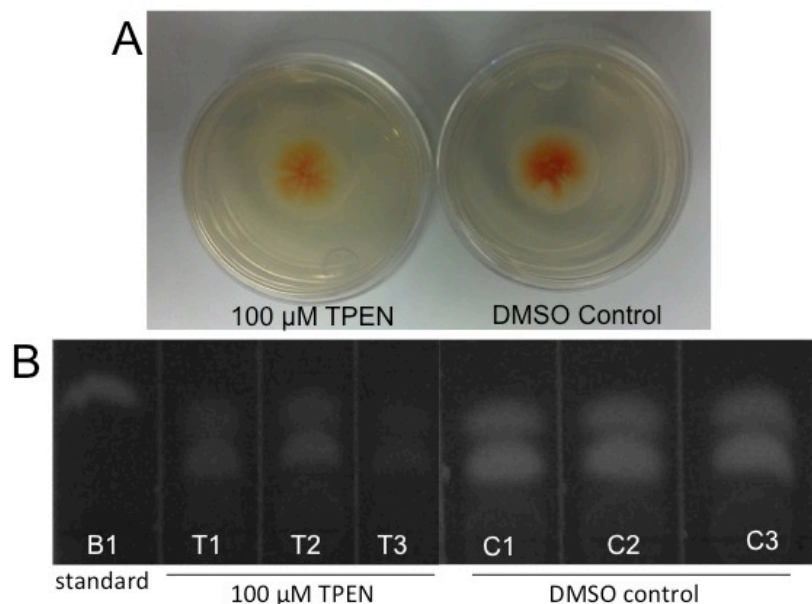


Figure 34 TPEN decreases aflatoxin biosynthesis on PDA solid media

A. parasiticus B62 (**Panel A**) or wild-type SU-1 (**Panel B**) were grown for 50 h on PDA under standard conditions (DMSO vehicle control) or treated with 100 μ M TPEN. The final dose, 100 μ M TPEN was established from preliminary dose response experiments on PDA and corresponded to the dose of TPEN that caused a maximal effect on aflatoxin production and minimal impact on fungal growth. TPEN was administered in the same volume as the DMSO control. Red color pigment visualized in Panel A is norsolorinic acid, an early pathway intermediate that serves as a useful indicator of aflatoxin accumulation. In **panel B**, aflatoxin was extracted from treated and control cultures and resolved by TLC. Preliminary observations indicate that 200 μ M TPEN reduced norsolorinic acid in B62 (Panel A) and aflatoxin levels in SU-1 (Panel B) grown on PDA media. Two biological replicates of the experiment were conducted, each with triplicate samples as indicated by the numbers 1, 2, and 3. Both experiments exhibited a similar trend in aflatoxin reduction. **Figure 35** represents a single biological experiment. B₁: aflatoxin B₁ standard (Sigma), T: TPEN, C: DMSO control.

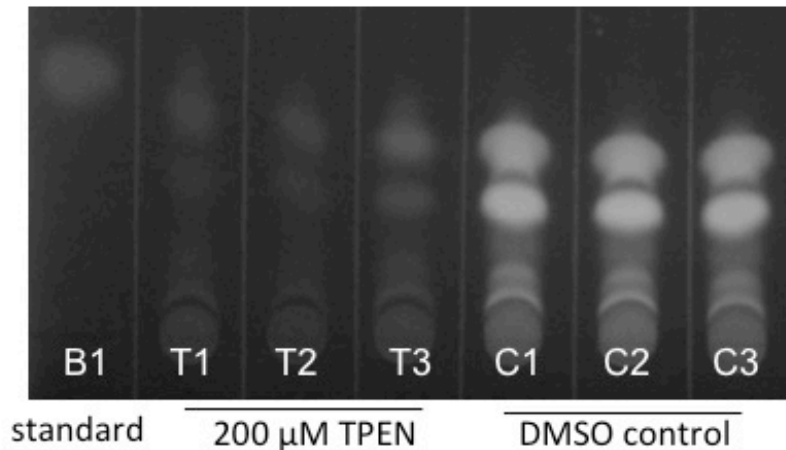


Figure 35 TPEN decreases aflatoxin biosynthesis in GMS

A. parasiticus SU1 grown for 120 h on GMS under standard conditions (DMSO vehicle control) or treated with 200 μ M TPEN. The final dose, 200 μ M TPEN was established from dose response experiments and corresponded to the dose of TPEN that caused a maximal effect on aflatoxin production and minimal impact on fungal growth. TPEN was administered in the same volume as the DMSO control. Aflatoxin was extracted from treated and control cultures and resolved by TLC. These preliminary observations indicate that 200 μ M TPEN reduced aflatoxin levels in SU-1 grown on GMS media. Two biological experiments were conducted in triplicate as indicated by the numbers 1, 2, and 3 and both experiments exhibited a similar trend in aflatoxin reduction. Figure 35 represents a single replicate of experiment. B₁: aflatoxin B₁ standard (Sigma), T: TPEN, C: DMSO control.

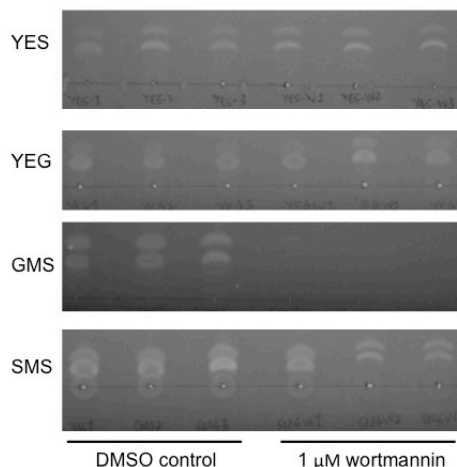


Figure 36 Wortmannin differentially affects aflatoxin synthesis on solid media

A. parasiticus SU-1 was grown on YES and YEG solid media (rich medium in the presence of sucrose or glucose) as well as GMS and SMS solid media (minimal media in the presence of sucrose or glucose) under standard conditions with DMSO vehicle control or 1 μ M wortmannin. Cultures were grown in triplicate. 1 μ M wortmannin was previously shown to inhibit aflatoxin synthesis and to decrease aflatoxin gene expression. Aflatoxin was extracted from control and wortmannin treated cultures and resolved by TLC. Preliminary observations indicate that wortmannin causes a differential effect in inhibition of aflatoxin production in the presence of glucose compared to sucrose in minimal media. Growth on GMS media results in maximal inhibition of aflatoxin in the presence of wortmannin as compared to SMS on which a slight inhibition was observed (data from, triplicate samples not consistent). In contrast, wortmannin treatment did not generate any observable effect in cultures grown on YES and YEG media. These data suggest that the regulation of the fungal cAMP/PKA pathway (cellular target of wortmannin) is different in rich media as compared to minimal media. Another possible explanation is that minimal media mimics the fungal natural environment more closely compared to rich media.

FUTURE STUDIES

1. Characterize the differential effect of inhibitors in minimal versus rich media and glucose versus sucrose as a carbon source. I suspect that the differential effect can be measured at the level of cAMP/PKA activity and/or in pools of precursors such as acetyl-CoA or acetate.
2. Further elucidate the role of zinc chelators on aflatoxin biosynthesis: Is the inhibitory effect of TPEN caused by direct chelation of intracellular zinc? Does DMPS (another zinc chelator) cause similar effects on aflatoxin production under standard conditions? Preliminary observations suggest that TPEN does not affect the level of aflatoxin gene expression (for *ver-1*, *nor-1*, and *afIR*). Thus, we hypothesize that TPEN causes an effect at the protein level and/or by altering levels of TCA cycle precursors such as acetyl-CoA as previously reported. Ongoing studies in the laboratory include measurement of zinc levels in the presence of TPEN by confocal laser microscopy using a fluorescent probe, Zynpyr-1 as well as measurement of acetyl-CoA levels using mass spectrometry.

APPENDIX C:
HETEROLOGOUS EXPRESSION AND PURIFICATION OF THE *ASPERGILLUS*
***PARASITICUS* ATFB DNA BINDING DOMAIN**

This work was conducted at the Department of Molecular and Applied Microbiology, Hans Knoll Institute, Jena, Germany under the guidance of Dr. Daniel Scharf, Dr. Peter Hortshansky, and Prof. Dr. Axel A. Brakhage. The work was funded by a research and travel grant by Michigan State University awarded to Josephine Wee and a partial scholarship obtained through the Jena Graduate School of Microbial Communication under the German Excellence Program.

BACKGROUND

In *Aspergillus parasiticus*, the bZIP transcription factor AtfB physically interacts with a C6 zinc binuclear cluster protein and positive aflatoxin pathway regulator, AflR. This interaction likely impacts expression of *nor-1* (an early structural gene) at the level of promoter activity. Our data suggest that AtfB binding is driven by the presence of a functional cAMP-response element (designated CRE1; TGACATAA) immediately upstream of *nor-1*. CHIP studies utilizing highly specific anti-AtfB demonstrated that AtfB binds to promoters of seven aflatoxin genes (including *nor-1*) containing CRE1-like sites under aflatoxin-inducing conditions but does not bind to promoters lacking CRE sites. EMSA studies expanded on this analysis and found that AtfB binds to promoters of at least two oxidative stress response genes, *MnSOD* and *catalase1* (*cat1*). We recently conducted gene disruption of AtfB in *A. parasiticus*. Disruption strains accumulated

lower levels of aflatoxin and AtfB protein and exhibited decreased levels of conidiospores and conidiospore pigment. Our data also suggest that at the molecular level, AtfB likely impact networks that regulate secondary metabolism (SM), stress response (SR), and conidiospore development (CD). The association between AtfB function and gene regulatory networks is supported by RNA Seq analysis, which was validated by RT-PCR analysis. Taken together, the data support an overall down regulation of expression in the aflatoxin gene cluster as well as in target genes related to SR as well as CD. Although promoter binding and loss of AtfB function suggest that AtfB regulates SM, SR, and CD, details of the cis-acting sites and affinity for AtfB binding to these sites are still unknown. The objectives of the current work were to (1) **express and purify the DNA binding domain of *A. parasiticus* AtfB (recombinant protein designated ApAtfB)** and (2) analyze the binding affinity of ApAtfB to previously identified cis-acting sites such as CRE1 in the *nor-1* promoter and promoters in the AtfB regulatory network using Surface Plasmon Resonance (SPR).

PRELIMINARY STUDIES

Determination of the AtfB DNA binding domain

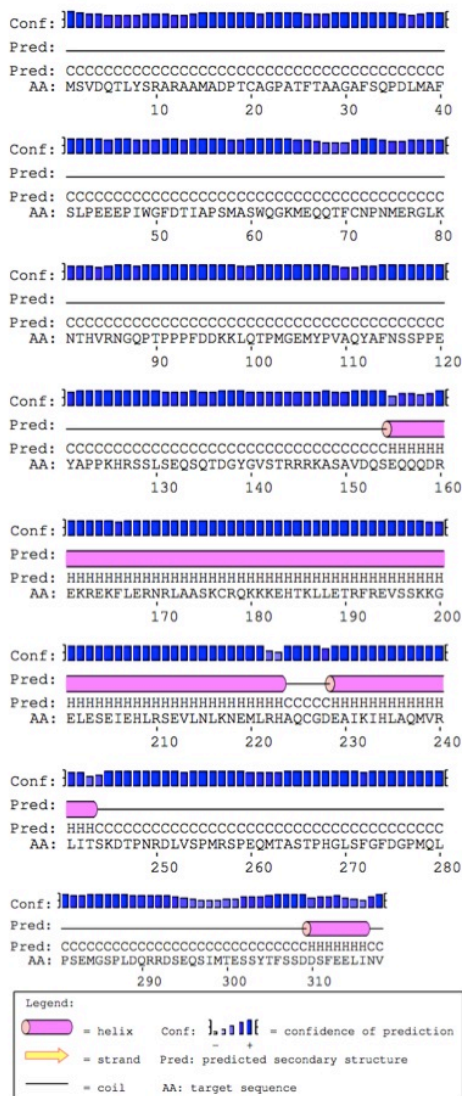


Figure 37 Secondary structure prediction of ApAtfB

A 318 amino acid sequence of *A. parasiticus* AtfB (GenBank: ADZ06147.1) was used to predict the secondary structure using Psipred (<http://bioinf.cs.ucl.ac.uk/psipred/>). Pred: Pink regions highlight the helix region; Conf: blue bar graphs indicate degree of confidence in prediction; the direction of the strand is from N- to C-terminus; solid black lines represent coiled regions. AA: the input ApAtfB amino acid sequence.

Predicted characteristics of ApAtfB

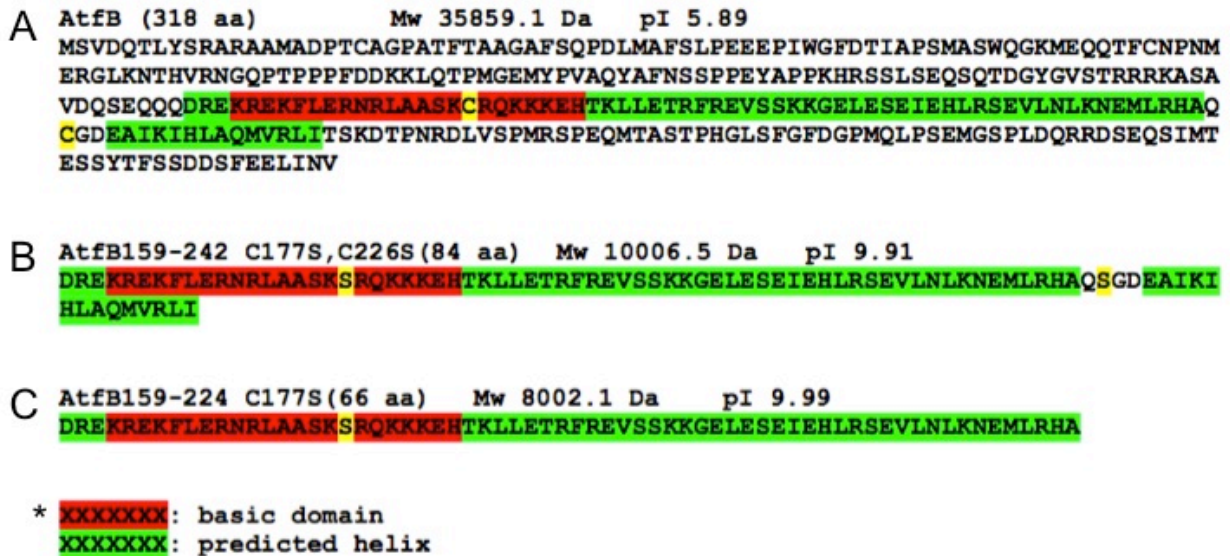


Figure 38 Physicochemical properties of ApAtfB

Panel A: full length ApAtfB amino acid sequence with basic domain highlighted in red, predicted helix highlighted in green, and cysteine residues highlighted in yellow. **Panel B and C.** Long (84 aa) and short (66 aa) fragments of DNA binding domain sequence used to design synthetic gene construct. Cysteine residues (highlighted in yellow) were modified to serine residues to overcome solubility problems. *color codes for basic domain and predicted helix

```

>1DH3:A_Creb (mouse)
KREVRMLMKNREAARESRRKKKEYVKSLENRVAVLENQNKTLIEELKALKDLYSHK
>1T2K:D_At2f (human)
KRRKFLEARNRAAASRSRQKRKVWVQSLEKKAEDLSSLNGQLQSEVTLLRNEVAQLKQLLLA

```

CLUSTAL O(1.2.1) multiple sequence alignment

```

AtfB           MSVDQTLYSRARAAMADPTCAGPATFTAAGAFSQPDLMAFSLPEEEPIWGFDTIAPSMAS 60
1DH3:A_Creb    ----- 0
1T2K:D_At2f    ----- 0

AtfB           WQGKMEQQTFCNPNMERGLKNTHVRNGOPTPPPFDDKQLQTPMGEMYPVAQYAFNSSPPE 120
1DH3:A_Creb    ----- 0
1T2K:D_At2f    ----- 0

AtfB           YAPPKHRSSLSEQSQTGDYGVSTRRRKASAVDQSEQQQDREKREKFLERNRLAASKCRQK 180
1DH3:A_Creb    -----KREVRMLMKNREAARESRRK 19
1T2K:D_At2f    -----KRRKFLEARNRAAASRSRQK 19
                **  * :** ** .*:

AtfB           KKEHTKLETRFREVSSKKGEESEIEHLRSEVLNLKNEMLRHAQCGDEAIKIHLAQMVR 240
1DH3:A_Creb    KKEYVKSLENRVAVLENQNKTLIEELKALKDLYSHK----- 55
1T2K:D_At2f    RKVWVQSLEKKAEDLSSLNGQLQSEVTLLRNEVAQLKQLLLA----- 61
                :*  .: **: .: .: * .: *:.

AtfB           LITSKDTPNRDLVSPMRSPEQMTASTPHGLSFGFDGPMQLPSEMGSPLDQRRDSEQSIMT 300
1DH3:A_Creb    ----- 55
1T2K:D_At2f    ----- 61

AtfB           ESSYTFSSDDSFEEELINV 318
1DH3:A_Creb    ----- 55
1T2K:D_At2f    ----- 61

```

Figure 39 Sequence comparison of Atf2, CREB, and ApAtfB

The DNA binding regions of the bZIP transcription factor CREB (mouse) and ATF2 (human). Multiple sequence alignment analysis using Clustal Omega (<http://www.ebi.ac.uk/Tools/msa/clustalo/>) highlights sequence similarity in the DNA binding domain of ApAtfB, CREB, and AtfB.

Synthetic gene construct

A synthetic gene AtfB159-242_C2S (267 bp) was assembled from synthetic oligonucleotides and/or PCR products based on the 84 aa long fragment seen in **Figure 38 (Panel B)**. The fragment was inserted into a pMA-T vector (**Figure 40**). The plasmid DNA was purified from transformed *E.coli* K12 (*dam+* *dcm+* *tonA*) and concentration determined by UV spectroscopy. The final construct was verified by sequencing. The sequence congruence within the insertion sites was 100%.

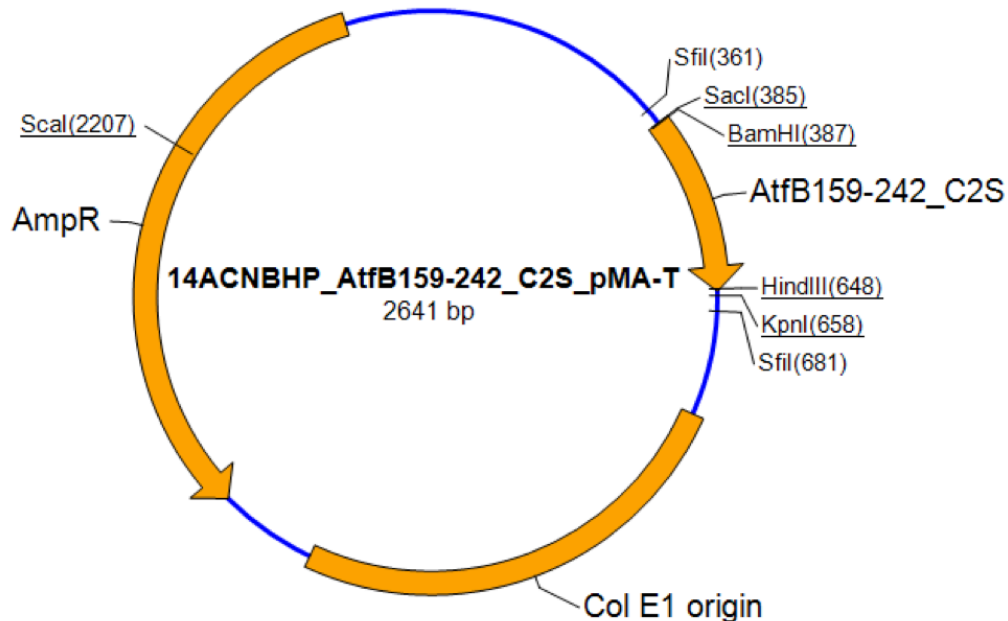


Figure 40 Plasmid map of synthetic gene construct ApAtfB159-242_C2S

A *Bam*HI-site inserted at the 5'-end and a *Hind*III-site was created at the 3'-end for easy insertion into a *Bam*HI-*Hind*III vector.

Protein production and purification of ApAtfB

A *Bam*HI-*Hind*III fragment containing the 267 bp DNA binding domain of ApAtfB (codon optimized for *E. coli*) was synthetically constructed by Life Technologies (Invitrogen) as shown in **Figure 40**. ApAtfB159-242_C2S_pMA-T was digested using *Bam*HI and *Hind*III to obtain the 267 bp ApAtfB159-242_C2S fragment. The 267 bp fragment was inserted into a *Bam*HI-*Hind*III-digested pET28aH6TEV (Kan^R) vector (Peter Hortschansky) and transformed into *E. coli* α -select [*rep* (pMB1), *eco47IR*, Amp^R] (Fermentas, St. Leon-Rot) resulting in pET28aH6TEV-ApAtfB159-242C2S. The integration of ApAtfB159-242_C2S into pET28aH6TEV was confirmed by PCR analysis and subsequently used for expression of ApAtfB. Nucleotide sequence of two clones, plasmid ApAtfB159-242_C2S (1728/1/1 and 1728/1/2) was submitted to the plasmid collection and also confirmed by sequencing.

ApAtfB protein was produced by autoinduction in BL21 (DE3) [*E. coli* B F⁻ *dcm ompT hsdS*(r_B⁻ m_B⁻) *gal* λ (DE3)] (Agilent Technologies) cells grown at 30°C for 24 h in 1 L Overnight Express Instant TB Medium (Novagen) supplemented with 5 μ g/mL kanamycin. 7 g (wet weight) of cells were collected by centrifugation (20,000 rpm for 20 min at 4°C), resuspended in 100 mL Lysis Buffer (50 mM NaH₂PO₄ pH 7.5, 300 mM NaCl, 6M urea, 20 mM imidazole), and homogenized 3 times using an Emulsiflex C5 high-pressure homogenizer (Avestin). The homogenized lysate (L) was centrifuged for 20 min at 20,000 rpm at 4°C. After centrifugation, the supernatant was passed through a 1.2 μ m filter and 100 ml Column Buffer A (20 mM NaH₂PO₄, pH 7.5, 300 mM NaCl, 6M urea, 20 mM imidazole) was added (1:1 lysis buffer to Buffer A). The pellet (P) was resuspended in 200 mL Column Buffer A and a small volume was taken for SDS-Page

analysis. The 6xHis-ApAtfB recombinant protein was purified using a 5 mL HisTrap™FF column at a flow rate of 5 mL/min. ApAtfB was eluted with Buffer B (20 mM NaH₂PO₄, pH 7.5, 300 mM NaCl, 6M urea, 250 mM imidazole) using a 0% - 100% Buffer B gradient (**Figure 41**).

The separation of proteins was carried out on a pre-cast SDS-polyacrylamide gel (NuPAGE 4-12% Bis-Tris gel; Invitrogen). The protein samples were adjusted to the appropriate concentration using the Sample NuPAGE LDS Buffer (4x) and denatured at 70°C for 10 minutes. All samples were treated with 50 mM dithiothreitol (DTT) to reduce disulfide bridges and to prevent formation of multi-mers. The separation of the proteins was performed at 200 V for 30 min. The BenchMark™ Protein Ladder was used as a molecular mass marker standard (Invitrogen). Protein gels were placed in a Coomassie staining solution (0.2% (w/v) Coomassie R-250, 45% (v/v) MeOH, 10% (v/v) acetic acid) for 20 min with gentle shaking. The protein gel was subsequently placed in a destaining solution (20% (v/v) methanol, 10% (v/v) acetic acid) with gentle shaking overnight prior to visualization.

Fractions A2, A4, and A5 were pooled (highest concentration) and subjected to slow dialysis overnight in the presence of 25 mM MES (2-(N-morpholino)ethanesulfonic acid, pH 6.0). 3.5 mL soluble protein was recovered and centrifuged at 13,000 rpm for 5 min. The solution recovered after dialysis was slightly cloudy but with no signs of precipitation. The pellet and supernatant were subjected to SDS-Page analysis (**Figure 43, top panel**). 0.8228 mg/mL of ApAtfB was recovered and visualized by UV/Vis spectroscopy (**Figure 43, bottom panel**).

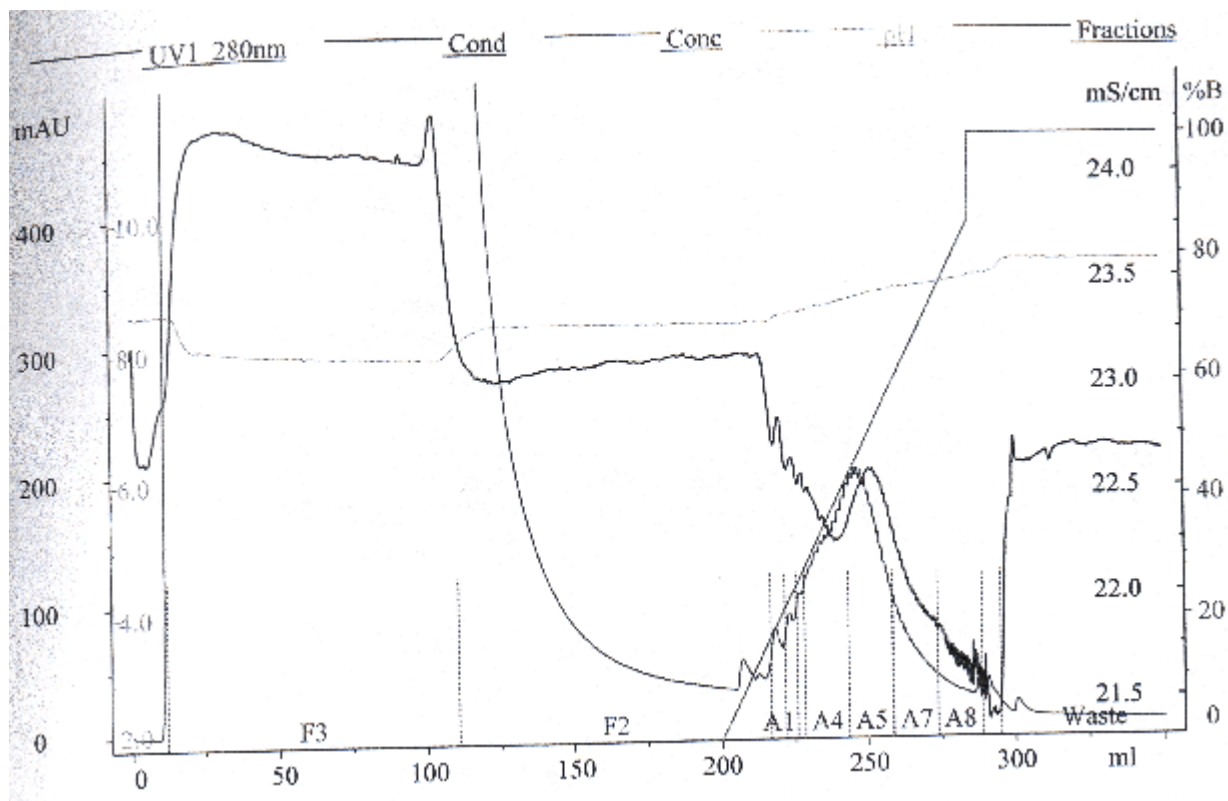


Figure 41 Purification of recombinant 6xHis-ApAtfB (column fractionation)

Chromatogram obtained from the HisTrap™FF column fractionation. Fractionation peaks A1, A2, A4, A5, A7, A8, A9 were collected in separate collection tubes for further analysis.

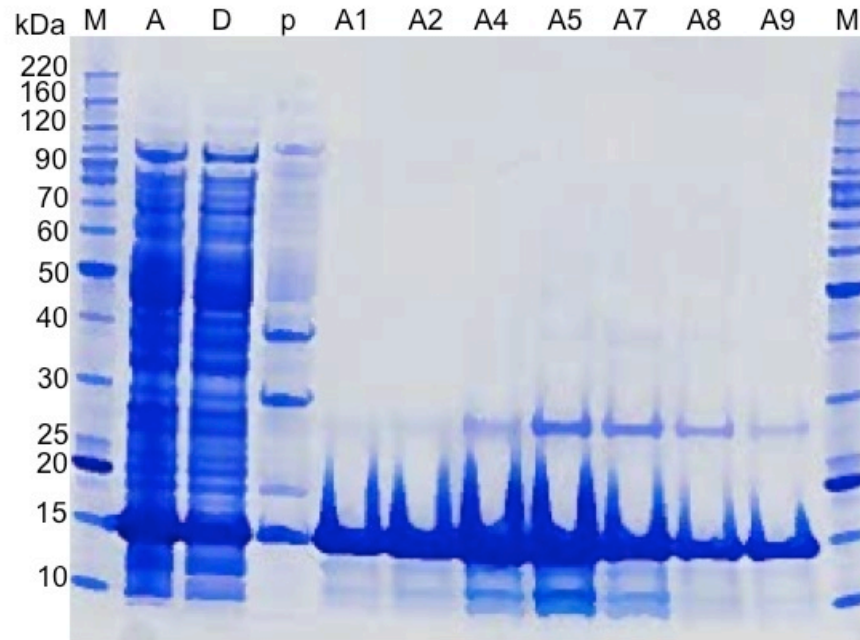


Figure 42 Purification of the recombinant 6xHis-ApAtfB (SDS-Page analysis)

Coomassie Blue-stained SDS-Page of the samples from column purification. A: Lysate (supernatant) obtained from *E. coli*, (D) column flow through, p: pellet obtained after centrifugation of *E. coli*, A1-A9: elution fractions from HisTrap™FF with a 0-100% Buffer B gradient.

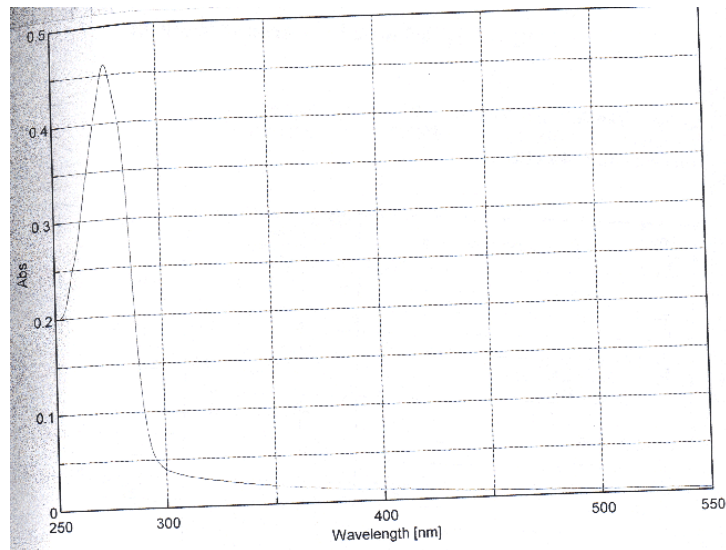
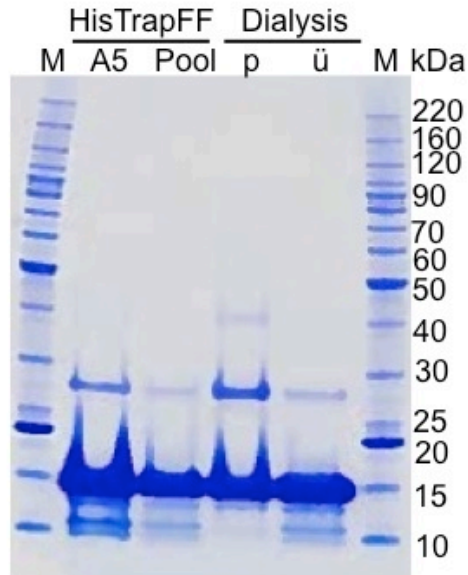


Figure 43 Purification of ApAtfB

Top panel: SDS-Page analysis of HisTrap™FF elution fractions, A5: representative single elution, Pool: pooled elution fractions A2, A4, A5, p: resuspension of pellet obtained after MES dialysis, ü: supernatant obtained after MES dialysis. **Bottom panel:** UV/Vis chromatogram of ApAtfB obtained after MES dialysis.

FUTURE STUDIES

Heterologous expression and subsequent purification of recombinant ApAtfB enables follow up studies on binding and kinetic data of ApAtfB to sequence-specific sites within promoters. I highlight some suggestions below:

1. ApAtfB can be used for SPR analysis (assessment of binding affinity) of the *nor-1* promoter (NorR, NorM, NorL subfragments) previously shown to bind AtfB.
2. ApAtfB can be used for SPR analysis of the *ver-1* promoter (highest binding through ChIP studies), *Mn SOD* and *cat1* (identified through EMSA).
3. Negative controls should be established for AtfB binding such as in the *vbs* and *laeA* promoter (no binding by ChIP studies) or by shuffling of the 8-mer motif.
4. Binding studies can also be expanded to novel promoters identified through disruption of AtfB such as the actin/cytoskeleton transport and heat shock proteins.
5. Crystallization studies of ApAtfB bound to the *nor-1* promoter.

BIBLIOGRAPHY

BIBLIOGRAPHY

1. Brakhage, A. A. Regulation of fungal secondary metabolism. *Nat. Rev. Microbiol.* **11**, 21–32 (2013).
2. Bennett, J. W. & Klich, M. Mycotoxins. *Clin. Microbiol. Rev.* **16**, 497–516 (2003).
3. Keller, N. P., Turner, G. & Bennett, J. W. Fungal secondary metabolism - from biochemistry to genomics. *Nat. Rev. Microbiol.* **3**, 937–47 (2005).
4. Jenke-Kodama, H., Müller, R. & Dittmann, E. in *Natural Compounds as Drugs Volume I SE - 3* (eds. Petersen, F. & Amstutz, R.) **65**, 119–140 (Birkhäuser Basel, 2008).
5. Hawksworth, D. L. The magnitude of fungal diversity: the 1.5 million species estimate revisited. *Mycol. Res.* **105**, 1422–1432 (2001).
6. Linz, J. E., Wee, J. & Roze, L. V. *Aspergillus parasiticus* SU-1 Genome Sequence, Predicted Chromosome Structure, and Comparative Gene Expression under Aflatoxin-Inducing Conditions: Evidence that Differential Expression Contributes to Species Phenotype. *Eukaryot. Cell* **13**, 1113–23 (2014).
7. Sargeant, K., Sheridan, A., O’Kelly, J. & Carnaghan, R. B. A. Toxicity associated with Certain Samples of Groundnuts. *Nature* **192**, 1096–1097 (1961).
8. Nesbitt, B. F., O’Kelly, J., Sargeant, K. & Sheridan, A. *Aspergillus flavus* and turkey X disease. Toxic metabolites of *Aspergillus flavus*. *Nature* **195**, 1062–1063 (1962).
9. Diener, U. L. & Davis, N. D. Aflatoxin formation by *Aspergillus flavus*. *Aflatoxin* (Elsevier, 1969). doi:10.1016/B978-0-12-395513-5.50007-6
10. Wannop, C. C. The Histopathology of Turkey ‘X’ Disease in Great Britain. *Avian Dis.* **5**, pp. 371–381 (1961).
11. Council for Agricultural Science and Technology (CAST). *Mycotoxins: risks in plant, animal and human systems*. CAST Task Force (2003).
12. Carnaghan, R. B. A., Hartley, R. D. & O’Kelly, J. Toxicity and Fluorescence Properties of the Aflatoxins. *Nature* **200**, 1101 (1963).
13. Squire, R. A. Ranking animal carcinogens: a proposed regulatory approach. *Science* **214**, 877–880 (1981).

14. Bbosa, G. S., Kitya, D., Lubega, A., Anokbonggo, W. W. & Kyegombe, D. B. in *Aflatoxins - Recent Advances and Future Prospects*
15. Koehler, P. E., Hanlin, R. T. & Beraha, L. Production of Aflatoxins B(1) and G(1) by *Aspergillus flavus* and *Aspergillus parasiticus* Isolated from Market Pecans. *Appl. Microbiol.* **30**, 581–583 (1975).
16. Yu, J., Bhatnagar, D. & Ehrlich, K. C. Aflatoxin biosynthesis. *Rev. Iberoam. Micol.* **19**, 191–200 (2002).
17. Yu, J. *et al.* Clustered Pathway Genes in Aflatoxin Biosynthesis MINIREVIEW Clustered Pathway Genes in Aflatoxin Biosynthesis. *Appl. Environ. Microbiol.* **70**, 1253–1262 (2004).
18. Yabe, K. & Nakajima, H. Enzyme reactions and genes in aflatoxin biosynthesis. *Appl. Microbiol. Biotechnol.* **64**, 745–755 (2004).
19. Liu, Y., Chang, C.-C. H., Marsh, G. M. & Wu, F. Population attributable risk of aflatoxin-related liver cancer: systematic review and meta-analysis. *Eur. J. Cancer* **48**, 2125–36 (2012).
20. Wild, C. P. & Gong, Y. Y. Mycotoxins and human disease: a largely ignored global health issue. *Carcinogenesis* **31**, 71–82 (2010).
21. Liu, Y. & Wu, F. Global burden of aflatoxin-induced hepatocellular carcinoma: A risk assessment. *Environ. Health Perspect.* **118**, 818–824 (2010).
22. Khlangwiset, P., Shephard, G. S. & Wu, F. Aflatoxins and growth impairment: A review. *Crit. Rev. Toxicol.* **41**, 740–755 (2011).
23. Cotty, P. J. & Jaime-Garcia, R. Influences of climate on aflatoxin producing fungi and aflatoxin contamination. *Int. J. Food Microbiol.* **119**, 109–115 (2007).
24. Khlangwiset, P. & Wu, F. Costs and efficacy of public health interventions to reduce aflatoxin-induced human disease. *Food Addit. Contam. Part A. Chem. Anal. Control. Expo. Risk Assess.* **27**, 998–1014 (2010).
25. Wu, F. Mycotoxin reduction in Bt corn: Potential economic, health, and regulatory impacts. *Transgenic Res.* **15**, 277–289 (2006).
26. Cotty, P. J. & Bhatnagar, D. Variability among atoxigenic *Aspergillus flavus* strains in ability to prevent aflatoxin contamination and production of aflatoxin biosynthetic pathway enzymes. *Appl. Environ. Microbiol.* **60**, 2248–2251 (1994).

27. Cotty, P. J. Influence of field application of an atoxigenic strains of *Aspergillus flavus* on the populations of *A. flavus* infection cotton balls and on the aflatoxin content of cottonseed. *Phytopathology* **84**, 1270–1277 (1994).
28. Atehnkeng, J. *et al.* Evaluation of atoxigenic isolates of *Aspergillus flavus* as potential biocontrol agents for aflatoxin in maize. *Food Addit. Contam. Part A. Chem. Anal. Control. Expo. Risk Assess.* **25**, 1264–1271 (2008).
29. Phillips, T. D. *et al.* Reducing human exposure to aflatoxin through the use of clay: a review. *Food Addit. Contam. Part A. Chem. Anal. Control. Expo. Risk Assess.* **25**, 134–145 (2008).
30. Kabak, B., Dobson, A. D. W. & Var, I. Strategies to prevent mycotoxin contamination of food and animal feed: a review. *Crit. Rev. Food Sci. Nutr.* **46**, 593–619 (2006).
31. Bandyopadhyay, R., Kumar, M. & Leslie, J. F. Relative severity of aflatoxin contamination of cereal crops in West Africa. *Food Addit. Contam.* **24**, 1109–1114 (2007).
32. Tang, L. *et al.* Modulation of aflatoxin biomarkers in human blood and urine by green tea polyphenols intervention. *Carcinogenesis* **29**, 411–417 (2008).
33. Egner, P. A. *et al.* Chlorophyllin intervention reduces aflatoxin-DNA adducts in individuals at high risk for liver cancer. *Proc. Natl. Acad. Sci. U. S. A.* **98**, 14601–14606 (2001).
34. Jubert, C. *et al.* Effects of chlorophyll and chlorophyllin on low-dose aflatoxin B 1 pharmacokinetics in human volunteers. *Cancer Prev. Res.* **2**, 1015–1022 (2009).
35. Magan, N. Effect of climate change on *Aspergillus flavus* and aflatoxin B1 production. *Front. Microbiol.* **5**, 1–7 (2014).
36. Rohlf, M., Albert, M., Keller, N. P. & Kempken, F. Secondary chemicals protect mould from fungivory. *Biol. Lett.* **3**, 523–525 (2007).
37. Yin, W.-B. *et al.* An *Aspergillus nidulans* bZIP response pathway hardwired for defensive secondary metabolism operates through aflR. *Mol. Microbiol.* **83**, 1024–34 (2012).
38. Yu, J.-H. & Keller, N. Regulation of secondary metabolism in filamentous fungi. *Annu. Rev. Phytopathol.* **43**, 437–458 (2005).
39. Trail, F. *et al.* Physical and transcriptional map of an aflatoxin gene cluster in *Aspergillus parasiticus* and functional disruption of a gene involved early in the aflatoxin pathway. *Appl. Environ. Microbiol.* **61**, 2665–2673 (1995).

40. Hoffmeister, D. & Keller, N. P. Natural products of filamentous fungi: enzymes, genes, and their regulation. *Nat. Prod. Rep.* **24**, 393–416 (2007).
41. Osbourn, A. Secondary metabolic gene clusters: evolutionary toolkits for chemical innovation. *Trends Genet.* **26**, 449–57 (2010).
42. Chang, P., Skory, C. D. & Linz, J. E. Cloning of a gene associated with aflatoxin B1 biosynthesis in *Aspergillus parasiticus*. **24690**, 2–4 (1992).
43. Skory, C. D., Chang, P. K., Cary, J. & Linz, J. E. Isolation and characterization of a gene from *Aspergillus parasiticus* associated with the conversion of versicolorin A to sterigmatocystin in aflatoxin biosynthesis. *Appl. Environ. Microbiol.* **58**, 3527–3537 (1992).
44. Skory, C. D., Chang, P. K. & Linz, J. E. Regulated expression of the nor-1 and ver-1 genes associated with aflatoxin biosynthesis. *Appl. Environ. Microbiol.* **59**, 1642–1646 (1993).
45. Trail, F., Chang, P. K., Cary, J. & Linz, J. E. Structural and functional analysis of the nor-1 gene involved in the biosynthesis of aflatoxins by *Aspergillus parasiticus*. *Appl. Environ. Microbiol.* **60**, 4078–4085 (1994).
46. Yu, J. *et al.* Comparative mapping of aflatoxin pathway gene clusters in *Aspergillus parasiticus* and *Aspergillus flavus*. *Appl. Environ. Microbiol.* **61**, 2365–2371 (1995).
47. Yu, J., Bhatnagar, D. & Cleveland, T. E. Completed sequence of aflatoxin pathway gene cluster in *Aspergillus parasiticus*. *FEBS Lett.* **564**, 126–30 (2004).
48. Georgianna, D. R. *et al.* Beyond aflatoxin: Four distinct expression patterns and functional roles associated with *Aspergillus flavus* secondary metabolism gene clusters. *Mol. Plant Pathol.* **11**, 213–226 (2010).
49. Georgianna, D. R. & Payne, G. A. Genetic regulation of aflatoxin biosynthesis: from gene to genome. *Fungal Genet. Biol.* **46**, 113–25 (2009).
50. Yu, J. Current understanding on aflatoxin biosynthesis and future perspective in reducing aflatoxin contamination. *Toxins (Basel)*. **4**, 1024–1057 (2012).
51. Cary, J. W. *et al.* Regulatory elements in aflatoxin biosynthesis. *Mycotoxin Res.* **22**, 105–109 (2006).
52. Chang, P. K. *et al.* Cloning of the *Aspergillus parasiticus* apa-2 gene associated with the regulation of aflatoxin biosynthesis. *Appl. Environ. Microbiol.* **59**, 3273–3279 (1993).

53. Roze, L. V., Chanda, A., Wee, J., Awad, D. & Linz, J. E. Stress-related Transcription Factor AtfB Integrates Secondary Metabolism with Oxidative Stress Response in Aspergilli. *Journal of Biological Chemistry* **286**, 35137–35148 (2011).
54. Miller, M. J., Roze, L. V., Trail, F. & Linz, J. E. Role of cis-acting sites NorL, a TATA box, and AflR1 in nor-1 transcriptional activation in *Aspergillus parasiticus*. *Appl. Environ. Microbiol.* **71**, 1539–1545 (2005).
55. Roze, L. V., Miller, M. J., Rarick, M., Mahanti, N. & Linz, J. E. A novel cAMP-response element, CRE1, modulates expression of nor-1 in *Aspergillus parasiticus*. *J. Biol. Chem.* **279**, 27428–39 (2004).
56. Hong, S.-Y., Roze, L. V., Wee, J. & Linz, J. E. Evidence that a transcription factor regulatory network coordinates oxidative stress response and secondary metabolism in aspergilli. *Microbiologyopen* **2**, 144–60 (2013).
57. Jayashree, T. & Subramanyam, C. Oxidative stress as a prerequisite for aflatoxin production by *Aspergillus parasiticus*. *Free Radic. Biol. Med.* **29**, 981–985 (2000).
58. Narasaiah, K. V., Sashidhar, R. B. & Subramanyam, C. Biochemical analysis of oxidative stress in the production of aflatoxin and its precursor intermediates. *Mycopathologia* **162**, 179–89 (2006).
59. Sakamoto, K. *et al.* *Aspergillus oryzae* atfB encodes a transcription factor required for stress tolerance in conidia. *Fungal Genet. Biol.* **45**, 922–932 (2008).
60. Sakamoto, K. *et al.* *Aspergillus oryzae* atfA controls conidial germination and stress tolerance. *Fungal Genet. Biol.* **46**, 887–897 (2009).
61. Reverberi, M. *et al.* Modulation of antioxidant defense in *Aspergillus parasiticus* is involved in aflatoxin biosynthesis: a role for the ApyapA gene. *Eukaryot. Cell* **7**, 988–1000 (2008).
62. Chanda, A. *et al.* A key role for vesicles in fungal secondary metabolism. *Proc. Natl. Acad. Sci. U. S. A.* **106**, 19533–19538 (2009).
63. Liang, S. H., Skory, C. D. & Linz, J. E. Characterization of the function of the ver-1A and ver-1B genes, involved in aflatoxin biosynthesis in *Aspergillus parasiticus*. *Appl. Environ. Microbiol.* **62**, 4568–4575 (1996).
64. Roze, L. V., Arthur, A. E., Hong, S.-Y., Chanda, A. & Linz, J. E. The initiation and pattern of spread of histone H4 acetylation parallel the order of transcriptional activation of genes in the aflatoxin cluster. *Mol. Microbiol.* **66**, 713–726 (2007).

65. Hicks, J. K., Yu, J. H., Keller, N. P. & Adams, T. H. *Aspergillus* sporulation and mycotoxin production both require inactivation of the FadA Gα protein-dependent signaling pathway. *EMBO J.* **16**, 4916–4923 (1997).
66. Roze, L. V, Beaudry, R. M., Keller, N. P. & Linz, J. E. Regulation of aflatoxin synthesis by FadA/cAMP/protein kinase A signaling in *Aspergillus parasiticus*. *Mycopathologia* **158**, 219–232 (2004).
67. Shimizu, K. & Keller, N. P. Genetic involvement of a cAMP-dependent protein kinase in a G protein signaling pathway regulating morphological and chemical transitions in *Aspergillus nidulans*. *Genetics* **157**, 591–600 (2001).
68. Calvo, A. M., Wilson, R. a, Bok, J. W. & Keller, N. P. Relationship between secondary metabolism and fungal development. *Microbiol. Mol. Biol. Rev.* **66**, 447–459, table of contents (2002).
69. Calvo, A. M. & Cary, J. W. Association of Fungal Secondary Metabolism and Sclerotial Biology. *Front. Microbiol.* **6**, (2015).
70. Mahanti, N., Bhatnagar, D., Cary, J. W., Joubran, J. & Linz, J. E. Structure and function of fas-1A, a gene encoding a putative fatty acid synthetase directly involved in aflatoxin biosynthesis in *Aspergillus parasiticus*. *Appl. Environ. Microbiol.* **62**, 191–195 (1996).
71. Zhou, R., Rasooly, R. & Linz, J. E. Isolation and analysis of fluP, a gene associated with hyphal growth and sporulation in *Aspergillus parasiticus*. *Mol. Gen. Genet.* **264**, 514–520 (2000).
72. Bennett, J. W., Silverstein, R. B. & Kruger, S. J. Isolation and characterization of two nonaflatoxigenic classes of morphological variants of *Aspergillus parasiticus*. *J. Am. Oil Chem. Soc.* **58**, A952–A955 (1981).
73. Kale, S. P., Cary, J. W., Bhatnagar, D. & Bennett, J. W. Characterization of experimentally induced, nonaflatoxigenic variant strains of *Aspergillus parasiticus*. *Appl. Environ. Microbiol.* **62**, 3399–3404 (1996).
74. Bayram, Ö. *et al.* VelB/VeA/LaeA Complex Coordinates Light Signal with Fungal Development and Secondary Metabolism. *Sci.* **320** , 1504–1506 (2008).
75. Calvo, A. M., Bok, J., Brooks, W., Keller, P. & Keller, N. P. veA Is Required for Toxin and Sclerotial Production in *Aspergillus parasiticus*. **70**, 4733–4739 (2004).
76. Menke, J., Weber, J., Broz, K. & Kistler, H. C. Cellular development associated with induced mycotoxin synthesis in the filamentous fungus *Fusarium graminearum*. *PLoS One* **8**, e63077 (2013).

77. Lim, F. Y. & Keller, N. P. Spatial and temporal control of fungal natural product synthesis. *Nat. Prod. Rep.* **00**, 1–10 (2014).
78. Lawellin, D. W., Grant, D. W. & Joyce, B. K. Aflatoxin localization by the enzyme-linked immunocytochemical technique. *Appl. Environ. Microbiol.* **34**, 88–93 (1977).
79. Lee, L.-W., Chiou, C.-H., Klomparens, K. L., Cary, J. W. & Linz, J. E. Subcellular localization of aflatoxin biosynthetic enzymes Nor-1, Ver-1, and OmtA in time-dependent fractionated colonies of *Aspergillus parasiticus*. *Arch. Microbiol.* **181**, 204–214 (2004).
80. Lee, L. W., Chiou, C. H. & Linz, J. E. Function of native OmtA in vivo and expression and distribution of this protein in colonies of *Aspergillus parasiticus*. *Appl. Environ. Microbiol.* **68**, 5718–5727 (2002).
81. Hong, S.-Y. & Linz, J. E. Functional expression and subcellular localization of the aflatoxin pathway enzyme Ver-1 fused to enhanced green fluorescent protein. *Appl. Environ. Microbiol.* **74**, 6385–96 (2008).
82. Hong, S. Y. & Linz, J. E. Functional expression and sub-cellular localization of the early aflatoxin pathway enzyme Nor-1 in *Aspergillus parasiticus*. *Mycol. Res.* **113**, 591–601 (2009).
83. Chanda, A., Roze, L. V., Pastor, A., Frame, M. K. & Linz, J. E. Purification of a vesicle-vacuole fraction functionally linked to aflatoxin synthesis in *Aspergillus parasiticus*. *J. Microbiol. Methods* **78**, 28–33 (2009).
84. Ohsumi, K., Arioka, M., Nakajima, H. & Kitamoto, K. Cloning and characterization of a gene (*avaA*) from *Aspergillus nidulans* encoding a small GTPase involved in vacuolar biogenesis. *Gene* **291**, 77–84 (2002).
85. Menke, J., Weber, J., Broz, K. & Kistler, H. C. Cellular development associated with induced mycotoxin synthesis in the filamentous fungus *Fusarium graminearum*. *PLoS One* **8**, e63077 (2013).
86. Roze, L. V *et al.* Ethylene modulates development and toxin biosynthesis in aspergillus possibly via an ethylene sensor-mediated signaling pathway. *J. Food Prot.* **67**, 438–447 (2004).
87. Gunterus, A., Roze, L. V., Beaudry, R. & Linz, J. E. Ethylene inhibits aflatoxin biosynthesis in *Aspergillus parasiticus* grown on peanuts. *Food Microbiol.* **24**, 658–663 (2007).

88. Lee, J.-W., Roze, L. V & Linz, J. E. Evidence that a wortmannin-sensitive signal transduction pathway regulates aflatoxin biosynthesis. *Mycologia* **99**, 562–568 (2007).
89. Roze, L. *et al.* Willow volatiles influence growth, development, and secondary metabolism in *Aspergillus parasiticus*. *Appl. Microbiol. Biotechnol.* **92**, 359–370 (2011).
90. Holmes, R. a, Boston, R. S. & Payne, G. a. Diverse inhibitors of aflatoxin biosynthesis. *Appl. Microbiol. Biotechnol.* **78**, 559–72 (2008).
91. Tian, C., Li, J. & Glass, N. L. Exploring the bZIP transcription factor regulatory network in *Neurospora crassa*. *Microbiology* **157**, 747–59 (2011).
92. Hong, S.-Y., Roze, L. V & Linz, J. E. Oxidative stress-related transcription factors in the regulation of secondary metabolism. *Toxins (Basel)*. **5**, 683–702 (2013).
93. Liu, J. *et al.* Genome-wide analysis and expression profile of the bZIP transcription factor gene family in grapevine (*Vitis vinifera*). *BMC Genomics* **15**, 281 (2014).
94. Amare, M. G. & Keller, N. P. Molecular mechanisms of *Aspergillus flavus* secondary metabolism and development. *Fungal Genet. Biol.* (2014). doi:10.1016/j.fgb.2014.02.008
95. Khaldi, N. *et al.* SMURF: Genomic mapping of fungal secondary metabolite clusters. *Fungal Genet. Biol.* **47**, 736–741 (2010).
96. Medema, M. H. *et al.* antiSMASH: rapid identification, annotation and analysis of secondary metabolite biosynthesis gene clusters in bacterial and fungal genome sequences. *Nucleic Acids Res.* **39**, W339–46 (2011).
97. Inglis, D. O. *et al.* Comprehensive annotation of secondary metabolite biosynthetic genes and gene clusters of *Aspergillus nidulans*, *A. fumigatus*, *A. niger* and *A. oryzae*. *BMC Microbiol.* **13**, 91 (2013).
98. Yin, W.-B. *et al.* bZIP transcription factors affecting secondary metabolism, sexual development and stress responses in *Aspergillus nidulans*. *Microbiology* **159**, 77–88 (2013).
99. Horng, J. S., Chang, P. K., Pestka, J. J. & Linz, J. E. Development of a homologous transformation system for *Aspergillus parasiticus* with the gene encoding nitrate reductase. *Mol. Gen. Genet.* **224**, 294–296 (1990).

100. Skory, C. D., Horng, J. S., Pestka, J. J. & Linz, J. E. Transformation of *Aspergillus parasiticus* with a homologous gene (pyrG) involved in pyrimidine biosynthesis. *Appl. Environ. Microbiol.* **56**, 3315–3320 (1990).
101. Schneider, C. a, Rasband, W. S. & Eliceiri, K. W. NIH Image to ImageJ: 25 years of image analysis. *Nat. Methods* **9**, 671–675 (2012).
102. Xie, C. *et al.* KOBAS 2.0: a web server for annotation and identification of enriched pathways and diseases. *Nucleic Acids Res.* **39**, W316–22 (2011).
103. Supek, F., Bošnjak, M., Škunca, N. & Šmuc, T. REVIGO Summarizes and Visualizes Long Lists of Gene Ontology Terms. *PLoS One* **6**, e21800 (2011).
104. Sekonyela, R. *et al.* RsmA Regulates *Aspergillus fumigatus* Gliotoxin Cluster Metabolites Including Cyclo(L-Phe-L-Ser), a Potential New Diagnostic Marker for Invasive Aspergillosis. *PLoS One* **8**, 1–10 (2013).
105. Cui, Y. *et al.* ExpR, a LuxR homolog of *Erwinia carotovora* subsp. *carotovora*, activates transcription of *rsmA*, which specifies a global regulatory RNA-binding protein. *J. Bacteriol.* **187**, 4792–803 (2005).
106. Kang, K. W., Ryu, J. H. & Kim, S. G. Activation of phosphatidylinositol 3-kinase by oxidative stress leads to the induction of microsomal epoxide hydrolase in H4IIE cells. *Toxicol. Lett.* **121**, 191–197 (2001).
107. Mackman, N. & Guha, M. The Phosphatidylinositol 3-Kinase-Akt Pathway Limits Lipopolysaccharide Activation of Signaling Pathways and Expression of Inflammatory Mediators in Human Monocytic Cells *. **277**, 32124–32132 (2002).
108. Nakaso, K. *et al.* PI3K is a key molecule in the Nrf2-mediated regulation of antioxidative proteins by hemin in human neuroblastoma cells. *FEBS Lett.* **546**, 181–184 (2003).
109. Slessareva, J. E., Routt, S. M., Temple, B., Bankaitis, V. A. & Dohlman, H. G. Activation of the phosphatidylinositol 3-kinase Vps34 by a G protein alpha subunit at the endosome. *Cell* **126**, 191–203 (2006).
110. Dienstmann, R., Rodon, J., Serra, V. & Tabernero, J. Picking the Point of Inhibition: A Comparative Review of PI3K/AKT/mTOR Pathway Inhibitors. *Mol. Cancer Ther.* 1021–1031 (2014). doi:10.1158/1535-7163.MCT-13-0639
111. Sánchez, S. *et al.* A cAMP-activated pathway, including PKA and PI3K, regulates neuronal differentiation. *Neurochem. Int.* **44**, 231–242 (2004).
112. Shepherd, P. R., Withers, D. J. & Siddle, K. Phosphoinositide 3-kinase : the key switch mechanism in insulin signalling. **490**, 471–490 (1998).

113. Gillooly, D. J. *et al.* Localization of phosphatidylinositol 3-phosphate in yeast and mammalian cells. *EMBO J.* **19**, 4577–4588 (2000).
114. Jaber, N. *et al.* Class III PI3K Vps34 plays an essential role in autophagy and in heart and liver function. *Proc. Natl. Acad. Sci.* **109**, 2003–2008 (2012).
115. Chanda, A., Roze, L. V & Linz, J. E. A possible role for exocytosis in aflatoxin export in *Aspergillus parasiticus*. *Eukaryot. Cell* **9**, 1724–7 (2010).
116. Linz, J. E. *et al.* Proteomic and biochemical evidence support a role for transport vesicles and endosomes in stress response and secondary metabolism in *Aspergillus parasiticus*. *J. Proteome Res.* **11**, 767–75 (2012).
117. Bhaya, D., Davison, M. & Barrangou, R. CRISPR-Cas Systems in Bacteria and Archaea: Versatile Small RNAs for Adaptive Defense and Regulation. *Annual Review of Genetics* **45**, 273–297 (2011).
118. Sander, J. D. & Joung, J. K. CRISPR-Cas systems for editing, regulating and targeting genomes. *Nat Biotech* **32**, 347–355 (2014).
119. Ochsner, U. a, Glumoff, V., Kälin, M., Fiechter, a & Reiser, J. Genetic transformation of auxotrophic mutants of the filamentous yeast *Trichosporon cutaneum* using homologous and heterologous marker genes. *Yeast* **7**, 513–524 (1991).
120. Wu, Y. T. *et al.* Dual role of 3-methyladenine in modulation of autophagy via different temporal patterns of inhibition on class I and III phosphoinositide 3-kinase. *J. Biol. Chem.* **285**, 10850–10861 (2010).
121. Heckmann, B. L., Yang, X., Zhang, X. & Liu, J. The autophagic inhibitor 3-methyladenine potently stimulates PKA-dependent lipolysis in adipocytes. *Br. J. Pharmacol.* **168**, 163–171 (2013).
122. Gibbons, J. G. & Rokas, A. The function and evolution of the *Aspergillus* genome. *Trends in Microbiology* **21**, 14–22 (2013).
123. Dobson, A. *Yeast and molds: Aspergillus flavus*. *Encyclopedia of Dairy Sciences* (Elsevier, Ltd., New York, NY, 2011). doi:10.1016/B978-0-12-374407-4.00367-8
124. Geiser, D. M. *et al.* The current status of species recognition and identification in *Aspergillus*. *Stud. Mycol.* **59**, 1–10 (2007).
125. Liang, S. H., Wu, T. S., Lee, R., Chu, F. S. & Linz, J. E. Analysis of mechanisms regulating expression of the *ver-1* gene, involved in aflatoxin biosynthesis. *Appl. Environ. Microbiol.* **63**, 1058–1065 (1997).

126. Cihlar, R. L. & Sypherd, P. S. The organization of the ribosomal RNA genes in the fungus *Mucor racemosus*. *Nucleic Acids Res.* **8**, 793–804 (1980).
127. Horng, J. S., Linz, J. E. & Pestka, J. J. Cloning and characterization of the *trpC* gene from an aflatoxigenic strain of *Aspergillus parasiticus*. *Appl. Environ. Microbiol.* **55**, 2561–2568 (1989).
128. Langmead, B. & Salzberg, S. L. Fast gapped-read alignment with Bowtie 2. *Nat Meth* **9**, 357–359 (2012).
129. Camacho, C. *et al.* BLAST+: architecture and applications. *BMC Bioinformatics* **10**, 421 (2009).
130. Roberts, A., Pimentel, H., Trapnell, C. & Pachter, L. Identification of novel transcripts in annotated genomes using RNA-Seq. *Bioinformatics* **27**, 2325–9 (2011).
131. Pan, T. & Coleman, J. E. GAL4 transcription factor is not a ‘zinc finger’ but forms a Zn(II)₂Cys₆ binuclear cluster. *Proc. Natl. Acad. Sci. U. S. A.* **87**, 2077–2081 (1990).
132. MacPherson, S., Larochele, M. & Turcotte, B. A fungal family of transcriptional regulators: the zinc cluster proteins. *Microbiol. Mol. Biol. Rev.* **70**, 583–604 (2006).
133. Woloshuk, C. P. *et al.* Molecular characterization of *aflR*, a regulatory locus for aflatoxin biosynthesis. *Appl. Environ. Microbiol.* **60**, 2408–2414 (1994).
134. Bailey, T. L. & Elkan, C. Fitting a mixture model by expectation maximization to discover motifs in biopolymers. *Proc. Int. Conf. Intell. Syst. Mol. Biol.* **2**, 28–36 (1994).
135. Maston, G. a, Evans, S. K. & Green, M. R. Transcriptional regulatory elements in the human genome. *Annu. Rev. Genomics Hum. Genet.* **7**, 29–59 (2006).
136. O’Dell, B. L., Burpo, C. E. & Savage, J. E. Evaluation of zinc availability in foodstuffs of plant and animal origin. *J. Nutr.* **102**, 653–660 (1972).
137. Jones, F. T., Jr, W. M. H., Hamilton, P. B., Hagler, W. M. & Hamilton, P. a T. B. Correlation of Aflatoxin Contamination With Zinc Content of Chicken Feed. **47**, 3–6 (1984).
138. Gupta, S. K., Maggon, K. K. & Venkitasubramanian, T. a. Effect of Zinc on tricarboxylic acid cycle intermediates and enzymes in relation to aflatoxin biosynthesis. *J. Gen. Microbiol.* **99**, 43–48 (1977).

139. Gupta, S. K. & Venkitasubramanian, T. A. Production of Aflatoxin on Soybeans. *Appl. Microbiol.* **29**, 834–836 (1975).